Master's thesis

Petrology and Economic Geology

Petrography, Geochemistry and Geochronology of the Post-kinematic A-type Intrusions of the Sorsavesi Area, Central Finland

Maija Pietilä

2020

Supervisors: Perttu Mikkola, Tapani Rämö

Master's Programme in Geology and Geophysics

Faculty of Science

Tiedekunta – Fakultet – Faculty	Laitos – Institution – Department
Faculty of Science	Department of Geosciences and Geography

Tekijä – Författare – Author

Maija Pietilä

Työn nimi – Arbetets titel – Title

Petrography, Geochemistry and Geochronology of the Post-kinematic A-type Intrusions of the Sorsavesi Area, Central Finland

Oppiaine – Läroämne – Subject

Geology

Työn laji – Arbetets art – Level	Aika – Datum – Month and year	Sivumäärä – Sidoantal – Number of pages
Master's Thesis	1.12.2020	80

Tiivistelmä – Referat – Abstract

Geological Survey of Finland conducted bedrock mapping in the eastern parts of Central Finland Granitoid Complex (CFGC) and the area next to the Archean craton in the 1990s. The area consists mainly of Paleo-proterozoic paragneisses, with minor volcanic rocks present. The granitoids belonging to the Central Finland Granitoid Complex make up part of the bedrock in the area. The granitoids of CFGC are divided into a 1.89-1.88 Ga syn-kinematic group, and a crosscutting, 1.88-1.87 Ga post-kinematic group. In this Master's thesis, three post-kinematic granitoid intrusions of Löytölamminvuori, Sorsakoski and Karvalevä are studied, covering their lithological, petrographical and geochemical features. The intrusions are non-foliated, porphyritic granites and quartz-monzonites, with a minor mafic phase of mostly dioritic composition in the Karvalevä intrusion. The main mafic silicates in the granite phase are biotite and hornblende, in the quartz-monzonite and mafic phases also clino- and orthopyroxene are present. Resembling the other post-kinematic plutons of the CFGC, the studied intrusions are geochemically high in Al_2O_3, FeO and K_2O, and low in MgO, CaO and Sr. One U-Pb age of 1876±6 Ma has been measured for the Löytölamminvuori intrusion, which places the intrusion at the same time frame as the other post-kinematic plutons.

Geochemically the intrusions show A-type affinity and close similarities to the post-kinematic pluton Types 2 and 3, fitting best with the Type 3a, which is transitional between the two. The magmas forming Löytölamminvuori, Sorsakoski and Karvalevä were derived from partial melting of mantle derived basalts, which underwent crustal contamination by partial melts from the lower crust. Slight deviation in composition from the strictly A-type magma and the volcanic arc affinity can be explained by the crustal component. The mafic phases show more primitive geochemistry, and thus present the mantle-derived source component with less crustal assimilation in the source.

The intrusions show signs of bimodal mafic-felsic magmatism, the dioritic phases in Karvalevä intrusion and one syn-plutonic dyke in Sorsakoski intrusion representing the mafic component. The mafic magmatism was cogenetic with the felsic phases, but not comagmatic, the diorites intruding simultaneously but slightly after the felsic phases. The mafic phases show a continuum in chemical composition to the granites and quartz-monzonites, but with a slight compositional gap.

Avainsanat – Nyckelord – Keywords

Granitoid, Petrography, Geochemistry, Geochronology, U-Pb, A-type, Bimodal, Central Finland Granitoid Complex, CFGC

Ohjaaja tai ohjaajat – Handledare – Supervisor or supervisors

Perttu Mikkola, Tapani Rämö

Säilytyspaikka – Förvaringställe – Where deposited

Muita tietoja – Övriga uppgifter – Additional information

Tiedekunta – Fakultet – Faculty	Laitos – Institution – Department
Matemaattis-luonnontieteellinen tiedekunta	Geotieteiden ja maantieteen laitos

Tekijä – Författare – Author
Maija Pietilä

Työn nimi – Arbetets titel – Title
Keski-Suomen Sorsaveden alueen postkinemaattisten A-tyypin intruusioiden petrografia, geokemia ja geokronologia

Oppiaine – Läroämne – Subject
Geologia

Työn laji – Arbetets art – Level	Aika – Datum – Month and year	Sivumäärä – Sidoantal – Number of pages
Pro gradu	1.12.2020	80

Tiivistelmä – Referat – Abstract

Geologian tutkimuskeskus suoritti laaja-alaisia kallioperäkartoituksia Keski-Suomen granitoidikompleksin itäisillä alueilla ja itäreunalla 1990-luvulla. Alue koostuu pääasiassa paleoproterotsooisista paragneisseistä ja vähäisistä vulkaanisista kivistä. Alueella esiintyvät Keski-Suomen granitoidikompleksiin kuuluvat granitoidit muodostavat osan alueen kallioperästä. Granitoidikompleksin granitoidit voidaan jakaa 1.89–1.88 Ga ikäisiin synkinemaattisiin intruusioihin ja näitä leikkaaviin 1.88–1.87 Ga ikäisiin postkinemaattisiin intruusioihin. Tässä pro gradu -työssä kolmea postkinemaattista intruusiota, Löytölamminvuori, Sorsakoski ja Karvalevä, on tutkittu niiden litologian, petrografian ja geokemian pohjalta. Intruusiot ovat suuntautumattomia, pofyyrisiä graniitteja ja kvartsimontsoniitteja, joiden lisäksi pieni, koostumukseltaan enimmäkseen dioriittinen osio esiintyy Karvalevä intruusiossa. Mafiset silikaatit ovat graniittisessa osassa biotiitti ja sarvivälke, kvartsimontsoniitti ja mafiset osat sisältävät myös klino- ja ortopyrokseenia. Kuten muissakin postkinemaattisissa granitoidikompleksin plutoneissa, on näissä korkeat pitoisuudet Al_2O_3, FeO ja K_2O ja matalat pitoisuudet MgO, CaO ja Sr. Yksi U-Pb -iänmääritys on tehty zirkonista yksikidemenetelmällä Löytölamminvuoren kvartsimontsoniitille, antaen iän 1876±6 Ma, eli se on muodostunut samanaikaisesti muiden postkinemaattisten plutonien kanssa.

Geokemiallisesti tutkitut intruusiot kuuluvat A-tyypin granitoideihin ja ovat samankaltaisia post-kinemaattisten tyyppien 2 ja 3 kanssa, sopien parhaiten tyyppiin 3a, joka on transitionaalinen 2 ja 3 tyypin välillä. Intruusiot muodostaneet magmat ovat peräisin vaipasta lähtöisin olevien basalttien osittaisesta sulamisesta, ja muodostuneiden sulien sekoittumisesta kuoren alaosien osittaisiin suliin. Intruusioiden lievät koostumuserot tiukasti tulkittuun A-tyypin kemiaan, kuten tietyt vulkaanisten kaarten graniiteille tyypilliset geokemialliset piirteet ovat selitettävissä kuoren materiaalin osuudella. Mafiset osat ovat geokemialtaan primitiivisempiä ja edustavat vaipasta lähtöisin olevaa lähdettä vähäisemmällä kuoren assimilaatiolla.

Intruusioissa on havaittavissa bimodaalisen magmatismin piirteitä, Karvalevän dioriittisten osuuksien ja yhden Sorsakosken synplutonisen juonen edustaessa mafista komponenttia. Mafiset kivilajit muodostanut magma oli lähtöisin samoilta alueilta kuin felsinen, mutta magmatismi ei ollut täysin samanaikaista, mafiset intruusiot muodostuivat hieman felsisten jälkeen. Mafiset komponentit muodostavat geokemiallisen jatkumon intruusioiden felsisempiin osiin, vaikka pieni koostumuksellinen epäjatkumo on havaittavissa.

Avainsanat – Nyckelord – Keywords
Granitoidi, Petrografia, Geokemia, Geokronologia, U-Pb, A-tyyppi, Bimodaalinen, Keski-Suomen granitoidikompleksi, CFGC

Ohjaaja tai ohjaajat – Handledare – Supervisor or supervisors
Perttu Mikkola, Tapani Rämö

Säilytyspaikka – Förvaringställe – Where deposited

Muita tietoja – Övriga uppgifter – Additional information

TABLE OF CONTENTS

1. INTRODUCTION

Granitoids are the most abundant plutonic rock type in the Earth's continental crust and can be found on all continents and thus have been studied very thoroughly. The most voluminous granitoids can usually be found on areas of thickened continental crust, (usually either in continental arc or continent-continent collision setting). They are a largely diverse group of rocks both in appearance and in chemical composition. Mineralogically, granitoids are defined as plutonic rocks that contain 20-60% quartz relative to feldspars and one or two feldspars +- mafic minerals, e.g. biotite, hornblende, or pyroxenes. Using the Streckeisen (1967) QAP diagram (Fig. 1.), granitoids can be divided into different groups. Feldspathic rocks containing 5-20% quartz can often be found with granitoid suites.

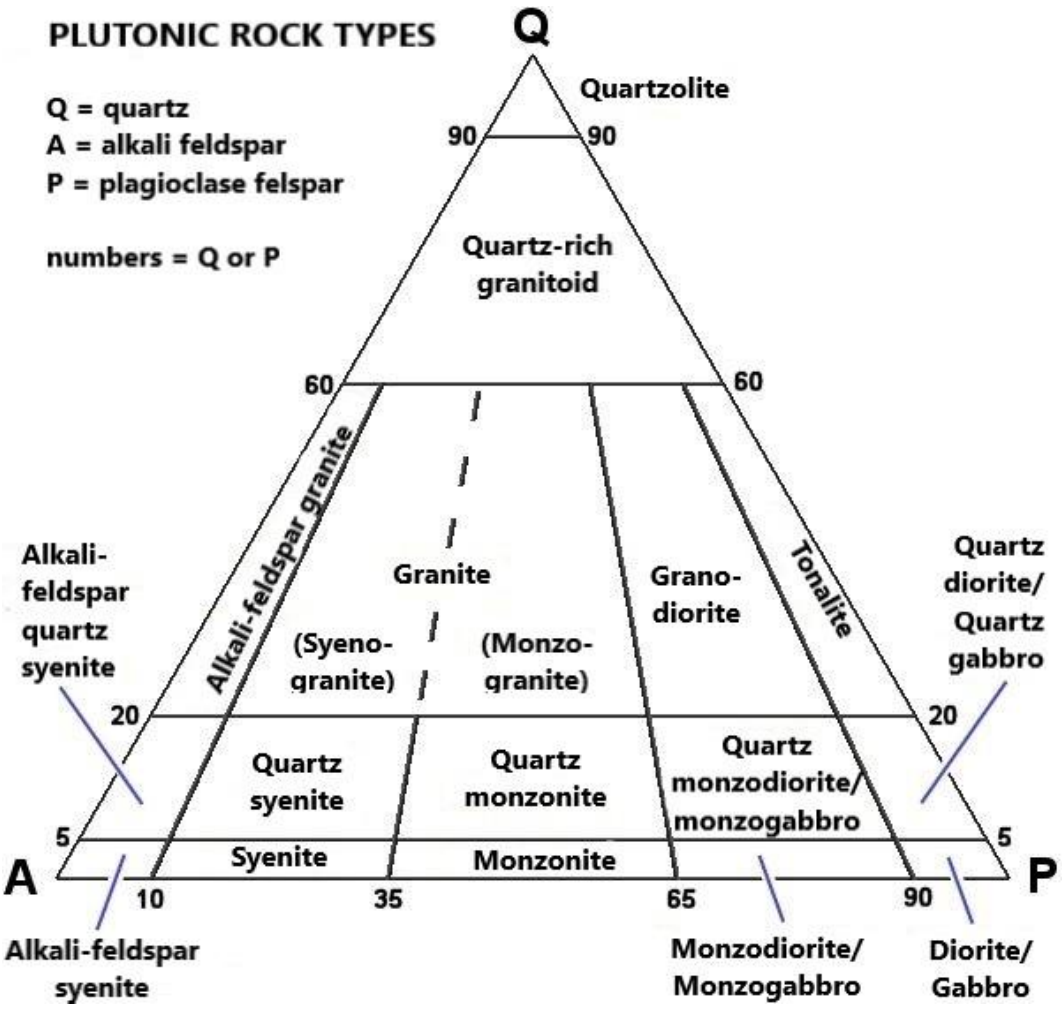

Figure 1. The QAP diagram, used for classifying granitic rocks (after Streckeisen 1967).

Due to slow cooling and the presence of volatiles, granitoids usually have a medium to coarse grain size. Large alkali-feldspar megacrysts are common. Biotite and hornblende are the main mafic phases in granitoids, clinopyroxene is usually more abundant in the mafic rocks of the rock suites. In addition to biotite, muscovite is common as a second mica in aluminous granitoids. Orthopyroxene and olivine are not usually found in granitoids. However, orthopyroxene can be found in anhydrous high-temperature granitoids and olivine in some alkaline varieties.

Numerous classification schemes have been invented and variably used, some overlapping each other. When classifying different granitoid types, the mostly used features are field and petrographical observations, mineral assemblages, isotopic and geochemical features. The difficulty when classifying granitoids is, that the typical main element composition and mineralogy of granites can be a result of many different processes and the sources for granitic rocks vary from only crustal sources to mantle origins, and different combinations of the two. Granitic melts also occur in almost all tectonic settings. All these features make granitoids extremely heterogenous rock group.

In this Master's Thesis, three intrusions located along the eastern boundary of the Central Finland Granitoid complex, approximately 50 km to the south-west of the city of Kuopio, are studied and analyzed using their mineralogy, petrography and geochemical composition. The data used in this Thesis was collected and comprised by the Geological Survey of Finland (GTK), mainly during the regional bedrock mapping (Mikkola et al. 2016). Additional samples were collected in summer 2018. The data comprises field observations, large petrographic material (thin sections) and whole-rock geochemical data, with one U-Pb age determination. The objective of this study is to classify the intrusions based on their petrography and geochemistry and determine their relation to the Central Finland Granitoid Complex (CFGC) and its plutonic rocks. The previous work done on the CFGC (Front and Nurmi 1987, Elliot et al. 1998, Nironen et al. 2000, Rämö et al. 2001) is used as reference material in this work, comparing the mineralogical, geochemical and spatial features in relation to the post-kinematic granitoids of the CFGC and their different subtypes.

2. GRANITOIDS

2.1. Granitoid classification

Because of the abundance and great variety of granitoid rocks, numerous different classification schemes have been invented and suggested for granitoids over many decades (e.g.,Winter 2001). The classifications are most commonly based on differences in mineralogical and geochemical composition of the granitoids. Using these features granitoids have been divided into different groups based by for example their petrogenetic conditions or tectonic settings. The three important and generally used geochemical parameters in granitoid-classification are: the Fe-number, the modified alkali-lime index (MALI) and the aluminum saturation index (ASI) (Fig. 2.) (Frost et al. 2001).

The Fe-number or the FeO / (FeO + MgO) ratio of the rock gives information about the differentiation history of the magma. This is based on the fact that there appears to be great differences between intrusions that go through iron enrichment while silica saturation remains low and rock suites that undergo silica enrichment while FeO remains low (relative to MgO) (Miyashiro, 1970). The terms used for these different types are, respectively, ferroan and magnesian. The second factor is the modified alkali-lime index (MALI) which is calculated as SiO_2 vs. $Na_2O + K_2O - CaO$, where at certain SiO_2 content the $Na_2O + K_2O$ equal CaO (Peacock 1931). The results are divided into four groups: alkalic, alkali-calcic, calc-alkalic and calcic. The third geochemical classification factor is the aluminum saturation index (ASI) which is defined as the molecular ratio Al / (Ca – 1.67P + Na + K) (Shand 1943). In this, apatite is subtracted so rocks that have ASI>1.0 are corundum-normative and so classified as peraluminous, meaning that they have more aluminum than can be carried by feldspars so they must have another aluminous phase (e.g. muscovite, cordierite, garnet etc.). If the ASI is < 1.0 but molecular Na + K < molecular Al, then the rock is metaluminous and there is usually excess Ca present, so these rocks contain calcic phases such as hornblende and augite. If ASI is <1.0 and Na + K > Al, then the rock is peralkaline. This means that the rock has more alkalis than is needed for the feldspars. In these rocks the excess of alkali metals, particularly Na, goes into ferro-magnesian silicates. If weakly peralkaline, the element might go into hornblende, but in more alkaline varieties sodic amphiboles and pyroxenes can be found.

These three geochemical parameters are the basic features when comparing granitoids and classifying them, since these traits and their different variations are good indicators of petrogenetic and tectonic conditions.

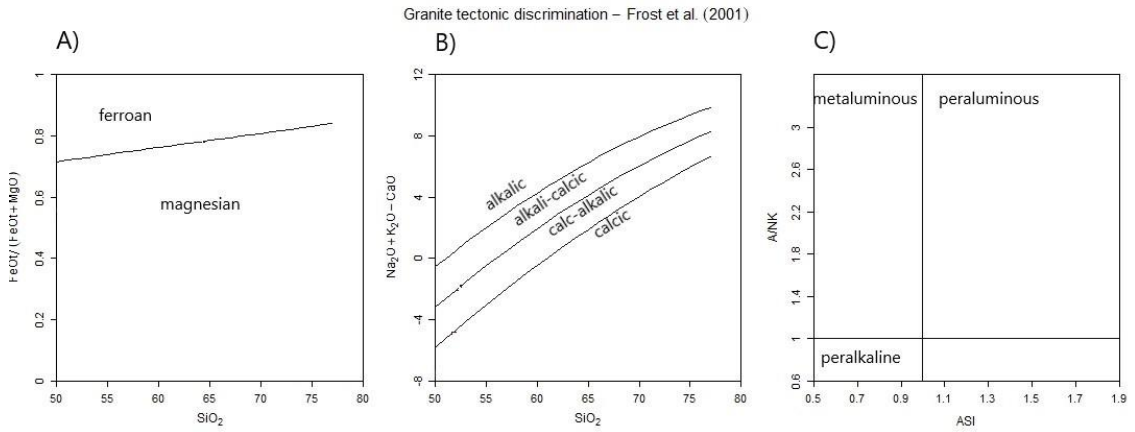

Figure 2. Tectonic discrimination diagrams for granitic rocks (after Frost et al. 2001). The diagrams are Fe-number vs. SiO_2 (A), modified alkali-lime index (MALI) vs. SiO2 (B), and aluminum saturation index (ASI) vs. inverse of agpaitic index (A/NK) (C).

The most commonly used petrogenetic classification scheme is the alphabetical S-I-A-M. This classification, first introduced by Chappell and White (1974), is based on field and petrographic differences as well as geochemical and isotopical characteristics. The four types are the I-type (igneous), S-type (sedimentary), M-type (mantle) and A-type (anorogenic). The I-type is thought to be formed by partial melting of a mafic igneous source material, probably a crustal underplate. I-type is the most dominant of granitoid types. This type can be petrologically variable, comprising mineralogically of quartz, plagioclase, K-feldspar and of lesser amounts hornblende, biotite, epidote, allanite, titanite and magnetite. Geochemically I-types are mostly metaluminous or sometimes weakly peraluminous and have a moderate depletion of Ba, Ti and P and have strong Nb-Ta depletion relative to Th ad l-REE. Tectonically, these granitoids are related to collisional setting or subduction in either island or continental arc and setting.

In comparison to the I-type, the S-type granitoids have the opposite chemical attributes. The S-type or sedimentary granitoids are always peraluminous and are produced by partial melting of sedimentary sources. They are biotite rich and also contain muscovite, aluminosilicates, titanite, ilmenite and for example garnet. Geochemically they are high in silica, and Li, B and F, with moderate depletion of Ba, Ti, and P. Tectonically S-type is found in syn- to post-tectonic regimes with continent-continent collisions.

The M-type stands for direct mantle source, as there are also granitoids forming from only mantle material, these being for example the immature arc plutons and the oceanic plagiogranites. They are formed by fractional crystallization of the Mid-Ocean Ridge Basalts (MORB). Mineralogically these granitoids contain hornblende, biotite, clinopyroxene and magnetite and geochemically are strongly metaluminous with A/CNK < 0.6 and are minorly depleted in Ba, Ti and P. Tectonically M-type granitoids are pre-tectonic, ophiolitic and occur in island arc settings.

For the A-type granitoids, the A stands for anorogenic, alkaline and anhydrous (Loiselle and Wones 1979). These granitoids are usually emplaced in non-orogenic settings and are formed by partial melting of lower crustal rocks with variable mantle source component. They may contain green biotite, fayalitic olivine, magnetite, apatite and for example fluorite. Geochemically, the A-type granitoids are metaluminous to weakly peraluminous and are high in silica, Na+K, Fe/Mg, Nb, Ta, Y, F and Ga with strong depletion of Ba, Ti and P. Tectonically, the A-type granitoids are found in anorogenic and post-orogenic settings, in extensional regions where there might be continental rifting and uplifting due to for example a hot-spot. Generally the A-type granitoids are a diverse group, both in their genesis and geochemically and they are not strictly bound to anorogenic setting either.

The alphabetic S-I-A-M classification is clear and quite simple way to differentiate between different type of granitoids, but in reality the boundaries between different types are usually never really clear and hybrid magmas are very common. I- and S-types are often only the end members of a granitoid series in for example an orogenic belt and I-type magma might take S-type characteristics by assimilating crustal material. And A-type magmas are not restricted to anorogenic settings, for they might also occur in orogenic belts. Because of the overlaps in and limitations of this classification, the classification by tectonic regimen is now-a-days growing in popularity. The A-type of the S-I-A-M scheme is already a tectonic-type classification.

Granitoid classification based on tectonic setting is also done using geochemical characteristics. Pearce et al. (1984) introduced a classifications scheme that uses certain trace elements and their occurrence in the granitoids. Granitoids are divided into four groups: 1) ocean ridge granites (ORG), 2) volcanic-arc granites (VAG), 3) within-plate granites (WPG) and 4) collisional granites (COLG) (Fig. 3.). The elements discriminating

granite tectonic types are Y, Yb, Rb, Ba, K, Nb, Ta, Ce, Sm, Zr and Hf. Discrimination diagrams based on variations of elements Rb-Y-Nb and Rb-Yb-Ta are the most useful when comparing the four types (Rollinson 1993). Another example of a classification scheme that uses geochemistry of the rocks, is the $R_1 - R_2$ tectonic discrimination diagram, which plots the samples on a multi-cationic diagram (De la Roche et al. 1980, Batchelor and Bowden 1985). This scheme depicts the change in magmatism type and tectonic setting through the orogenic cycle and the composition of the associated granites. There are typical geochemical features and mineralogy to different tectonic types, but often the geochemistry of granitoids is affected by the protolith of the granitoid. As such the tectonic discrimination should be used with caution. Many of these features are overlapping with for example the S-I-A-M classification and these are not exclusive. The alphabetical classification can be useful in some cases, the tectonic schemes in some other purposes.

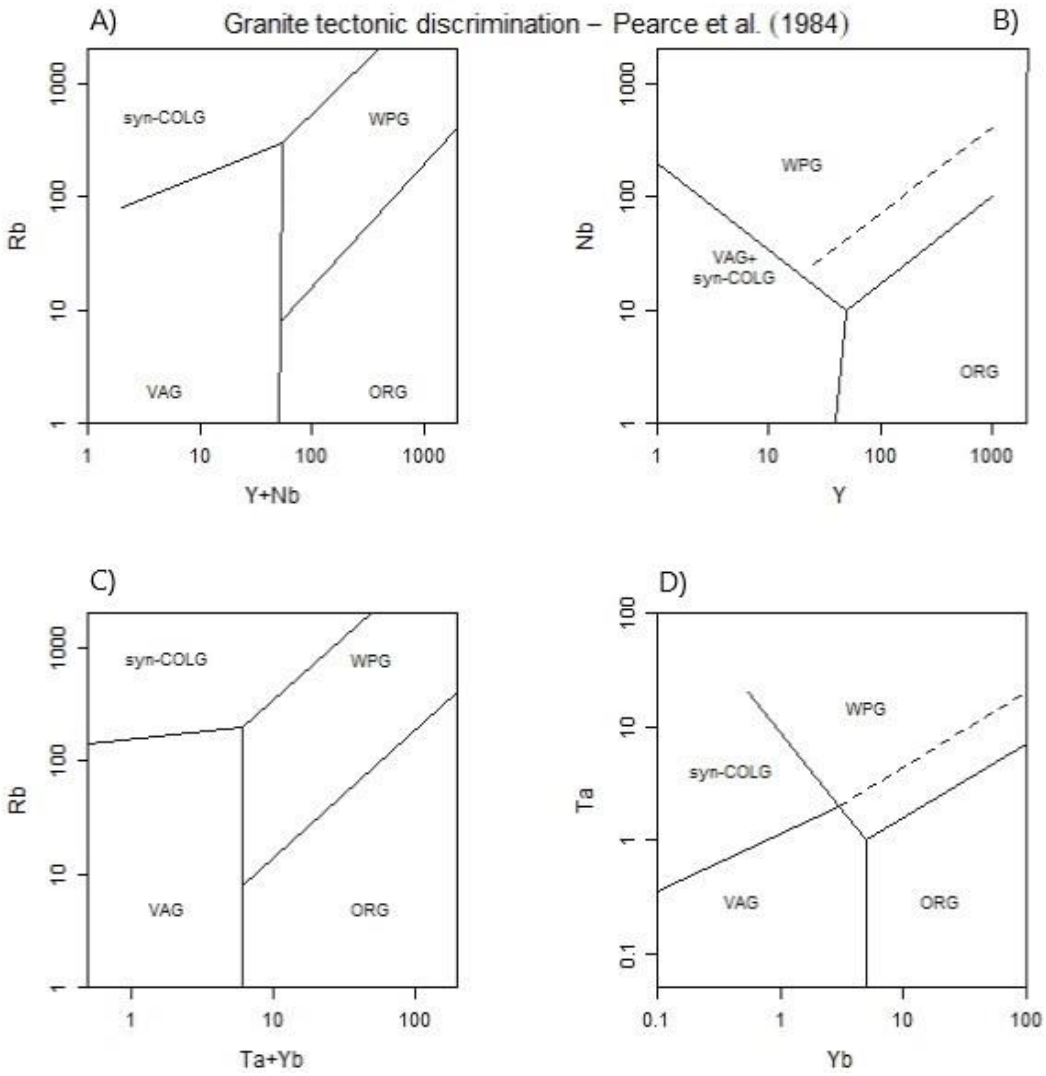

Figure 3. Tectonic discrimination diagrams of Rb vs. Y+Nb (A), Nb vs. Y (B), Rb vs. Ta+Yb (C), and Ta vs. Yb (D), showing the different fields for ocean ridge granites (ORG), volcanic arc granites (VAG), within plate granites (WPG), and (syn)-collisional granites (syn-COLG). (after Pearce et al. 1984).

2.2. Granitoid petrogenesis

For such a diverse group of rocks, granitoids are bound to have a wide range of sources and their formation is not restricted to only for example subduction processes. The petrogenesis of granitoids has been a topic of debate for over 200 years. It was suggested earlier that remelting of older crustal material is the source of granitoid magmas (Chappell and White 1974, Frost and Frost 1997). However, even as most of Earth's granitoids are found in the continental crust, some are also found in the oceanic crust; this shows that granitoids can be formed also by fractionation of a priori mantle-derived material. It is

now generally accepted that the majority of granitoids is generated by melting of pre-existing crust, but that mantle may also contribute. Mantle contribution may vary from providing a heat source to acting as granitoid's source material. As granitoids are plutonic rocks they are formed when melt ascents as diapirs or through fractures as dykes. The final shape of the intrusions depends on the depth of emplacement, the ductility and density of the surrounding country rocks and the magma, and the pre-existing structures of the country rocks. The initial granitoid melt composition is controlled by a variety of factors, the main ones being the composition of the source, temperature and pressure conditions, degree of partial melting and interaction with other melts or magmas.

3. GEOLOGICAL SETTING

3.1. Svecofennian orogeny

The Svecofennian orogeny produced the majority of the crustal material of central Finland. This involved multiple accretionary processes which caused the continental growth in Fennoscandia during Palaeoproterozoic. The orogen can be divided into different phases of Lapland-Savo, Fennia, Svecobaltic and Nordic orogens (Lahtinen et al. 2009). These are all separate but partly overlapping events, consisting of accretionary growth, continental collision and continental collapse which all together resulted in the anomalously thick Paleoproterozoic crust in central Finland (Fig.4.). The Svecofennian orogen is a collection of 2.1-2.0 Ga microcontinents and 2.02-1.82 Ga island arcs. The accretion of the central Finland island arc complex to the Archean continent took place at approximately 1.91 Ga. Following this, a subduction reversal and plate motion direction rotation, or convergence of another plate happened at 1.90 Ga. During 1.88 – 1.87 Ga the southern Finland arc complex collided against the Central Finland arc. This led to the disappearance of two subduction zones and the merging of accretionary prisms. The amalgamation took place between 1.92 Ga and 1.79 Ga. Andean type magmatic additions also added to the growth, especially around 1.89 and 1.8 Ga. The main collisional stage was around 1.89-1.87 Ga and was associated with voluminous continental growth in the

central part of the Fennoscandian shield and formation of the Central Finland Granitoid Complex (CFGC).

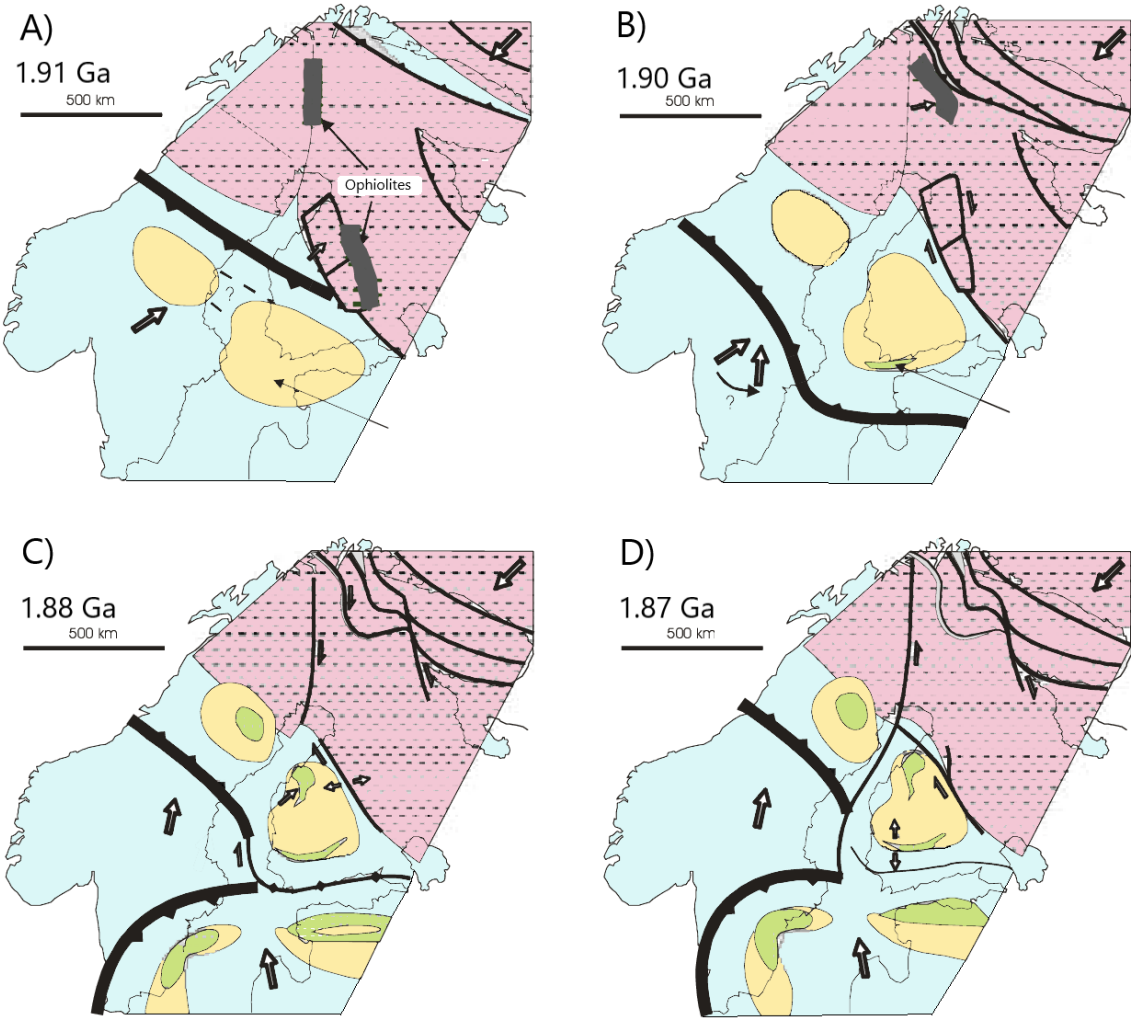

Figure 4. Tectonic model of the Svecofennian orogen after on Nironen (1997). The pink areas are Archean crust; the blue sedimentary rocks and oceanic crust; yellow areas arc complexes and green areas volcanic arcs. Scenario A depicts the accretion of the central Finland island arc complex to the Archean continent at approximately 1,91 Ga. B shows a subduction reversal and plate motion direction rotation, or convergence of another plate. C and D scenarios depict the collision of the southern Finland arc complex against the Central Finland arc. This led to the disappearance of two subduction zones and the merging of accretionary prisms.

3.2. Central Finland Granitoid Complex (CFGC)

The Central Finland Granitoid Complex (CFGC) covers an area of circa 44 000 km^2. It is predominantly made of felsic rocks, especially granites and granodiorites but also contains some mafic intrusions, mostly dioritic in composition (Fig.5.) (Front and Nurmi

1987, Nironen 2005). CFGC is the main core of the Keitele microcontinent (Lahtinen et al. 2009) which is surrounded by mainly Svecofennian gneisses.

3.3.1. Syn kinematic plutons of the CFGC

The plutonic rocks of the CFGC have been classified by texture, mineral and chemical composition, and degree of deformation (Front and Nurmi 1987, Rämö et al. 2001, Nironen 2005). On a larger scale the plutons have been divided into syn-kinematic and post-kinematic with respect to the regional deformation D2. Syn-kinematic rocks are dominant in the CFGC. These are aged 1.89-1.88 Ga and crosscut supracrustal rocks. Their deformation degree varies from slight preferred orientation to pervasive, sometimes folded foliation. The granites are even grained to porphyritic, usually medium to coarse grained, porphyritic varieties have feldspar phenocrysts of 1-3 cm up to 5 cm. The most dominant rock type among the syn-kinematic plutons are granodiorites. Small gabbro and diorite bodies are found through the CFGC and also a few ultramafics are present with the gabbros. The mafic rocks that are found together with the syn-kinematic plutons tend to have mingling textures with the felsic rocks. The main minerals of the syn-kinematic granitoids are quartz, plagioclase, K-feldspar, biotite, and hornblende. The main accessory minerals are apatite, magnetite, titanite and zircon. Geochemically they show affinities to volcanic arc type granitoids, tend to be calc-alkaline and thus plot in the Phanerozoic I-type field of granitoids (Front and Nurmi, 19897).

The syn-kinematic granitoids are crosscut by the post-kinematic series. Post-kinematic rocks are almost co-eval with the syn-kinematic rocks in the eastern parts of CFGC but slightly younger in the west, with ages of 1.88-1.87 Ga and 1.87 Ga, respectively. They are mostly weakly to non-foliated and represent the time at which the crust was stabilized. The post-kinematic intrusions differ from the syn-kinematic ones by texture, mineralogy, and geochemical composition (Nironen et al. 2000).

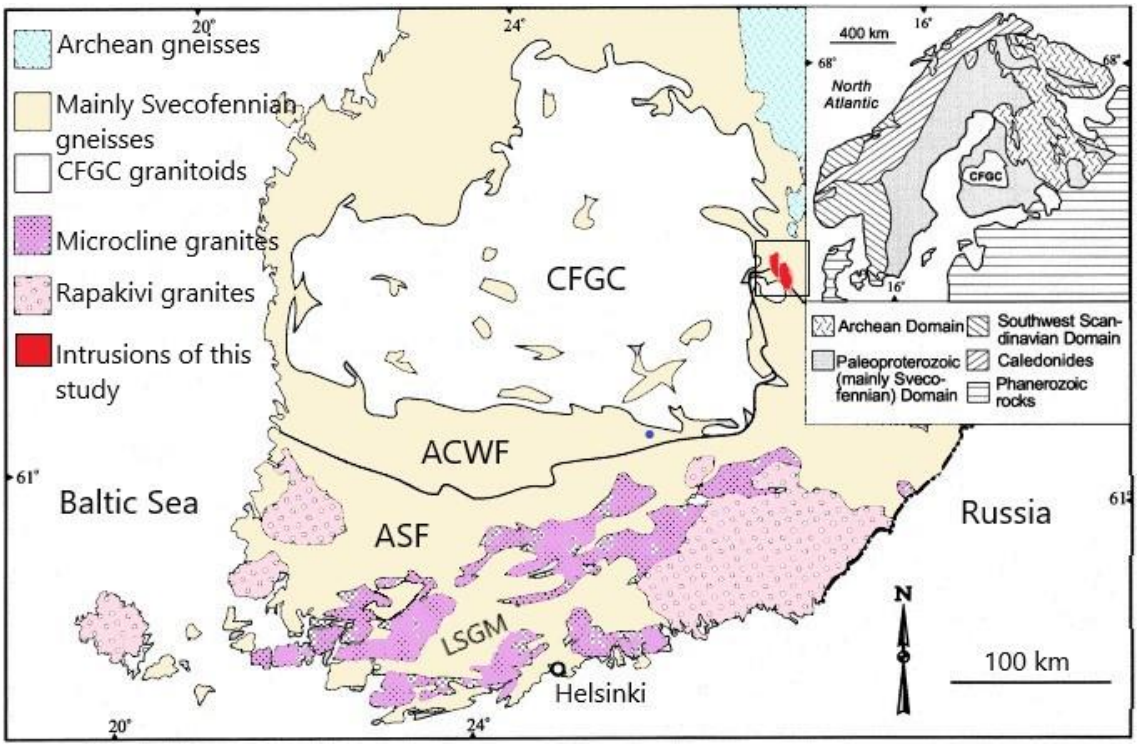

Figure 5. The bedrock map of southern and central Finland and tectonic setting of the Central Finland Granitoid Complex (CFGC), after Nironen et al. (2000). ACWF = Accretionary arc complex of central and western Finland, ASF = Accretionary arc complex of southern Finland, LSGM = Late Svecofennian granite-migmatite zone. The studied intrusions are located east of the CFGC, and are marked here in red.

3.3.2. Post-kinematic plutons of the CFGC

The post-kinematic plutons are found as numerous relatively small batholiths and stocks mainly in the CFGC area, some intrusions also outside of it (Fig.6.) (Elliott 2001). They are mostly quartz-monzonites, monzogranites and some granites, and mafic members are also found. Compared to the syn-kinematic rocks which are mostly I-type and calc-alkaline, the post-kinematic series have in general alkaline affinity and higher FeO_t, K_2O, TiO_2, Ba, Nb and Zr and lower MgO, CaO and Sr at a given SiO_2. As such they tend to plot more into the A-type granitoids and not the I-type (Elliott et al. 1998). The post-kinematic granitoids have been divided into three groups based on their petrographic, mineral, outcrop and geochemical and mineral chemical characteristics, the groups being Type 1, Type 2 and Type 3, the Type 3 is divided further into 3a and 3b (Table 1.) (Elliott et al. 1998, Nironen et al. 2000).

The Type 1 granitoids are discordant and slightly to non-foliated and are dominant in the southern parts of CFGC. They are mainly granodiorite or monzogranite and are even- to coarse-grained and usually porphyritic and white or gray to pink in color. Compared to

the Type 2 and Type 3 they have lower Fe/Mg and have more modal plagioclase. K-feldspar and plagioclase are typically resorbed and altered to sericite, and plagioclase is either replaced by secondary alkali-feldspar or surrounded by it. K-feldspar occurs as orthoclase megacrysts and medium-grained microcline. Quartz is usually interstitial. The Type 1 granitoids have usually biotite as the only mafic silicate. It is found as brown to light-brown euhedral and subhedral grains. Also reddish-brown biotite occurs but it is probably a reaction product of amphibole. Accessory minerals in Type 1 are fluorite, zircon, apatite and ilmenite. Geochemically the Type 1 plutons are peraluminous.

Table 1. Post-kinematic granitoids of Central Finland Granitoid Complex, the rock types and typical mineralogy after Front and Nurmi (1987), Elliott et al. (1998) and Rämö et al. (2001).

	Type 1	Type 2	Type 3a	Type 3b
Rock type	monzogranite, granodiorite	monzogranite	quartz-monzonite, monzogranite and quartz-syenite	quartz-monzonite and granodiorite
Main mafic silicates	biotite	biotite ± hornblende	biotite, hornblende ± pyroxene	biotite, hornblende, pyroxene ± olivine
Accessory minerals	apatite, ilmenite, zircon ± fluorite	apatite, allanite, fluorite, ilmenite, titanite, zircon	apatite, ilmenite, titanite, zircon ± magnetite	apatite, ilmenite, titanite, zircon ± magnetite

The Type 2 plutons are the most abundant of the post-kinematic types and are found in the southern and western parts of the CFGC (Elliott et al. 1998). They are, like the Type 1 intrusions, discordant, non-foliated and even- to coarse-grained and often porphyritic. The Type 2 plutons are mostly granites and red in color. Many of the plutons are associated with mafic plutonic rocks. Plagioclase is usually altered to sericite and largely replaced by alkali feldspar. Orthoclase megacrysts are occasionally surrounded by quartz and plagioclase mantles. Quartz is interstitial and appears often as inclusions in felspars. Biotite is the main mafic silicate but the plutons with less silica contain also amphibole. The amphibole is anhedral and green-brown pleochroic in color. On grain margins can be seen some alteration to biotite. Accessory minerals are fluorite, apatite, zircon, allanite and titanite. Epidote may also be present. Geochemically the type 2 plutons are marginally peraluminous and have high Fe/Mg which increases with SiO_2 content (Nironen et al. 2000).

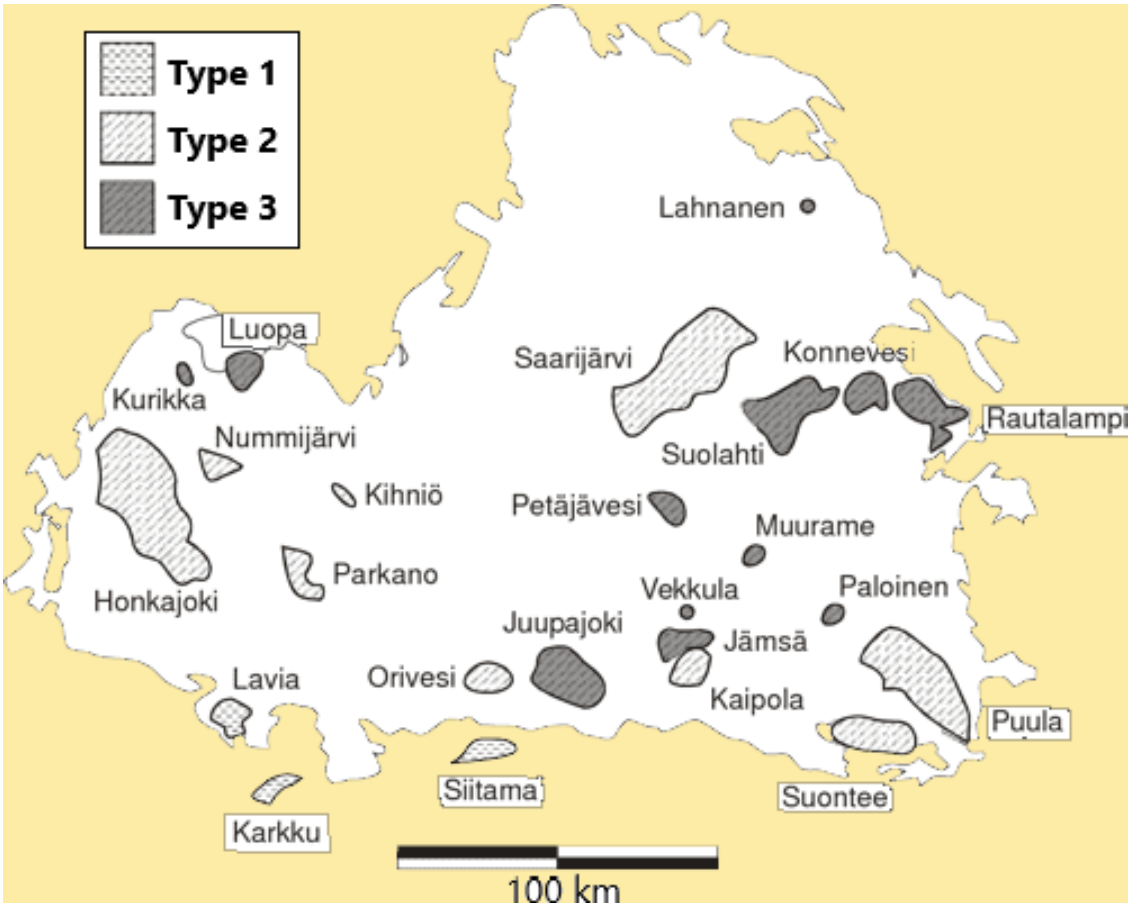

Figure 6. The distribution of the Type 1, 2 and 3 post-kinematic plutons of the Central Finland Granitoid Complex (after Elliott, 2001)

The Type 3 plutons are mostly quartz-monzonite and granite, usually discordant and even- and coarse-grained. They are often porphyritic and non-foliated and contain pyroxenes. The Type 3 plutons are most abundant in the eastern parts of CFGC. Type 3 is further divided into two groups: Type 3a has pyroxene-bearing margins or pyroxene-bearing bodies near the margin, Type 3b with pyroxene throughout the pluton. The change from the more pyroxene-bearing margin to the center is gradual and plutons show a decrease in Ti, Fe/Mg and K/Na from the margin towards the center. In general, the Type 3 pluton margins are pyroxene+-olivine bearing quartz-monzonite and the center biotite-hornblende monzogranite. Unlike in Types 1 and 2, plagioclase is unaltered and likely presents a late-stage cumulus phase. Alkali feldspar appears as perthitic orthoclase megacrysts which sometimes have quartz and plagioclase rims. The more mafic margins of Type 3 plutons contain fayalitic olivine, Fe-rich clino- and/or orthopyroxene, amphibole and biotite. Accessory minerals are apatite, zircon and secondary titanite. Geochemically the Type 3 plutons are marginally metaluminous to marginally

peraluminous. The Type 3a plutons have higher FeO_t and lower MgO content than type 3b at similar SiO_2 values.

4. MATERIALS AND METHODS

4.1. Materials

The material for this thesis was provided by GTK. The pre-existing materials consist of field observation and mapping data, 59 previously prepared thin sections, and 74 whole-rock geochemical analyses (Appendix 1.) of Löytölamminvuori, Sorsakoski and Karvalevä intrusions, and one U-Pb age analysis of Löytölamminvuori intrusion (Appendix 2.) (done by Hannu Huhma, 2016). To ensure even distribution of sample locations and coverage of data, three additional days of revision mapping and sampling of the area was performed for this study. The additional samples were collected from all three intrusions, but most of them from the mafic Karvalevä intrusion because of the lack of previous data. New materials consist of 22 thin sections and 18 whole-rock geochemical analyses (Appendix 1.).

4.2. Whole-rock geochemistry

Wave-length dispersive X-ray fluorescence (WD-XRF) method was used to analyze all major element oxides (SiO_2, TiO_2, Al_2O_3, Fe_2O_3, MnO, MgO, CaO, Na_2O, K_2O, and P_2O_5) and some of the trace elements (S, Cl, Cr, Ni, Cu, Zn, Ga, Sr, Ba and Pb). Inductively coupled plasma mass spectrometer (ICP-MS) was used to analyze the rest of the trace element (Sc, V, Rb, Y, Nb, Hf, Ta, Co, Pb, Th, U, La, Ce, Pr, Nd, Sm, Eu, Gd, Tb, Dy, Ho, Er, Tm, Yb and Lu). The WD-XRF measurements for the older, pre-existing samples were done in GTK, and the ICP-MS measurements for the old samples are from

Rasilainen et al. (2007). The measurements on the new samples from 2018 were done by Labtium Oy.

4.3. U-Pb zircon geochronology

Zircons from sample (A2434) were analyzed in GTK's isotope laboratory in Espoo directly from thin sections. The U-Pb dating analyses were done with a Nu Plasma Attom single collector ICP-MS connected to a Photon Machine Excite laser ablation system. He gas was used for the sample ablation within a HelEx ablation cell (Müller et al. 2009). The ablation conditions were as follows; beam diameter: 25 μm, pulse frequency: 5 Hz, beam energy density: 2 J/cm2.

Standards were run at the beginning and end of every analytical session and at regular intervals during sessions. The standards used were calibration standard GJ-1 (609+-1 Ma; Belousova et al. 2006) and in-house standard A382 (1877+-2 Ma; Huhma et al. 2012). The Glitter program was used to correct the raw data for the background, laser induced elemental fractionation, mass discrimination and drift in ion counter gains, and reduced to U-Pb isotope ratios by calibration to concordant reference zircons (Van Achterbergh et al. 2001). Age calculations and plotting of the U-Pb isotopic data were performed using the Isoplot/Ex 3 program (Ludwig 2003). The ages were calculated with 2σ errors and without decay constant errors. Data-point error ellipses in the figures are at the 2 σ level.

5. LITHOLOGY OF THE INTRUSIONS

The area comprises three intrusions, together approximately 50 by 20 km in the current level of erosion. The felsic intrusions, Löytölamminvuori and Sorsakoski, grade in composition from quartz-monzonite core to granite rims. Between these felsic intrusions there is a smaller, roundish Karvalevä intrusion that ranges in composition from granite to diorite (Fig. 7.). The intrusions are situated in the Palaeoproterozoic suture zone between the Central Finland Granitoid Complex in the west and Archean craton in the

east. The bedrock of the area consists mainly of Palaeoproterozoic paragneisses into which the granitoids have intruded. The bedrock is cut by many faults and shear zones which are connected to the Raahe-Ladoga shear-zone. The contacts the plutons have to the surrounding rocks are in general sharp and usually tectonic. The age of the suite has been estimated at approximately 1880 Ma by relation to the surrounding rocks (Lahtinen et al. 2016).

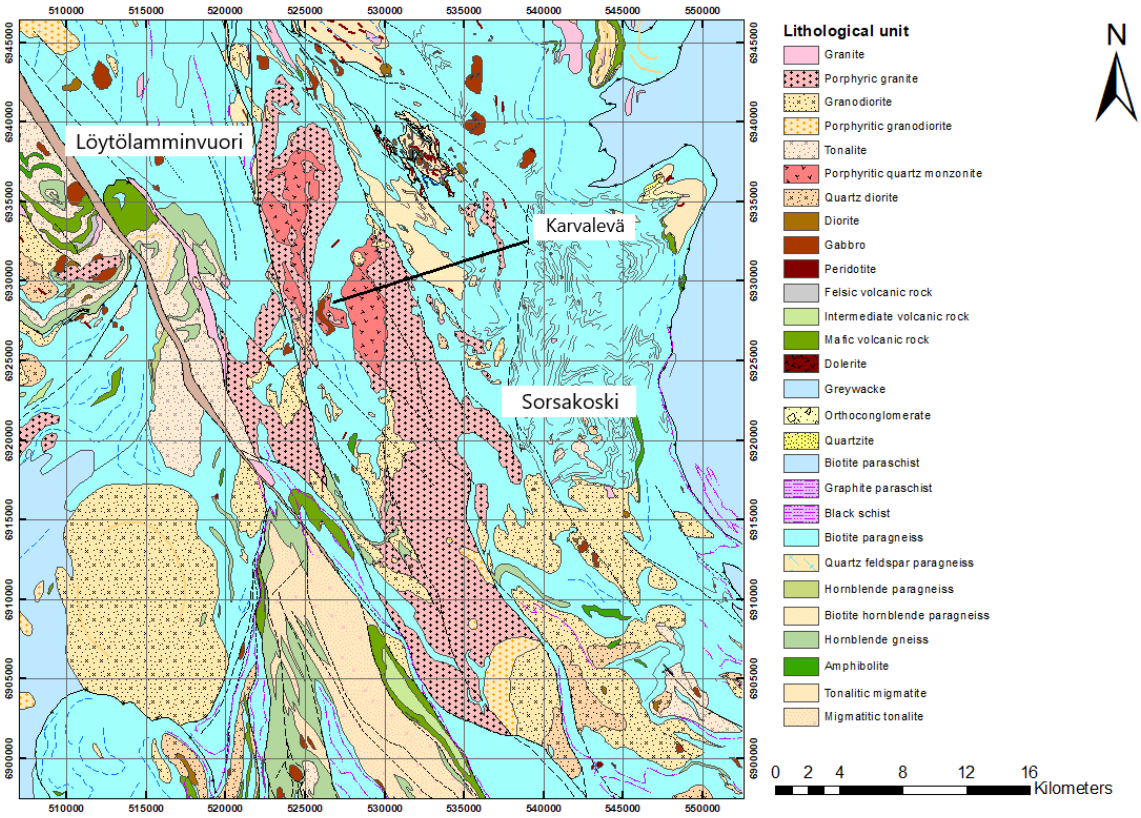

Figure 7. Bedrock map of the area and the three intrusions, Löytölamminvuori on the left, Sorsakoski on the right and Karvalevä in the middle. Bedrock map modified from Digital bedrock map of Finland (DigiKP).

5.1. Löytölamminvuori and Sorsakoski intrusions

The felsic intrusions of Löytölamminvuori and Sorsakoski (Fig. 7.) are so similar that they are considered together in this section. The Löytölamminvuori intrusion is the north-western one, approximately 20 x 5 km in size and grades in composition from inner quartz-monzonite phases to granite in the remainder of the intrusion. The Sorsakoski intrusion is the larger, south-western one with the size of approximately 30 x 5 km. It grades in composition from a small, northern quartz-monzonite phase to a granite in the

remainder of the intrusion. The rocks of both intrusions are generally non-foliated alkali feldspar porphyritic granites (Fig. 8.) and quartz-monzonites which at times show rapakivi-like ovoid-texture (Fig. 9.). Some even-grained variants (Fig. 12.) are found and the samples near the major shears show mylonitization.

Some inclusions of the surrounding rocks can be observed on the outcrops - mainly tonalites, granodiorites and paragneisses. The main minerals of the granite and quartz-monzonite phases are alkali feldspar, quartz, plagioclase, and biotite±hornblende and in the quartz-monzonite phases also ortho- and clinopyroxene. In the granite phases the alkali feldspar phenocrysts are euhedral to subhedral and compose generally 20-30% of the rocks, at times over 50%. Sometimes the phenocrysts are surrounded by thin plagioclase rims. The groundmass grain size is from 0.3 mm to 1 mm and the diameter of the alkali feldspar phenocrysts varies from 10 mm up to 40 mm. The mafic minerals are biotite and in lesser amounts hornblende. In a few granite samples garnet can be found, especially in the samples taken near the paragneiss inclusions. The quartz-monzonite phases are also alkali feldspar porphyritic and the amount of the phenocrysts is the same as in the granite phases. The difference is in the mafic minerals which in addition to biotite and hornblende, also include ortho- and clinopyroxene.

Figure 8. A typical porphyritic granite from Sorsakoski intrusion (PIM$-2018-51.1) with large alkali-feldspar crystals. Mafic silicates as interstitial grains. Diameter of the coin 2 cm.

Figure 9. A quartz-monzonite (PIM$-2018-49.1) from Sorsakoski intrusion. The outcrop exhibits same kind of porphyritic texture as the granite site with large alkali-feldspar crystals. Diameter of the coin 2 cm.

Figure 10. Granite site from the Löytölamminvuori intrusion (PIM$-2018-62.1). The grain size is a bit finer in this locality compared to Sorsakoski intrusion. Diameter of the coin 2 cm.

Figure 11. PIM$-2018-63.1 sample site of a quartz-monzonite from the Löytölamminvuori intrusion. Sample is porphyritic, but the alkali-feldspar grains are not as prominent as in the Sorsakoski intrusion. An slight orientation can be seen on the alkali-feldspars. Diameter of the coin 2 cm.

Figure 12. An example of the fine-grained variation from the Löytölamminvuori intrusion, a monzonite (PIM$-2018-65.1). Length of the compass is 12 cm.

5.2. Karvalevä intrusion

Karvalevä is a small, round intrusion located between Löytölamminvuori and Sorsakoski intrusions (Fig. 13.). This intrusion is compositionally heterogenous ranging from granite (Fig. 14.) to diorite (Fig. 16.), the majority being quartz-monzonite (Fig. 15.) with a small patch of granite and a diorite section cutting in middle in the north-south direction.

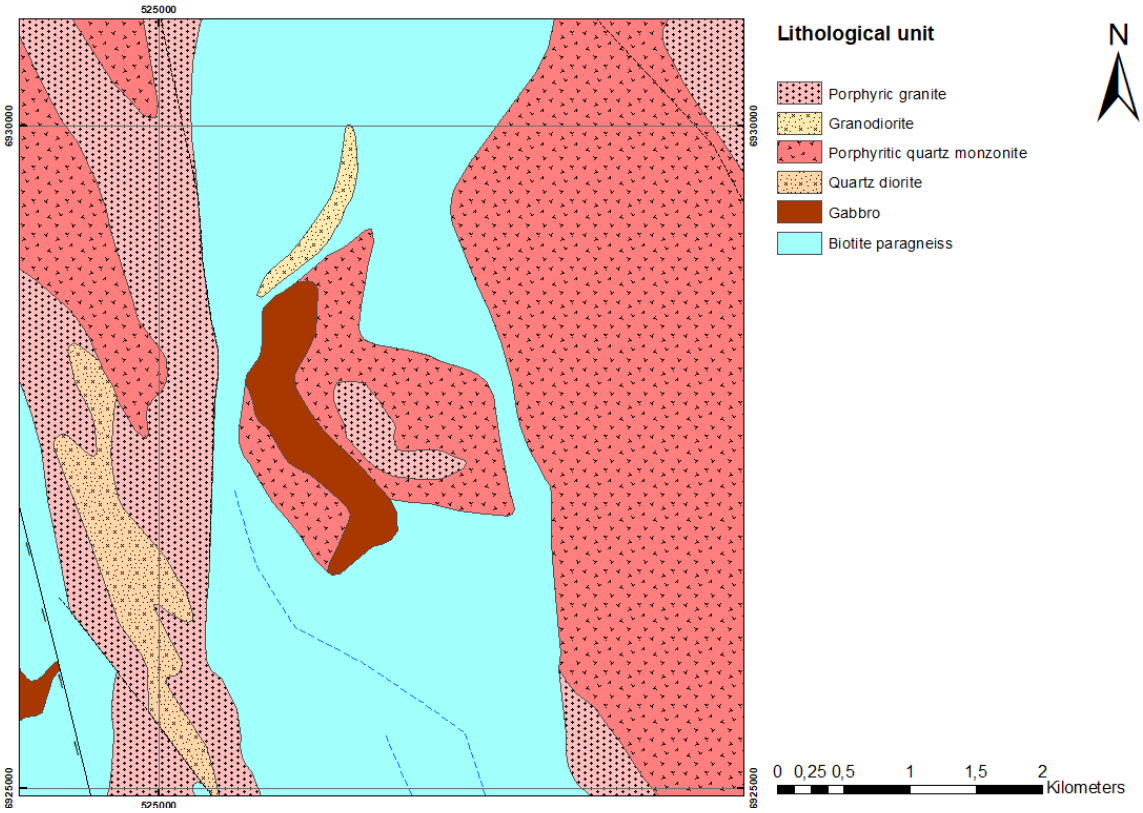

Figure 13. Bedrock map of Karvalevä intrusion, located between the more felsic intrusions of Löytölamminvuori and Sorsakoski. Bedrock map modified from Digital bedrock map of Finland (DigiKP).

The Karvalevä intrusion is approximately 2,5 x 2,5 km in size, with mafic phases primarily cutting the granitoid phase, although the two show some mixing on the boundaries. The main minerals in the granitoid phases are alkali feldspar, plagioclase, quartz with mafic silicates biotite, hornblende and ortho- and clinopyroxene. The main minerals in the mafic phases are plagioclase, biotite, hornblende and ortho- and clinopyroxene, with a more minor quartz and alkali-feldspar. The accessory minerals are zircon, monazite, chlorite, and apatite. The groundmass grain size varies from fine to medium. The felsic parts have similar texture compared to Löytölamminvuori and

Sorsakoski intrusions, with large alkali-feldspar phenocrysts (diameter 10mm to 30mm), some with plagioclase rims. The mafic phases have in general finer grainsize and show sometimes cumulus-texture.

Figure 14. A porphyritic granite from the Karvalevä intrusion (PIM$-2018-66.1). Porphyritic texture with larger alkali-feldspar grains and finer groundmass. Diameter of the coin 2 cm.

Figure 15. PIM$-2018-59.1 is a quartz-monzonite from the Karvalevä intrusion with large alkali-feldspar grain on the upper left corner. The mafic silicates are mostly as finer grains in the groundmass. Diameter of the coin 2cm.

Figure 16. A diorite sample from the Karvalevä intrusion (PIM$-2018-58.1). The grain size is considerably finer than in the more felsic sites. Diameter of the coin 2 cm.

6. PETROGRAPHY

6.1. Löytölamminvuori intrusion

6.1.1. General

A total of 16 thin sections from the Löytölamminvuori intrusion were studied, 8 from the quartz-monzonite phase and 8 from the granite phase. Most of the samples are porphyritic and have approximately the same amount of alkali feldspar and plagioclase in the groundmass. The alkali feldspar crystals are in general larger than other minerals and some have plagioclase rims around them, showing rapakivi-like textures. Quartz occurs both as smaller smush and as large crystals. The mafic minerals are in the groundmass and in addition to biotite, hornblende can be found in approximately half of the samples, in both quartz-monzonite and the granite phase. Both clino- and orthopyroxene are present in the quartz-monzonite phase but are absent in the granite part of the intrusion.

6.1.2. Main minerals

The main minerals are alkali feldspar, plagioclase, quartz, biotite, hornblende and, in the quartz-monzonite, also pyroxenes and all in all higher amount of biotite and hornblende. The alkali feldspar is in most samples orthoclase, except three samples which have microcline and one which has microperthite. The alkali feldspar is found as 0.5 mm to 1 mm in groundmass up to large megacrysts, usually euhedral grains that sometimes show growth-zoning. Alkali feldspars have small inclusions of other minerals, usually plagioclase and quartz. Orthoclase appears to be turning to microperthite in some of the samples, for example PIM$-2018-63.1 (Fig. 18.). Plagioclase occurs as 0.3 mm to 1 mm euhedral to subhedral grains, sometimes at the borders of the alkali feldspars with quartz forming rapakivi-texture. The crystals show almost always twinning and sometimes growth-zoning. Alkali feldspar and plagioclase have some intergrowths on their mutual grain boundaries. Both feldspars are often somewhat sericitized. Quartz is found as large undulating crystals and also as small grains on the borders of the feldspars where it shows intergrowth textures. It can also be found as totally recrystallized metamorphic small grains in-between larger plagioclase and feldspar grains. Biotite occurs both as primary, brown to light green flakes and as secondary darker brown crystals of medium grain size. The groundmass biotite is found as small flakes between larger grains, as interlocking mush with quartz. Hornblende is mostly subhedral, fractures crystals among the groundmass, and as pseudomorph where they have turned into biotite. Both biotite and hornblende are in some samples altered almost totally to chlorite. Ortho- and clinopyroxene are rounded and greatly fractured and have grain size varying from small to medium.

6.1.3. Accessory minerals

The accessory minerals of the Löytölamminvuori intrusion include apatite, zircon, rutile, tourmaline, titanite, epidote, chlorite, sericite, monazite, cummingtonite, and opaques. Apatite and zircon occur in almost all of the samples as small crystals. Rutile and tourmaline in one sample both. Chlorite occurs as alteration product of biotite and hornblende and sericite in feldspars. Cummingtonite is the alteration product of hornblende. Monazite is usually inside biotite as small clear fragments. Garnet is found in two granite samples, in N98302736 and PIM$-2018-62.1 (Fig. 17.), in the latter as 1 – 2 mm crystals within a rock fragment that appears to be foreign. The rock fragment is

from a fine and even-grained rock which consist of quartz and feldspars, which could be an assimilated fragment of the surrounding paragneiss.

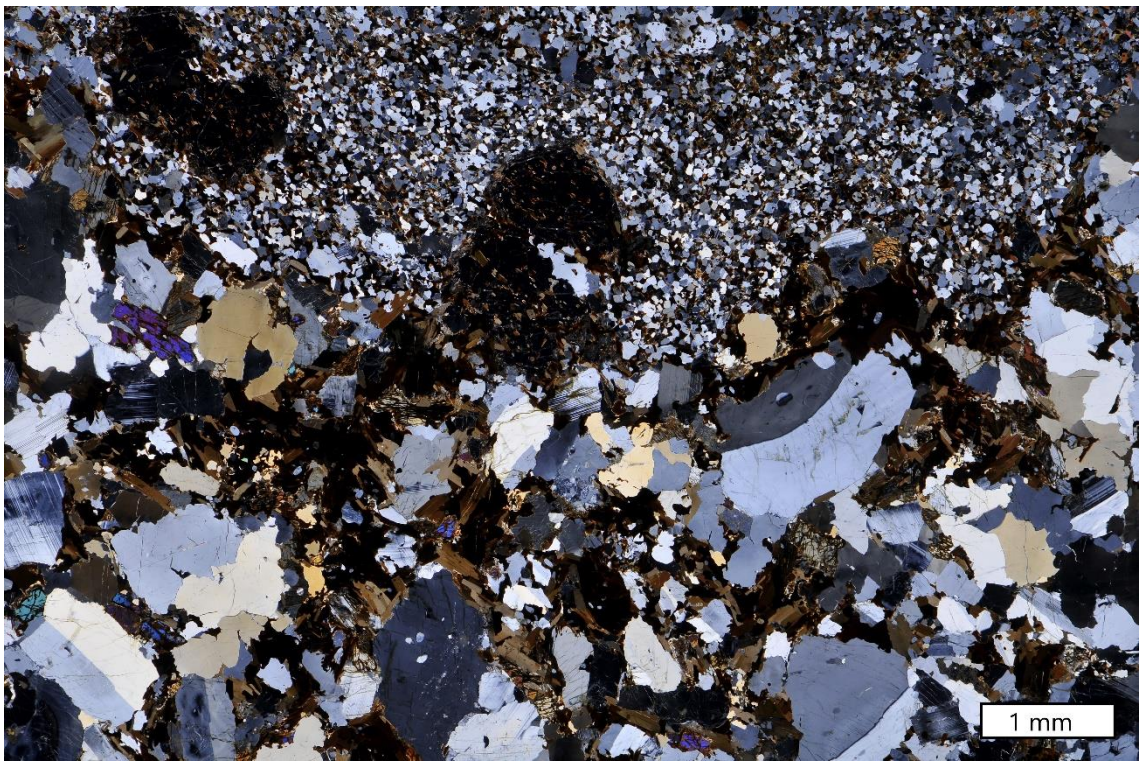

Figure 17. A thin section of a granite sample PIM$-2018-62.1 from the Löytölamminvuori intrusion. The sample is medium to coarse grained porphyritic granite. This sample includes garnet grains, which can be seen in the upper part as inclusions in the fine-grained rock fragment. Photomicrograph taken under crossed polarized light. Photo: Tarja Neuvonen/GTK

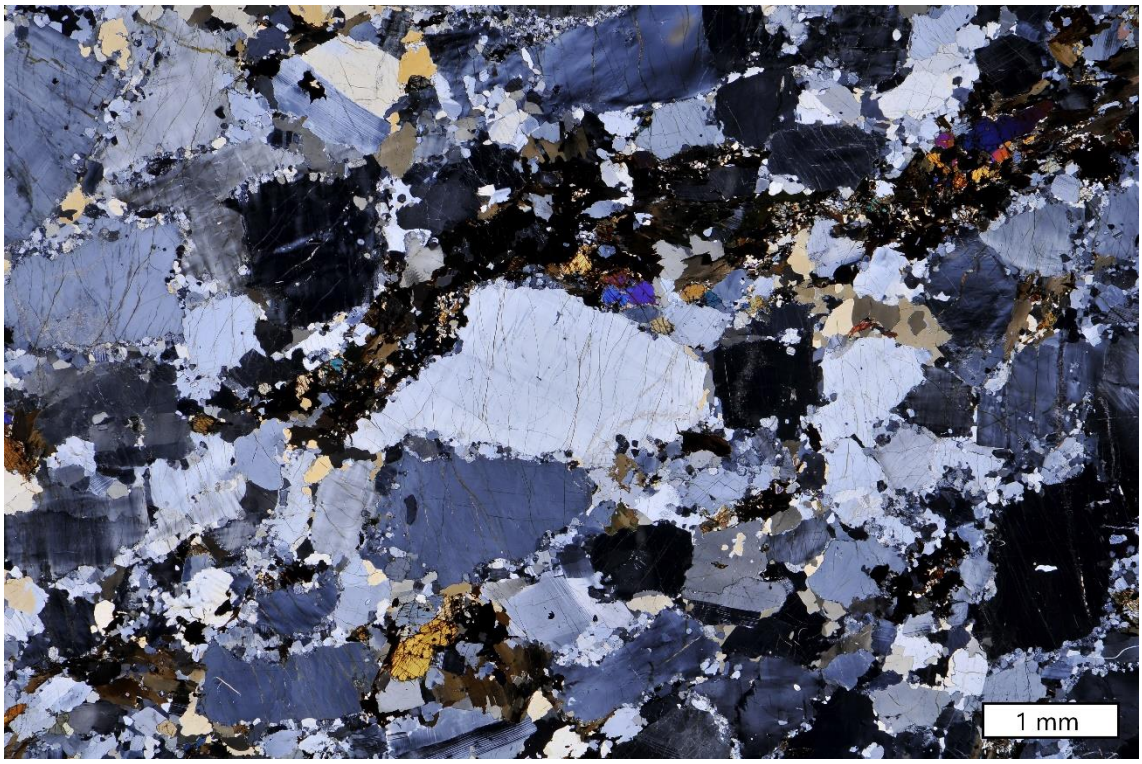

Figure 18. A quartz-monzonite sample from the Löytölamminvuori intrusion (PIM$-2018-63.1). A groundmass sample from porphyritic rock with larger alkali-feldspar crystals, some showing microperthitic structures. The mafic silicates are in the groundmass as fine-grained smush. Photomicrograph taken under crossed polarized light. Photo: Tarja Neuvonen/GTK

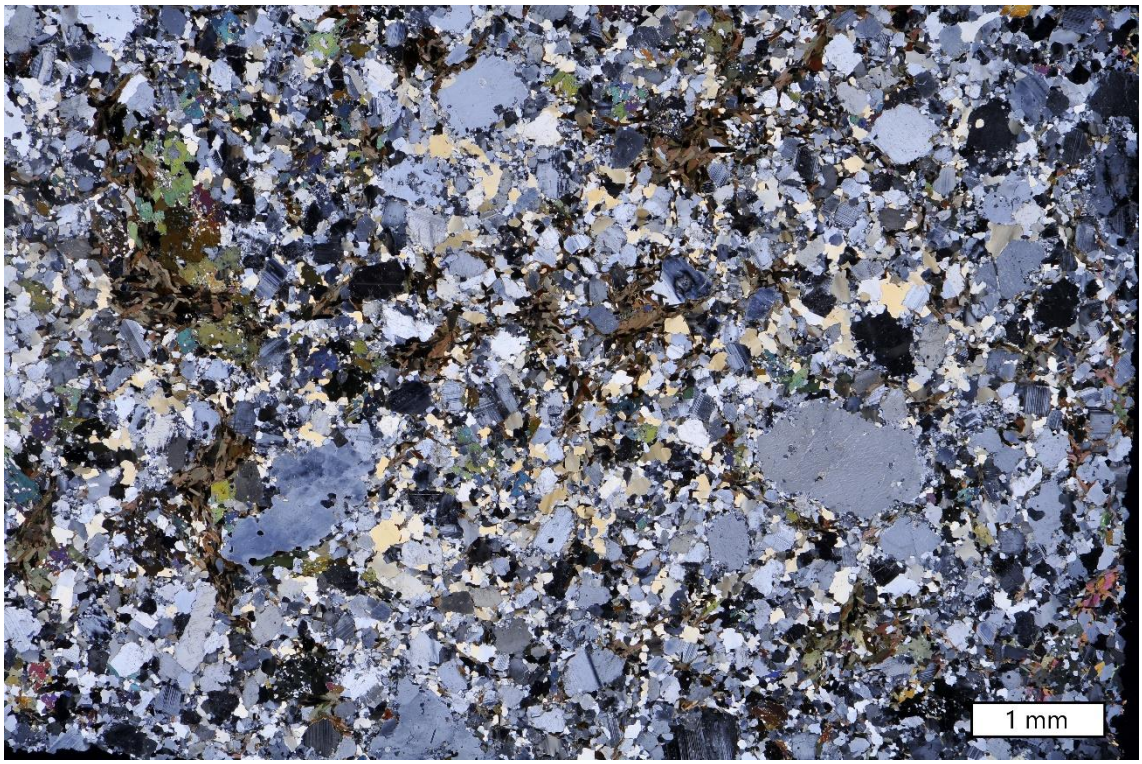

Figure 19. PIM$-2018-64.1is a quartz-monzonite, example of more fine-grained variation. Sample is quite even-grained and has an abundance of hornblende, which is strongly chloritized. Photomicrograph taken under crossed polarized light. Photo: Tarja Neuvonen/GTK

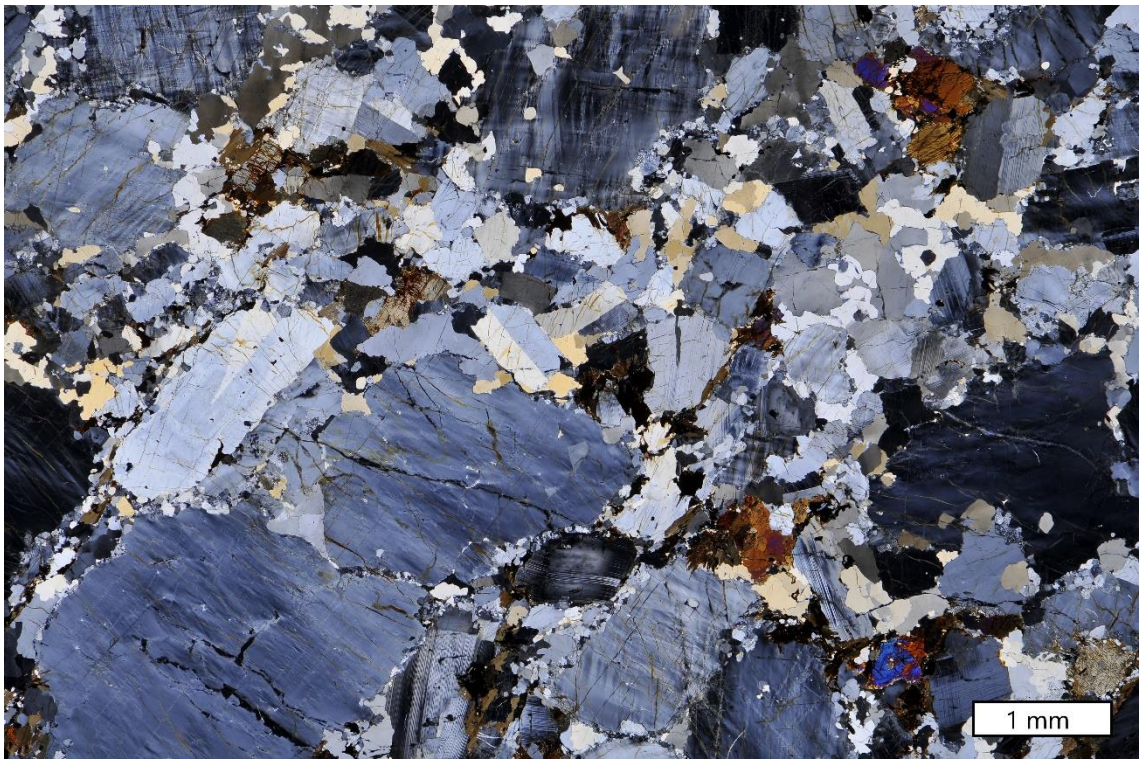

Figure 20. A porphyritic monzonite sample from Löytölamminvuori intrusion (PIM$-2018-65.1). Contains large alkali-feldspar crystals which sometimes have plagioclase and quartz rims around them. Quartz and plagioclase as smaller grains. Photomicrograph taken under crossed polarized light. Photo: Tarja Neuvonen/GTK

6.2. Sorsakoski intrusion

6.2.1. General

The petrographic features of the granite phase of Sorsakoski intrusion have been studied from 53 thin sections. Six of the samples are from dykes, one from a sedimentary rock and the rest from plutonic rocks. Four samples are from the quartz-monzonite phase in the northern part and the rest from the granite phase. The granite samples are almost all porphyritic with large alkali feldspar crystals and have protoclastic texture. Plagioclase and K-felspar occur approximately in equal amounts and some samples have rapakivi-texture with plagioclase rims around the K-felspar crystals. Quartz is found as larger crystal as well as smaller grains, and mafic silicates biotite and occasional hornblende in groundmass. The quartz-monzonite samples are similar to the granite samples with the exception of the presence of orthopyroxene.

6.2.2. Main minerals

The main minerals of Sorsakoski intrusion are quartz, alkali feldspar, plagioclase and biotite, and in a bit lesser amounts hornblende, and orthopyroxene in the quartz-monzonite. Both orthoclase and microcline occur as the alkali feldspar phase, but compared to the Löytölamminvuori, microcline is more dominant in the Sorsakoski intrusion. Some thin sections also have microperthite in them. The crystals in the groundmass are in general from 0.3 mm to 5 mm, and up to megacrysts, some are clear, and some have exsolution lamellae and are sericitized. Quartz and plagioclase occur as small inclusions in the feldspars and sometimes as rims around the grains forming rapakivi-texture. Plagioclase is in general more broken down than alkali feldspars, have exsolution lamellae and small holes in them. Like alkali feldspars the plagioclase is also sometimes strongly sericitized. The grain size varies from 0.3 mm to 3 mm, and almost all crystals show clear twinning. Quartz is found both as large crystals with clear boundaries and as small-grained metamorphic smush on the grain-boundaries of other minerals where it shows intergrowths with feldspars. Also, large, totally re-crystallized grains occur and some have clear three-point crystal-boundaries. Biotite occurs, similar to Löytölamminvuori, as primary phase as flaky, euhedral crystals and as re-crystallized grains. The grain size varies from medium sized flakes to small mush in the groundmass. The euhedral crystals are usually lighter in color and green-pleochroic and the re-crystallized are dark brown. In some samples biotite has very high interference colors and in some samples shows intergrowths with quartz. Hornblende can be found as cracked crystals, usually as pseudomorphs which have turned into biotite or chlorite. The grain size varies from small grains to medium sized.

6.2.3. Accessory minerals

The accessory minerals include muscovite, zircon, titanite, monazite, apatite, chlorite, sericite, epidote, garnet, carbonate, opaques, and cummingtonite in quartz-monzonite sample L04021013. Muscovite is found in a few samples and it occurs as small, secondary flakes. Zircon and apatite are common in almost all samples as small grain sized crystals. Titanite has small grain size and is common in the granite phase of Sorsakoski intrusion. Chlorite and sericite occur as alteration phases of biotite and hornblende, and feldspars

respectively. Garnet is found in sample N98002532 as fractured grains. Undefined carbonate mineral is found in three samples as small, rounded grains.

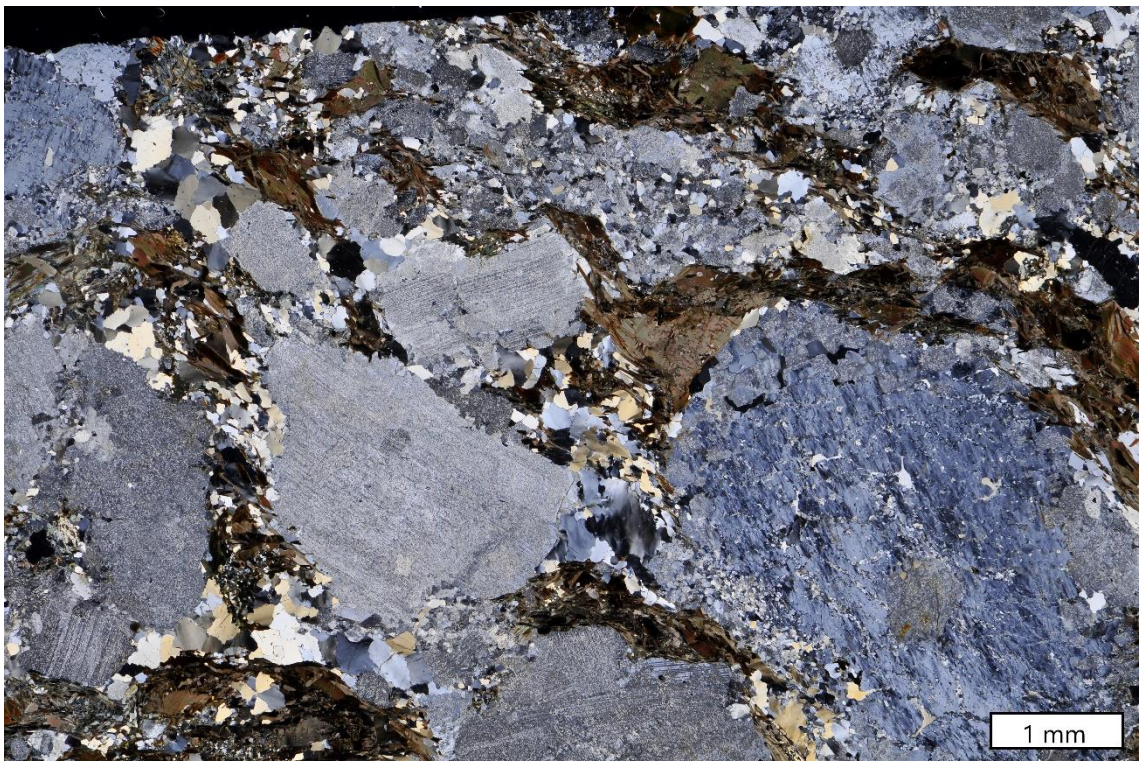

Figure 21. A porphyritic granite sample from Sorsakoski intrusion (PIM$-2018-51.1). Sample consists of large alkali-feldspar crystals, both orthocline and microcline, and interstitial quartz and biotite. Photomicrograph taken under crossed polarized light. Photo: Tarja Neuvonen/GTK

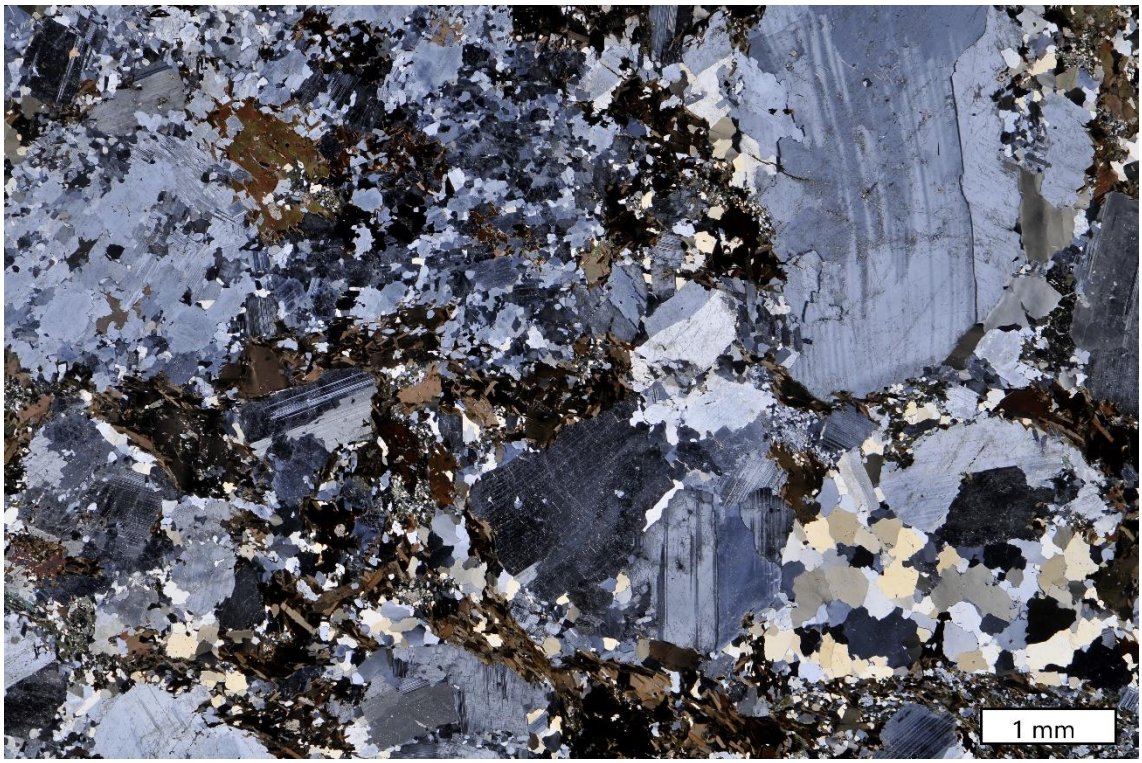

Figure 22. PIM$-2018-52.1 is a porphyritic granite sample, with large alkali-feldspar crystals, sometimes rimmed with plagioclase and quartz. The quartz in this sample shows recrystallization structures and the plagioclase on the upper right corner shows bended lamellae. Photomicrograph taken under crossed polarized light. Photo: Tarja Neuvonen/GTK

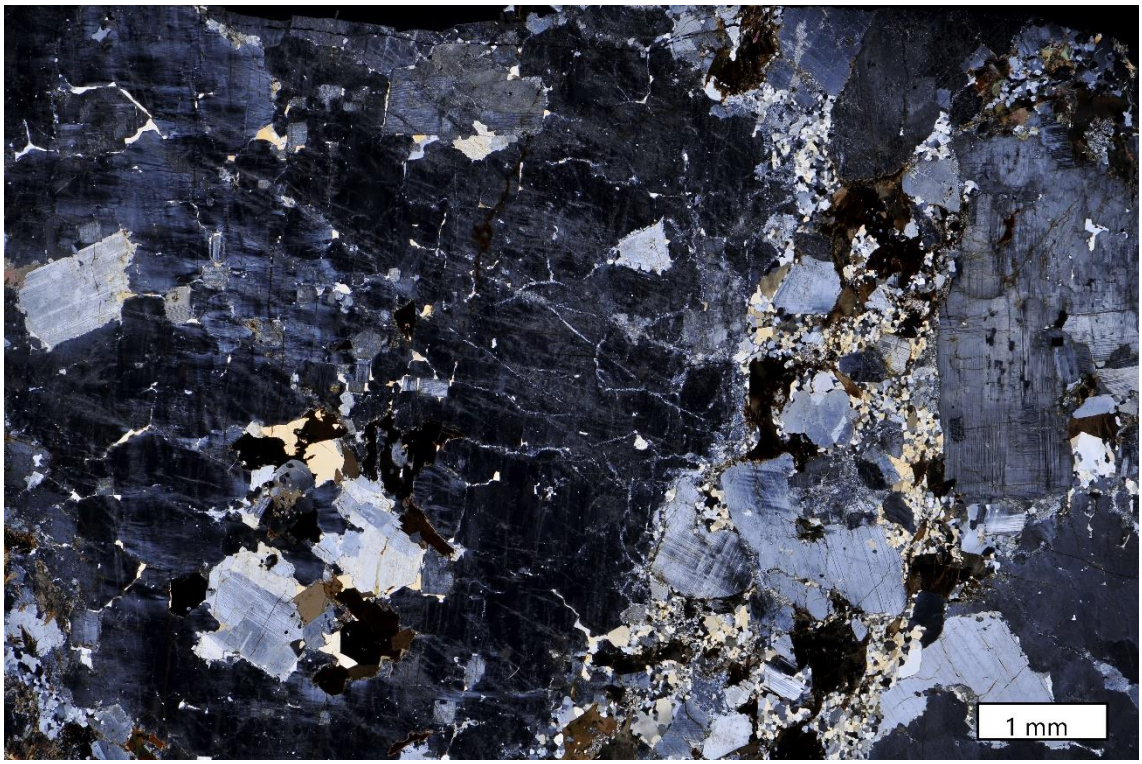

Figure 23. A porphyritic quartz-monzonite from Sorsakoski intrusion (PIM$-2018-49.1). The sample contains large alkali-feldspar crystals (microcline) which have quartz inclusions in them. Plagioclase and mafic silicates are in the groundmass. Photomicrograph taken under crossed-polarized light. Photo: Tarja Neuvonen/GTK

Figure 24. A quartz-monzonite sample from Sorsakoski intrusion (PIM$-2018-49.2). A more medium-grained variation compared to PIM$-2018-49.1. Alkali-feldspar is microcline and appears as larger crystals among the more fine-grained groundmass of mafic silicates. Photomicrograph taken under crossed polarized light. Photo: Tarja Neuvonen/GTK

6.3. Karvalevä intrusion

6.3.1. General

Nine thin sections from the Karvalevä intrusion were studied. The samples show a great variation. The samples from the granite and quartz-monzonite parts of the intrusion are similar to samples from Löytölamminvuori and Sorsakoski intrusions, with large alkali-feldspar grains, considerably smaller plagioclase crystals, and varying quartz-grainsize. In the more mafic samples, the alkali feldspar and quartz occur as smaller amounts and plagioclase is more dominant. Almost all of the samples have orthopyroxene and half have also clinopyroxene. Biotite is found in all of the samples. The grain size is finer in the gabbro phases than in the more felsic samples. A few mafic samples have cumulus-texture of plagioclase and pyroxenes. Two of the samples are greenstones and consist of plagioclase, biotite and chlorite smush.

6.3.2. Main minerals

The main minerals are plagioclase, alkali feldspar, quartz, biotite and both clino- and orthopyroxene. Alkali feldspars, when present, are, in general, orthoclase and can be found as euhedral crystals in groundmass in a few samples. The only sample with microcline as the alkali feldspar phase is PIM$-2018-54.1 (Fig. 28.). Plagioclase is more dominant in the mafic samples and occurs as stick-like crystals and forms cumulus-texture with pyroxenes. In samples PIM$-2018-55.1 and PIM$-2018-55.2 (Fig. 30.) can be seen a clear orientation in the minerals. Biotite is found in all of the samples and is often chloritized.

6.3.3. Accessory minerals

The accessory minerals in the Karvalevä intrusion are monazite, zircon, apatite, chlorite, garnet, and opaques. Apatite, zircon, and monazite are found in the more felsic samples of the intrusion and chlorite in the more mafic parts. Garnet is found in one sample, PIM$-2018-54.1 (Fig. 28.).

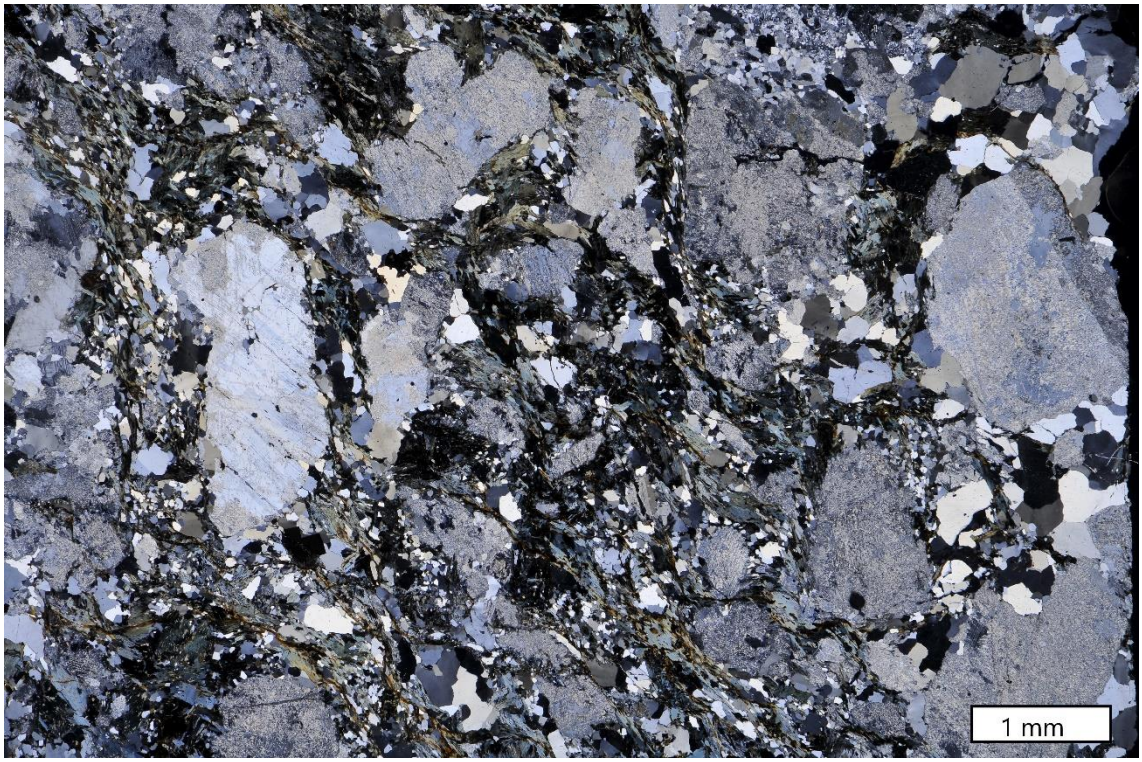

Figure 25. A porphyritic granite sample from the Karvalevä intrusion (PIM$-2018-57.1). The sample has large alkali-feldspar crystals (orthoclase) and quartz and plagioclase as smaller grains. Mafic silicates occur in the groundmass and biotite is chloritized. A slight orientation can be seen in the thin section. Photomicrograph taken under crossed polarized light. Photo: Tarja Neuvonen/GTK

Figure 26. A fine-grained diorite sample from Karvalevä intrusion (PIM$-2018-67.1), which shows cumulus texture with plagioclase as cumulus phase and pyroxenes as intercumulus. Pyroxene is locally been replaced by biotite and chlorite. Photomicrograph taken under crossed polarized light. Photo: Tarja Neuvonen/GTK

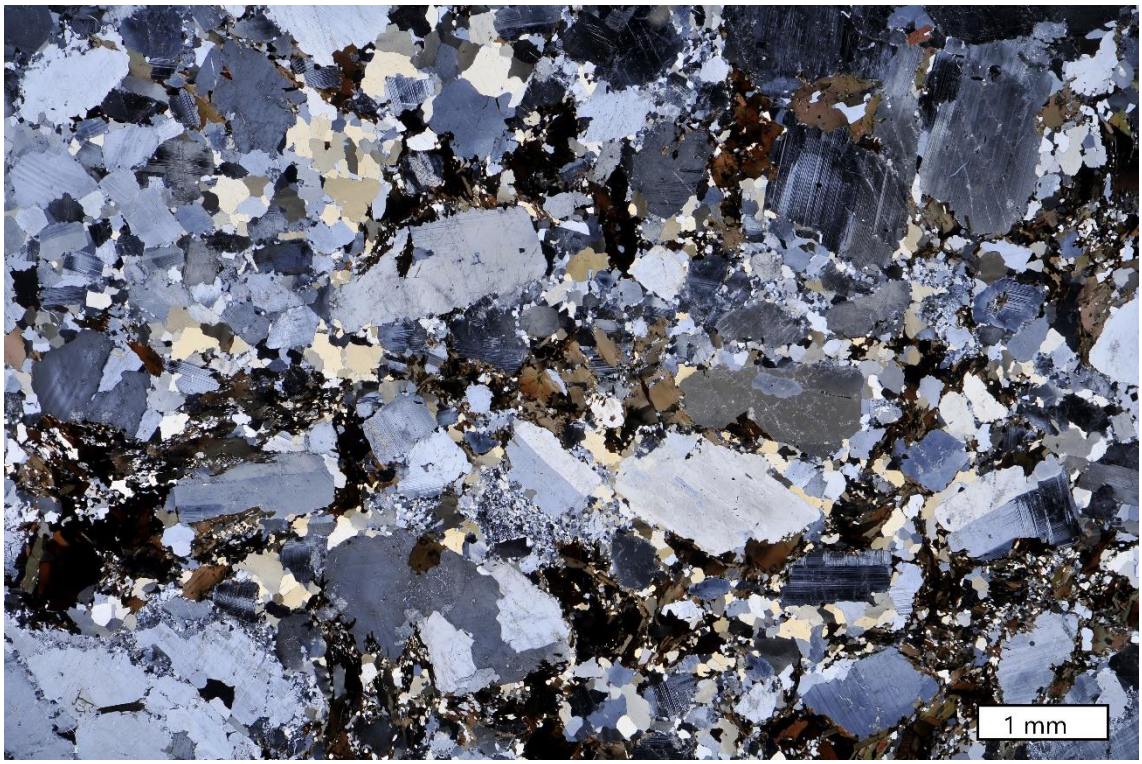

Figure 27. A porphyritic variation of quartz-monzonite in the Karvalevä intrusion (PIM$-2018.59.1). Quite similar to Sorsakoski and Löytölamminvuori samples. Alkali-feldspar occurs as larger crystals, plagioclase and quartz as bit smaller grains and mafic silicates in the groundmass. Two different generations of biotite can be recognized. Photomicrograph taken under crossed-polarized light. Photo: Tarja Neuvonen/GTK

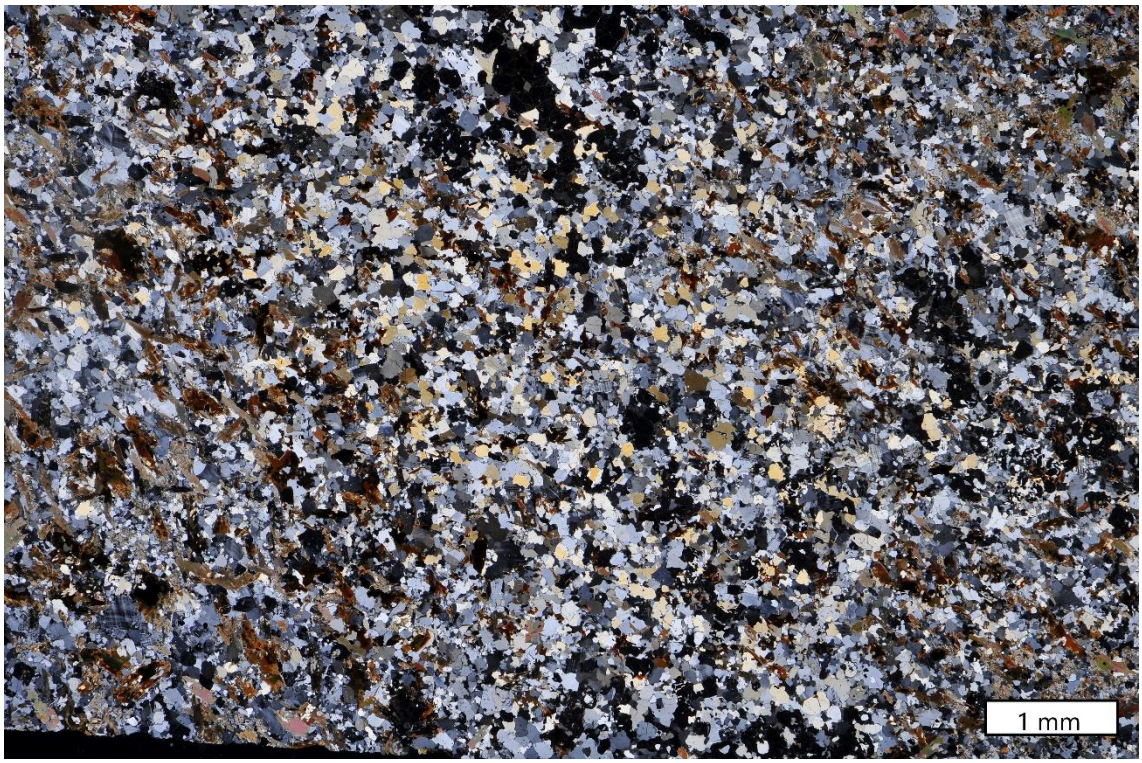

Figure 28. Monzonite sample PIM$-2018-54.1 is a very fine-grained variation in the Karvalevä intrusion. The alkali-feldspar is microcline and the sample has no visible orientation. Photomicrograph taken under crossed polarized light. Photo: Tarja Neuvonen/GTK

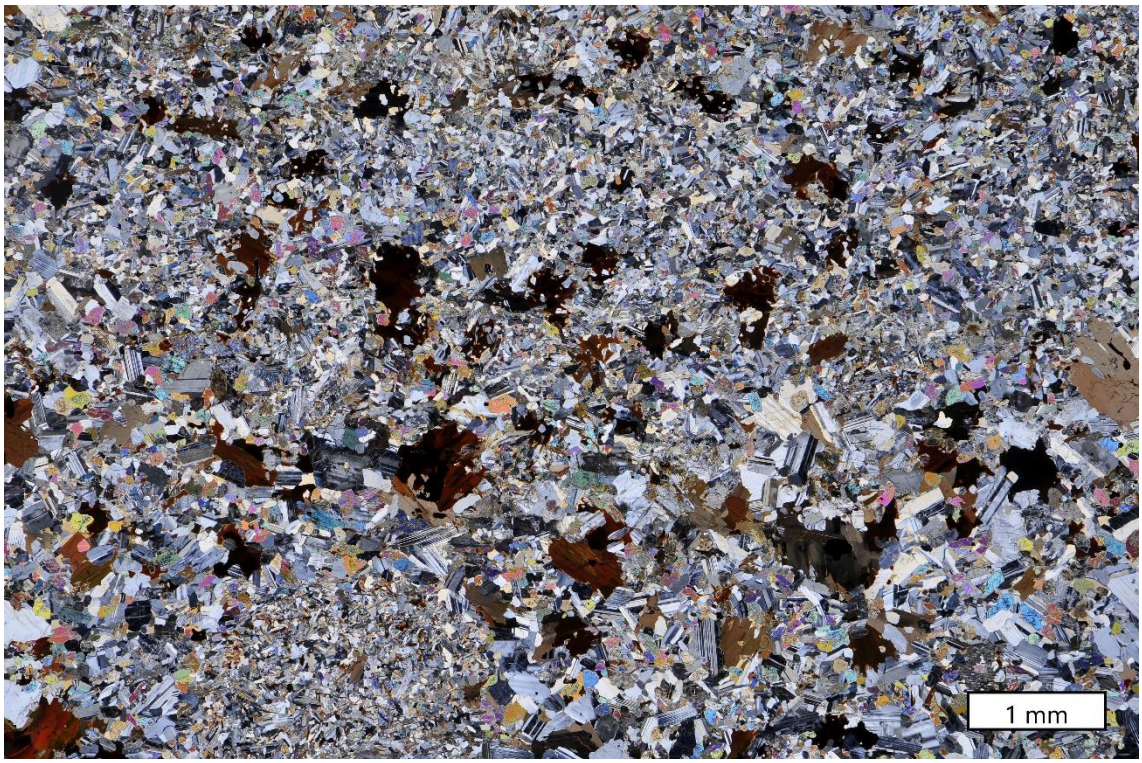

Figure 29. A diorite sample from the Karvalevä intrusion represents the more mafic end in the rock-type spectrum (PIM$-2018-58.1). It contains plagioclase, biotite and both ortho- and clinopyroxene. The grain size varies from medium to fine-grained and sample has a cumulus texture, with pyroxenes as cumulus phase and plagioclase as intercumulus. Photomicrograph taken under crossed polarized light. Photo: Tarja Neuvonen/GTK

Figure 30. A diabase sample from the Karvalevä intrusion (PIM$-2018-55.2). The rock is fine-grained plagioclase and pyroxene rock displaying weak orientation. Chloritization is strong. Photomicrograph taken under crossed polarized light. Photo: Tarja Neuvonen/GTK

7. WHOLE-ROCK GEOCHEMISTRY

7.1. Löytölamminvuori intrusion

7.1.1. Major element composition

The average SiO_2 content of the Löytölamminvuori intrusion is 63.7 wt%, the lowest being 56.5 wt% and the highest 69.2 wt%. The average A/CNK of the samples is 1.49, with values between 1.34 – 1.64. Compared to the post-kinematic plutons of the CFGC the A/CNK values of the Löytölamminvuori intrusion are slightly higher, and the samples are peraluminous (Fig. 31.c). The Al_2O_3 content is quite uniform from 14.4 wt% to 17.2 wt%, the average being 15.7 wt%. The Al_2O_3 content of Löytölamminvuori resembles most that of the Type 3 post-kinematic plutons. The total alkali content ($Na_2O + K_2O$) of the intrusion is on average 7.61 wt% and shows correlation with the SiO_2 content. The K_2O range is quite large (from 1.94 wt% to 6.57 wt%) with the average at 4.35 wt%. The

variation can be due to the porphyritic nature of the rocks, when the amount of alkali-feldspar in the sample varies greatly. The K_2O content correlates with the SiO_2 content and the samples belong to the high-K calc-alkaline and the shoshonite series (Fig. 36.). The values are quite similar to the post-kinematic plutons, mostly to Type 3b. The FeO/MgO ratio is 5.48 and the average FeO_t is 6.70 wt% and MgO is 1.39 wt%. The contents correlate with the SiO_2 and all the samples plot in the ferroan group (Fig. 31.a). The ratio resembles that of the type 3b plutons but the FeO_t is on average higher in the Sorsakoski area intrusions than in the post-kinematic series. The CaO content correlates well with the silica content and the average CaO is 3.00 wt% and resembles that of the type 3 plutons.

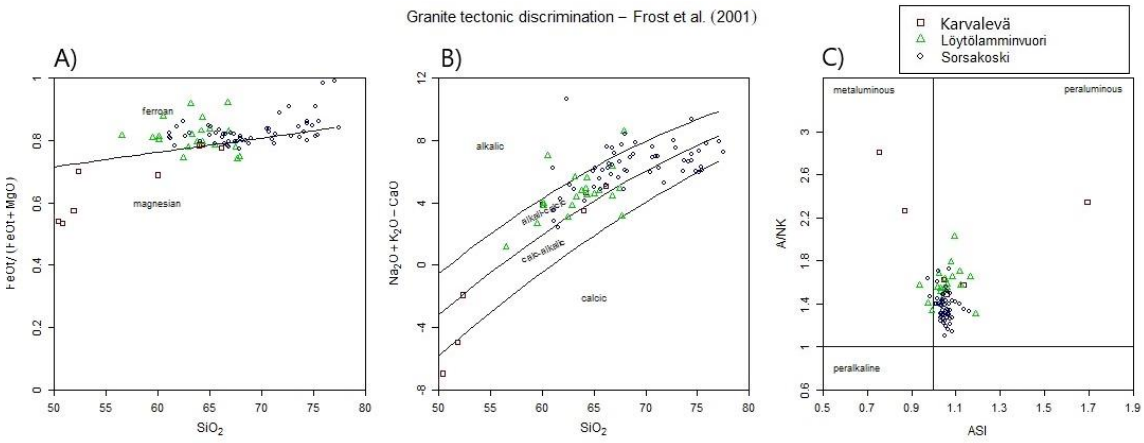

Figure 31. Tectonic discrimination diagrams for Löytölamminvuori, Sorsakoski and Karvalevä intrusions, using the Fe-number vs. SiO2 (A), MALI vs. SiO2 (B), and ASI vs. A/NK (C). The samples are mostly ferroan, alkali-calcic and peraluminous.

7.1.2. Trace element composition

The average Ba content of the Löytölamminvuori intrusion is 1403 ppm, with the highest value of 2774 ppm and the lowest 757 ppm, the lowest value found in the sample with the least SiO_2. The values are similar to the post-kinematic suite of CFGC. The average Zr content is 451 ppm and is similar to the post-kinematic plutons. The average Rb content is 117 ppm and it is slightly lower than in the Sorsakoski intrusion and resembles that of the Type 3 plutons. The Sr content of 282 ppm in contrast is higher in Löytölamminvuori and also similar to the type 3 intrusions. The Rb/Ba ratio is on average 0.08 and the Rb/Sr ratio is 0.41, both being lower than those measured from Sorsakoski intrusion. The ratios are similar to the type 3a margin and type 3b plutons, as in the phases which have pyroxenes in them.

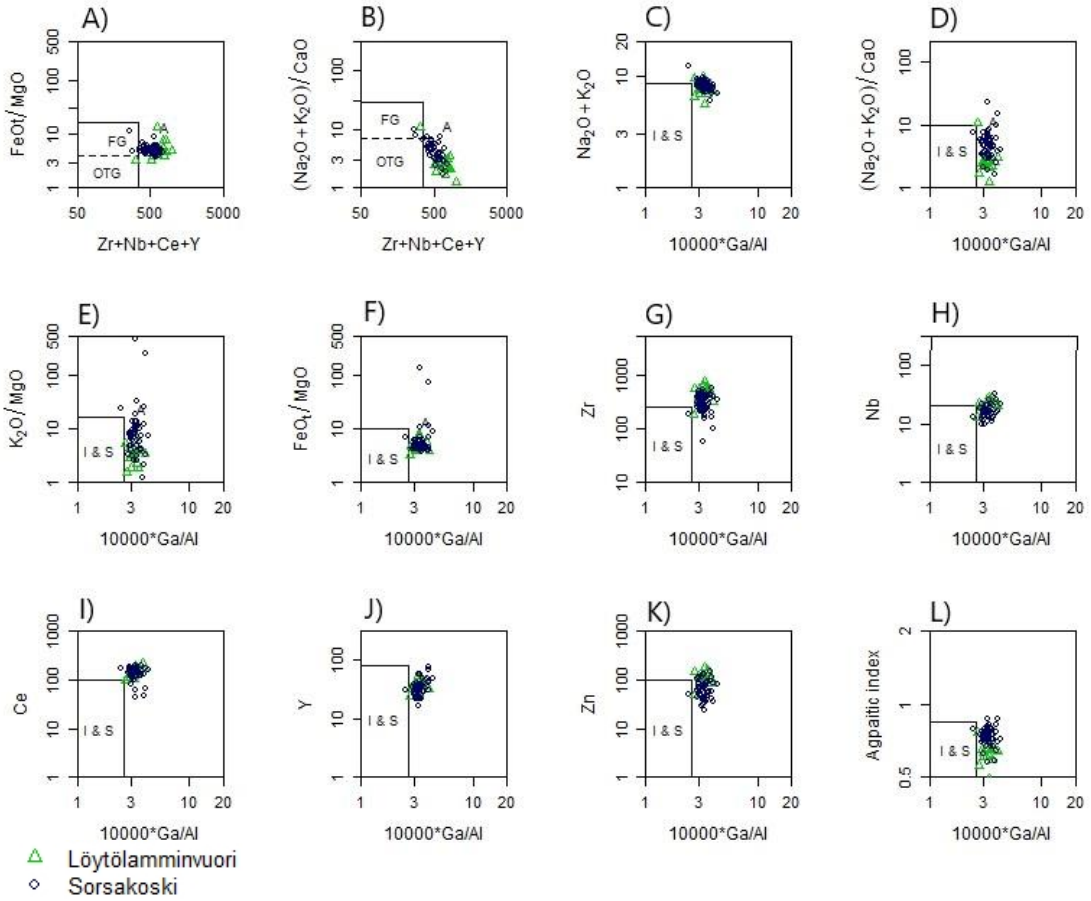

Figure 32. Distinguishing diagrams for A-type granitoids, (after Whalen 1987) for Löytölamminvuori and Sorsakoski intrusions. Distinguishing parameters include: FeO_t/MgO vs. Zr+Nb+Ce+Y (A), $(Na_2O+K_2O)/CaO$ vs. Zr+Nb+Ce+Y (B), Na_2O+K_2O vs. 10000*Ga/Al (C), $(Na_2O+K_2O)/CaO$ vs. 10000*Ga/Al (D), K_2O/MgO vs. 10000*Ga/Al (E), FeO_t/MgO vs. 10000*Ga/Al (F), Zr vs. 10000*Ga/Al (G), Nb vs. 10000*Ga/Al (H), Ce vs. 10000*Ga/Al (I), Y vs. 10000*Ga/Al (J), Zn vs. 10000*Ga/Al (K), and Agpaitic index vs. 10000*Ga/Al (L).

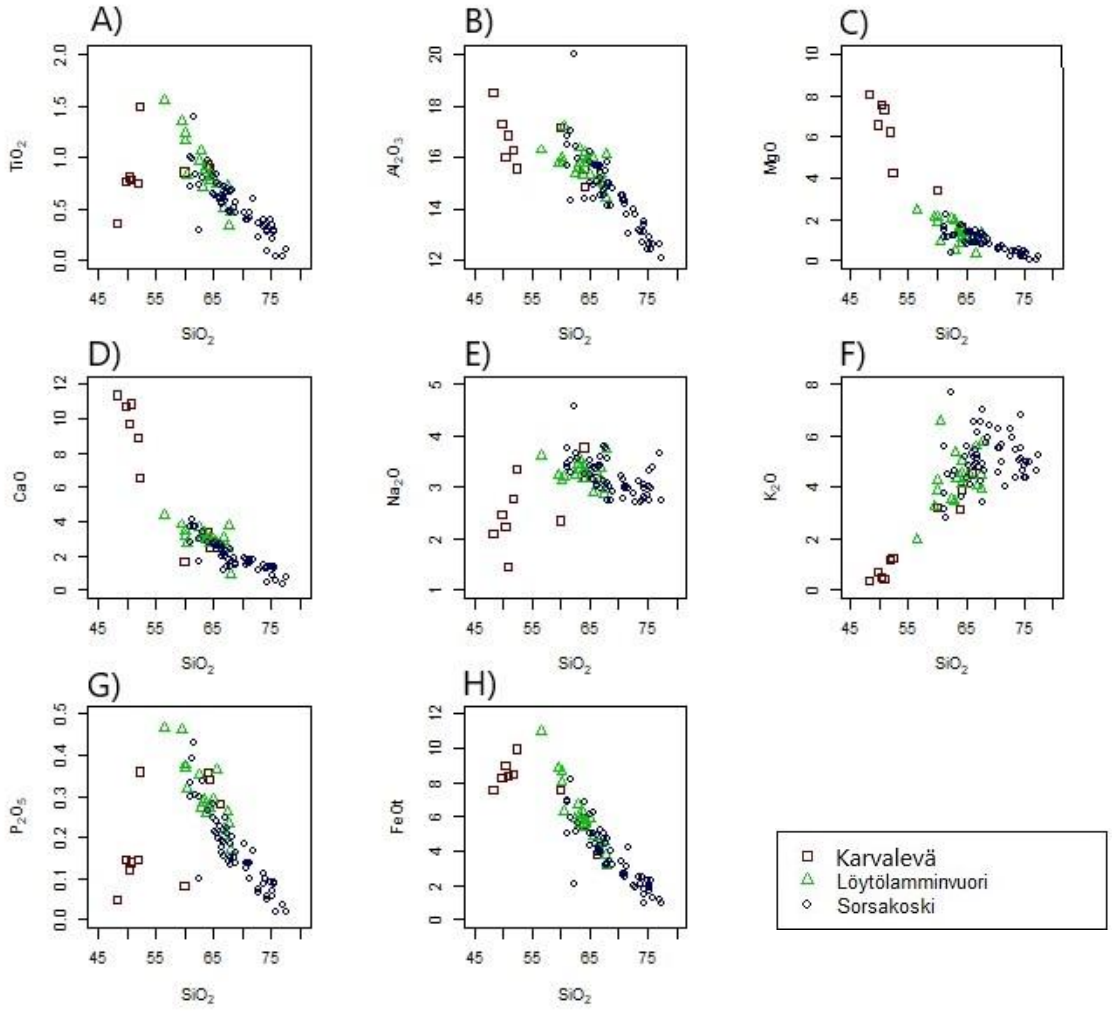

Figure 33. Multiple plots with SiO_2 vs. major elements for all three intrusions. Plots include: TiO_2 vs. SiO_2 (A), Al_2O_3 vs. SiO_2 (B), MgO vs. SiO_2 (C), CaO vs. SiO_2 (D), Na_2O vs. SiO_2 (E), K_2O vs. SiO_2 (F), P_2O_2 vs. SiO_2 (G), and FeO_t vs. SiO_2 (H). A clear continuous trend can be seen from Sorsakoski and Löytölamminvuori intrusion from granitoid phases to the quartz-monzonite phases. The more mafic samples from Karvalevä deviate somewhat from the other intrusions, while the felsic samples plot in the same group as other intrusions.

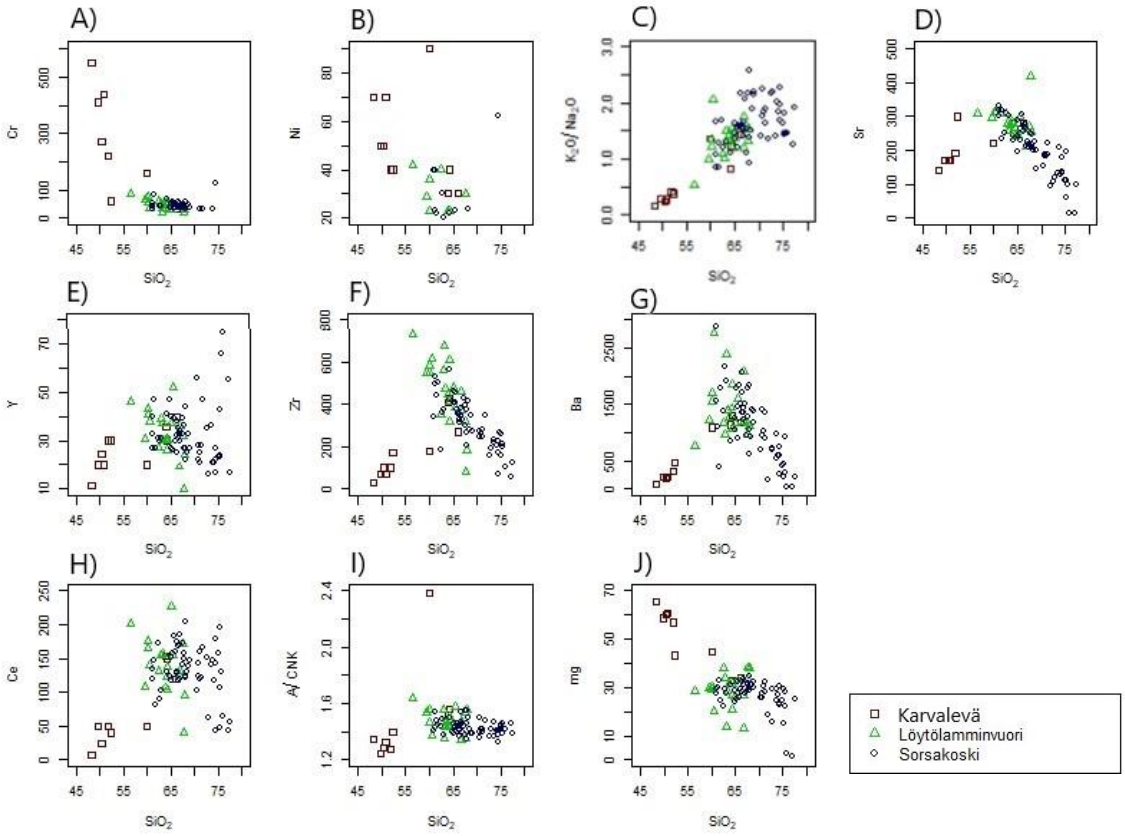

Figure 34. Multiple plots with SiO_2 vs. minor elements with all three intrusions. Plots include: Cr vs. SiO_2 (A), Ni vs. SiO_2 (B), K_2O/Na_2O vs. SiO_2 (C), Sr vs. SiO_2 (D), Y vs. SiO_2 (E), Zr vs. SiO_2 (F), Ba vs. SiO_2 (G), Ca vs. SiO_2 (H), A/CNK vs. SiO_2 (I), and Mg vs. SiO_2 (J). As with major elements, trace elements also show continuous trend in Löytölamminvuori and Sorsakoski. The more felsic samples from Karvalevä plot in the same group as Löytölamminvuori and Sorsakoski, the mafic samples show a differing trend.

7.2. Sorsakoski intrusion

7.2.1. Major element composition

The SiO_2 range of the Sorsakoski intrusion varies quite greatly from 61.1 wt% to 77.1 wt%, the average being 68.9 wt%, and thus is slightly higher than in Löytölamminvuori. The SiO_2 content of the intrusion resembles that of the Type 2 and 3a plutons. The samples are slightly peraluminous (Fig. 31.c) and show A/CNK values over 1.0 the average being 1.43 and lowest and highest 1.35 and 1.58 respectively. Similar to Löytölamminvuori, the A/CNK values are considerably higher than in the post-kinematic pluntons. The Al_2O_3 content of the rocks is on average 14.58 wt%, ranging from 12.4 wt% to as high as 20.0 wt% on one sample and correlates with the type 3a plutons of the CFGC. Total alkali content of the intrusion (Na_2O + K_2O) is slightly higher than in Löytölamminvuori, 8.28 wt% on average, and shows correlation with the SiO_2 content.

The average K_2O resembles that of the post-kinematic plutons and is relatively high at 5.09 wt%, the lowest being 2.77 wt% and the highest 7.7 wt% which when correlated with the SiO_2 content places the intrusion partly in the high-K calc-alkalic series and partly in the shoshonite series (Fig. 36.). The FeO_t of the intrusion is on average 4.11 wt% and the MgO as low as 0.83 wt%, the FeO_t/MgO ratio being 5.32. This places the samples to the ferroan series, although some samples close to the ferroan/magnesian border (Fig. 31.a). The values are quite similar to the post-kinematic plutons. The CaO content correlates well with the SiO_2 content, the average CaO of the samples being 1.93 wt% and is on average lower than in Löytölamminvuori and the post-kinematic plutons.

7.2.2. Trace element composition

The Ba content of the Sorsakoski intrusion varies widely, from 148 ppm to 2880 ppm, the average being 1088 ppm, which correlates well with the post-kinematic rocks of the CFGC (Nironen et al. 2000). Zr content is 305 ppm on average, which is similar to the post-kinematic series. Rb averages at 158 ppm and Sr at 202 ppm, with average Rb/Sr ratio of 0.77. This is on average similar to the post-kinematic plutons but varies between the pluton types. The Rb/Ba ratio is 0.15 and resembles that of the Type 1 and 2 plutons of the post-kinematic plutons but is considerably higher than in the Type 3 plutons. The samples have slightly negative Eu anomalies on average (Fig. 37.).

7.3. Karvalevä intrusion

SiO_2 of the felsic samples from the Karvalevä ranges between 64.1 wt% - 66,1 wt%, and the SiO_2 of the mafic phases between 48.3 wt% - 59.9 wt%. The Al_2O_3 content is quite uniform, the average being 16.3 wt% and the lowest and highest 14.9 wt% and 18.5 wt% respectively. The Al_2O_3 contents of the more felsic samples from Karvalevä are similar to the quartz-monzonite phases from Löytölamminvuori and Sorsakoski, the mafic samples have slightly higher Al_2O_3 (Fig. 33.b). When comparing other geochemical features of the more mafic intrusion to those of the granite and quartz-monzonite phases, the mafic phases of Karvalevä are enriched in FeO, MgO and CaO (Fig. 33.h,c,d, respectively). There seems to be a clear correlation between these parameters and the

SiO_2 content of the samples, and a straight continuum from the mafic phases through the monzonitic phases to granitic phases of the study area. The mafic phases are depleted in K_2O, Rb, Ba and Zr when compared to the felsic phases. The Sr content of Karvalevä, however, are quite similar to the more felsic intrusions. The absolute REE contents of the gabbro phases are generally lower than in the felsic phases, and the REE patterns also differ (Fig. 37.).

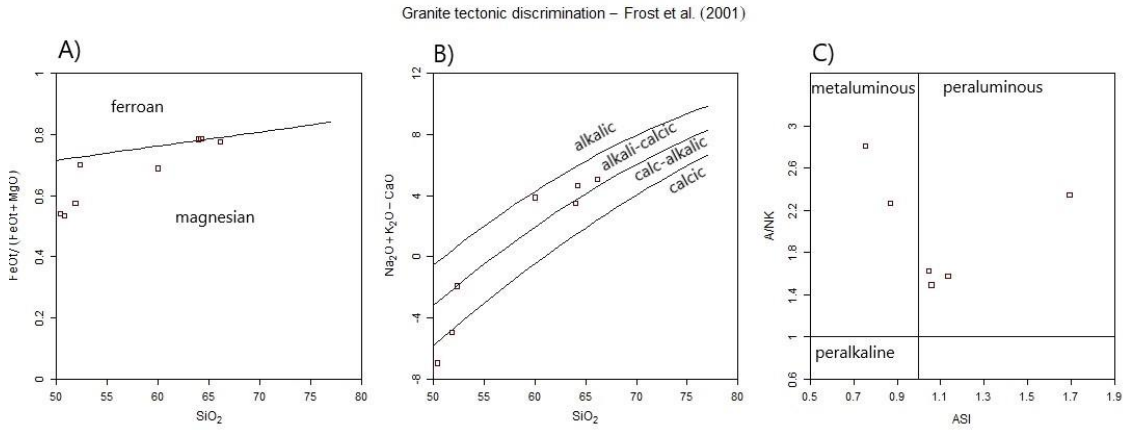

Figure 35. Tectonic discrimination diagrams for Karvalevä intrusion, using the Fe-number vs. SiO2 (A), MALI vs. SiO2 (B), and ASI vs. A/NK (C). The more felsic samples are marginally ferroan, alkali-calcic to calc-alkaline and peraluminous. The mafic samples are magnesian, calc-alkaline to calcic and metaluminous.

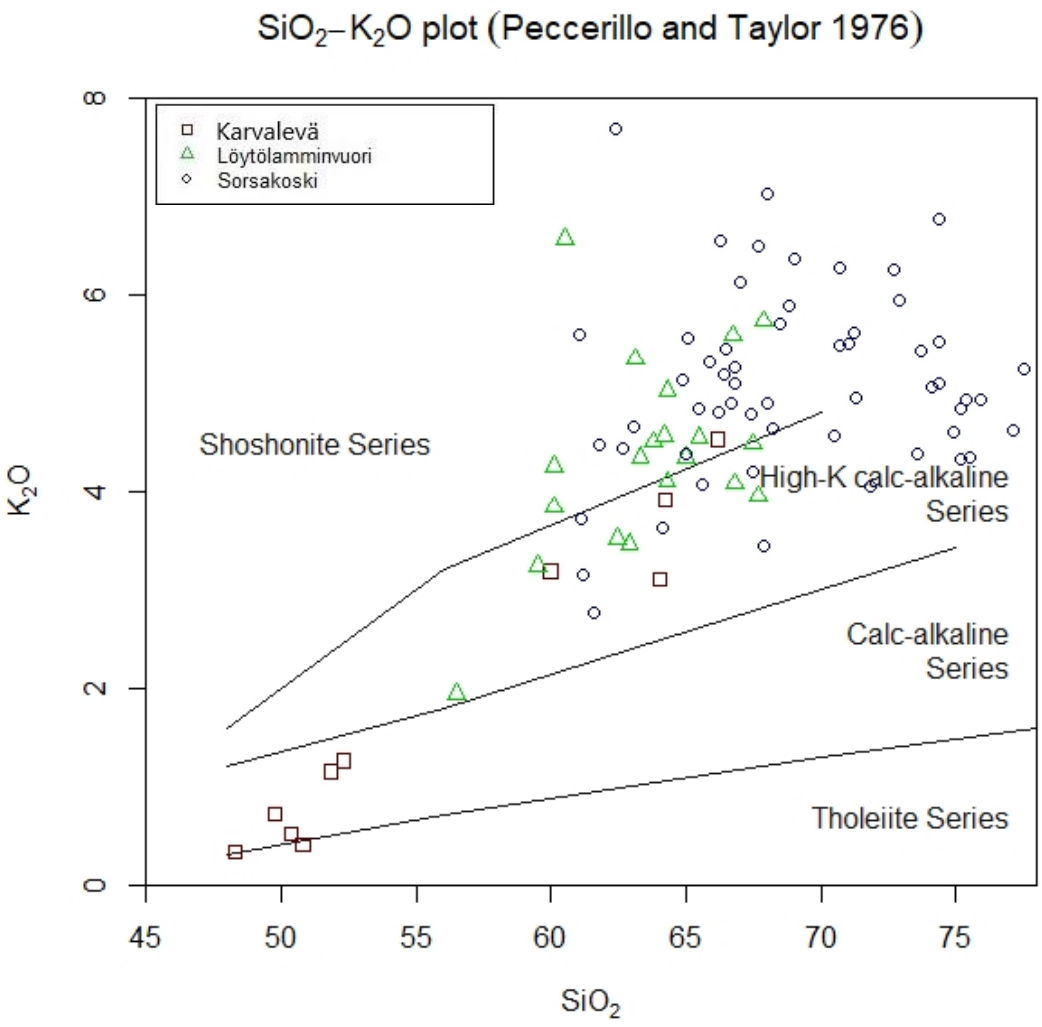

Figure 36. A SiO_2 vs. K_2O diagram for all the intrusions (after Peccerillo & Taylor 1976). Both Sorsakoski and Löytölamminvuori plot in the high-K calc-alkaline series and shoshonite series. The felsic parts of the Karvalevä intrusion plot in the same fields as Sorsakoski and Löytölamminvuori, the mafic parts plot in the calc-alkaline series.

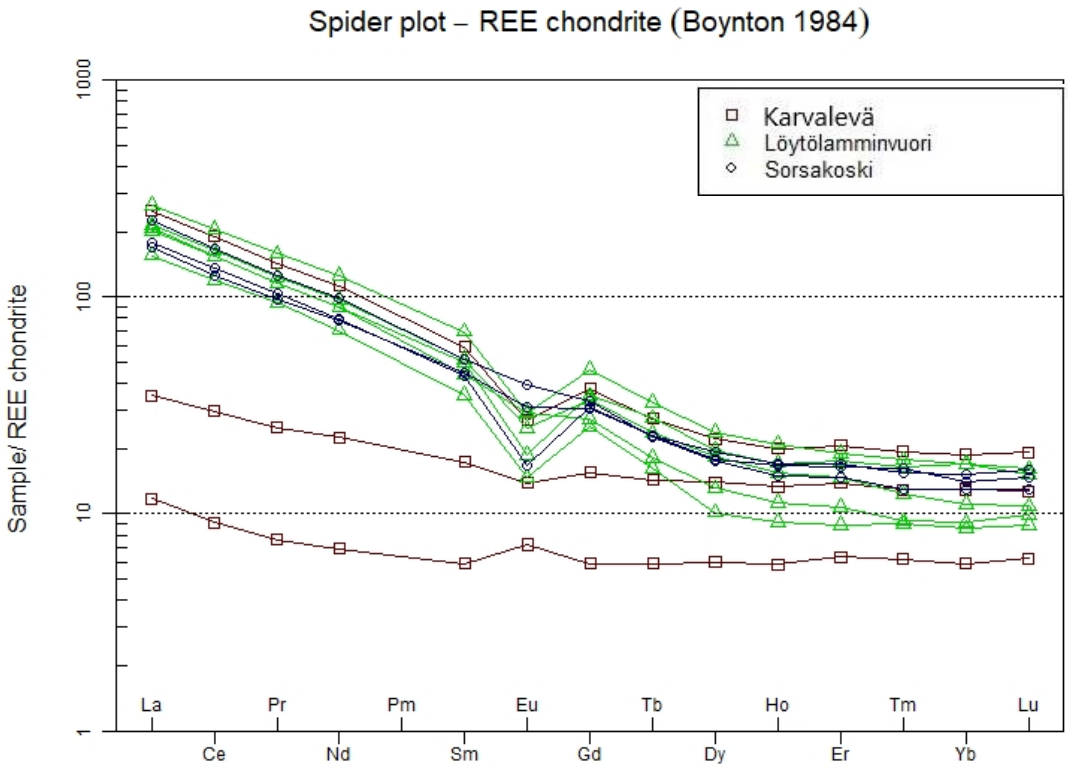

Figure 37. REE contents from Karvalevä, Löytölamminvuori and Sorsakoski have been normalized to chondritic composition (Boynton 1984). Löytölamminvuori and Sorsakoski, and the felsic samples from Karvalevä show slight Eu anomalies. Mafic Karvalevä samples deviate from the felsic samples.

8. U-PB GEOCHRONOLOGY

The age determination was made on a sample collected from the quartz-monzonite phase of the Löytölamminvuori intrusion. The sample A2434 is from a quartz-monzodiorite. The zircon crystals vary from circular and prismatic to elongated (Fig. 38.) The size of the grains varies between approximately 50-300 µm. Most of the grains appear to be homogenous. 35 zircons were included in the analysis and 51 spots were measured in total. The measurements used for the age calculation had U contents varying from 91 ppm to 2884 ppm. The ages were calculated with 2σ errors and without decay constant errors. The results were concordant but scattered preventing calculation of a Concordia age. One slightly older spot was rejected as inherited. Average $^{207}Pb/^{206}Pb$ age 1876±6 Ma calculated based on the remaining 50 spots can be regarded as best estimate for the crystallization age of this sample (Fig. 39.)

Figure 38. Back-scattered electron (BSE) images of two zircons from the Löytölamminvuori intrusion U-Pb age determination study. The size and shape of the zircons used in the analysis varies from roundish to elongated.

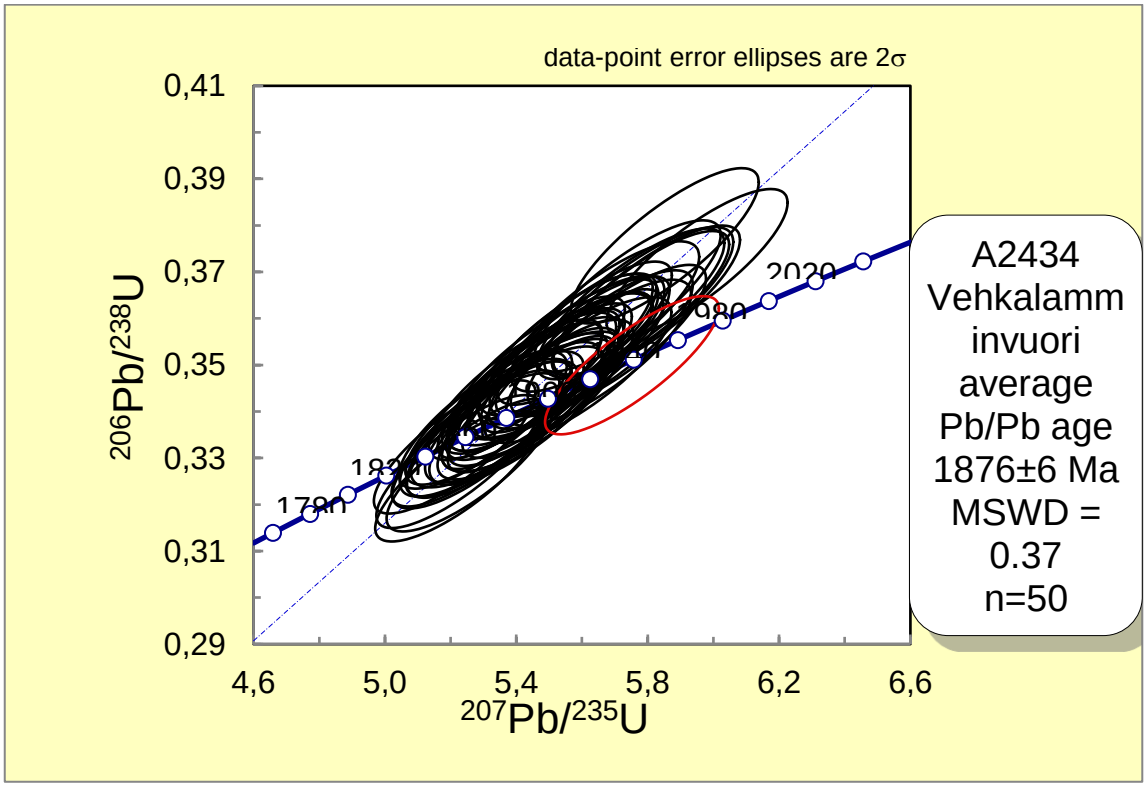

Figure 39. Average Pb/Pb age diagram, showing the result of single zircon U-Pb laser ablation inductively coupled plasma mass spectrometry (LA-ICP-MS) measurement.

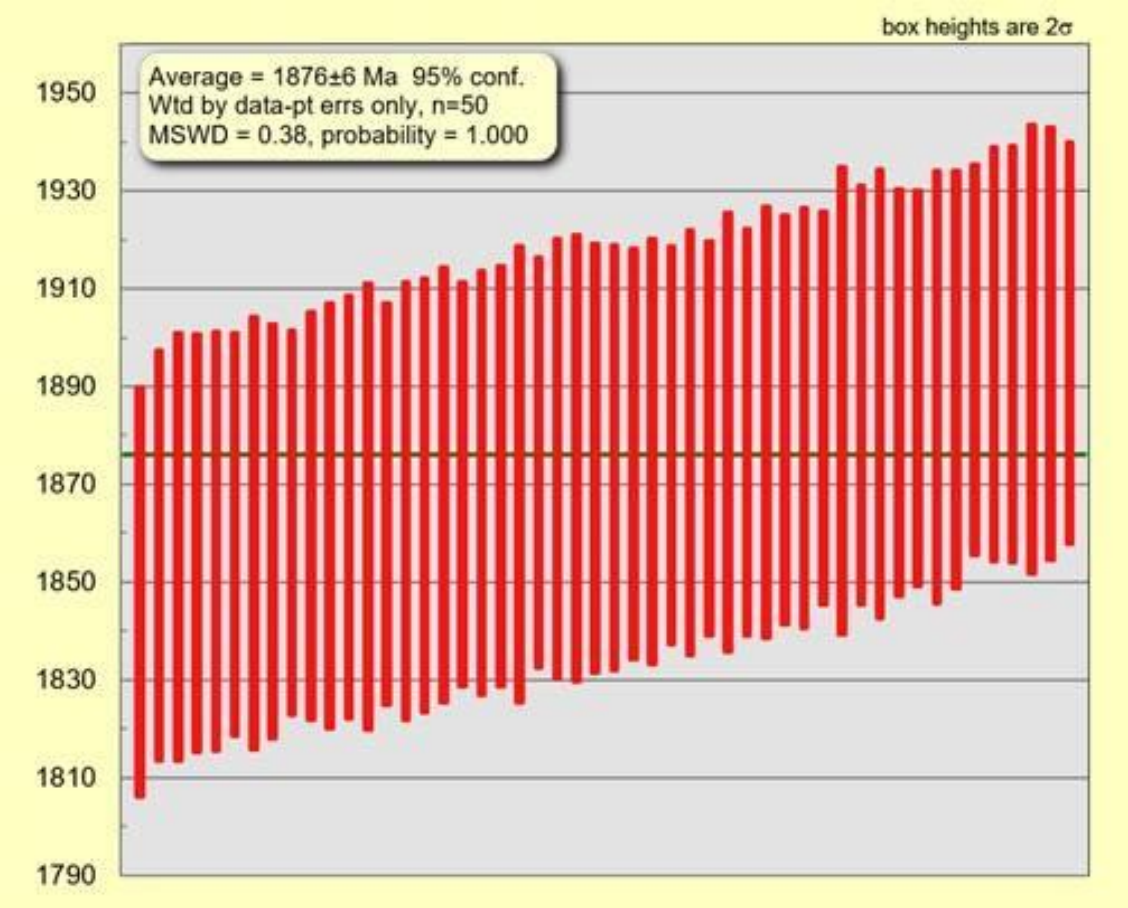

Figure 40. Weighted average $^{207}Pb/^{206}Pb$ age diagram showing the results of single zircon U-Pb laser ablation inductively coupled plasma mass spectrometry (LA-ICP-MS) measurement.

9. DISCUSSION

9.1. Classification of the intrusions

In the Central Finland Granitoid Complex (CFGC), two granitoid groups have been identified; the foliated, 1.89-1.88 Ga syn-kinematic granitoid group and the non-foliated 1.88-1.87 Ga post-kinematic group (Front and Nurmi 1987, Elliot et al. 1998, Nironen et al. 2000). Both of these types span across the complex equally, but they have been distinguished by their mineralogical and geochemical composition. The post-kinematic group has been divided further into sub-types Type 1, Type 2 and Types 3a and 3b (Elliot et al. 1998, Nironen et al. 2000). The granitoid intrusions of Löytölamminvuori,

Sorsakoski and Karvalevä, being A-type (Fig. 32.), ferroan granitoids, have mineralogical and geochemical affinities to the post-kinematic group of the CFGC. They are also non-foliated, which sets them apart from the syn-kinematic group. The one U-Pb age measurement of 1876±6 Ma places them in the early stages of the post-kinematic magmatism in the CFGC. Similar ages have been measured from other post-kinematic intrusions, for example the Puula intrusion with the age 1875±4 Ma (Rämö et al. 2001) and Riitalampi intrusion with the age 1879±4 Ma (Virtanen and Heilimo 2018).

The Löytölamminvuori and Sorsakoski intrusions show major similarities to the post-kinematic plutons of CFGC, especially to the Type 3a. Type 3a granitoid mafic silicates include biotite and hornblende throughout the intrusions, and pyroxenes on the outer rims (Elliott et al. 1998), so these have the most similar mineral assemblage to Sorsakoski and Löytölamminvuori (Table 2.). The exception is that in Sorsakoski and Löytölamminvuori the pyroxene-bearing phase does not form a rim-like structure, although pyroxenes do occur only locally and not throughout the intrusions. When comparing geochemical properties, Sorsakoski and Löytölamminvuori have the greatest affinity to the Type 3a plutons. Some overlapping with Types 1 and 2 does occur, for example in Al_2O_3 content and K_2O content, but these values are quite similar between all of the post-kinematic plutons of the CFGC (Nironen et al. 2000). However, the most silica rich, granitic parts of the plutons show some similarities to the Type 2 plutons.

In general, the geochemical characteristics of Sorsakoski and Löytölamminvuori are closest to the Type 3a plutons, having mostly similar major element concentrations, with similar SiO_2, Al_2O_3, K_2O, and CaO. The FeO/MgO ratios are also similar to the Type 3a plutons, but the FeO_t is on average higher in the Sorsakoski area intrusions than in the post-kinematic series. The trace element contents also resemble those of Type 3 plutons, with similar Ba, Zr, Rb and Sr. Differences are in the Rb/Ba and Rb/Sr ratios, which both are lower in Löytölamminvuori than in Sorsakoski. Löytölamminvuori ratios resemble those of the Type 3 and Sorsakoski those of Type 1 and 2, which could partly be explained by the slightly more granitic overall composition of Sorsakoski intrusion. Only major difference between the Type 3 post-kinematic plutons, and Sorsakoski and Löytölamminvuori intrusions is, that the latter are both peraluminous, while the Type 3 plot in the margin of metaluminous to peraluminous. In this sense the studied intrusions are similar to the Type 1, which are more peraluminous than Type 2 ja 3 plutons. In conclusion, Löytölamminvuori and Sorsakoski intrusions consist of non-foliated, A-type

granites and quartz-monzonites. Geochemically they belong to the high-K and shoshonitic series, are ferroan, alkali-calcic to calc-alkalic, and peraluminous.

Table 2. Rock types and mineralogical features of Löytölamminvuori, Sorsakoski and Karvalevä intrusions.

	Löytölamminvuori	Sorsakoski	Karvalevä felsic	Karvalevä mafic
Rock type	granite and quartz-monzonite	granite and quartz-monzonite	granite and quartz-monzonite	monzonite, diorite and diabase
Main mafic silicates	biotite, hornblende, clinopyroxene and orthopyroxene	biotite, hornblende and orthopyroxene	biotite, hornblende and orthopyroxene	biotite, hornblende, clinopyroxene and orthopyroxene
Typical accessory minerals	apatite, epidote, monazite, titanite, zircon ± rutile ± tourmaline ± garnet	apatite, epidote, monazite, titanite, zircon ± muscovite ± carbonate ± garnet	apatite, monazite, zircon	apatite, monazite, zircon ± garnet

The Karvalevä intrusion differs from Löytölamminvuori and Sorsakoski, for it has a major mafic component to it. The rock types in Karvalevä vary from diorite to granite, the SiO_2 content ranging from 48.3% to 66.2%. The felsic parts of the Karvalevä intrusion are similar as the quartz-monzonite phases of Sorsakoski and Löytölamminvuori both mineralogically and geochemically, having similar SiO_2, Al_2O_3, FeO, MgO, and K_2O contents, and also quite similar FeO/MgO ratios. So, they can be also classified as Type 3 post-kinematic plutons of the CFGC (Nironen et al. 2000). The mafic phases of the intrusion are enriched in Al_2O_3, FeO, MgO and CaO, and a continuum (with a slight gap) can be seen in the concentrations when comparing to the SiO_2 content, from mafic samples to quartz-monzonite to granite. The mafic phases are depleted in K_2O, Rb, Ba, and Zr, compared to the felsic phases and the REE concentrations are lower in the Karvalevä mafic phases, the patterns differ, and there is no visible depletion of Eu in the mafic samples.

Slightly to the west, mafic intrusions associated with post-kinematic granitoids, with Type 2 to Type 3a compositions, have been studied by Virtanen and Heilimo (2018). These intrusions range in composition from gabbros to tonalites and form a bimodal mafic-felsic system with the associated granitoids. The diorites occur as fine- to coarse grained, even-grained or slightly plagioclase porphyritic rocks (Mikkola et al. 2016). These mafic intrusions have many petrographical similarities to Karvalevä mafic phases,

with similar mineralogy as main mineral phases being plagioclase, biotite, hornblende, pyroxenes ± quartz. The intrusions show also roughly similar geochemical properties as Karvalevä diorites with similar Al_2O_3 and FeO concentrations. Karvalevä has slightly higher MgO and CaO, and lower Rb and Sr concentrations (Virtanen and Heilimo 2018). The roughly similar petrographic and geochemical properties, and the same kind of bimodal setting indicate similar sources for these mafic intrusions, but with less crustal assimilation for Karvalevä mafic phases, as they have a slightly more juvenile composition. Generally, the Karvalevä intrusion felsic phase is similar to the Sorsakoski and Löytölamminvuori. The mafic phases can be classified as diorites and monzodiorites, which are magnesian, calcic, and on the border of metaluminous to peraluminous.

9.2. Bimodal mafic-felsic magmatism

Bimodal rock suites are common in intracontinental orogens, and in CFGC there is also evidence for bimodal mafic-felsic magmatism in the form of microgranular mafic enclaves (MME), syn-plutonic mafic dykes and rare mafic plutons. According to Nironen et al. (2000) the post-kinematic granitoids and their associated mafic rocks have formed from two or more magma sources, and not by differentiation of a single parental magma. So, the dykes and mafic plutons likely represent cogenetic, but not comagmatic suites, with at least two different magmatic components. In Löytölamminvuori and Sorsakoski intrusions there is little evidence of bimodal magmatism, one syn-plutonic diorite dyke in Sorsakoski and one quartz-monzodioritic sample from Löytölamminvuori. The major evidence for bimodal magmatism in the studied intrusions is the Karvalevä intrusion between the two felsic intrusions.

The Karvalevä intrusion consist of a wide range of rock types from granite to diorite. The felsic phases were intruded first, and the mafic phases later, when the felsic intrusion was already crystallizing. Evidence for this is a clear compositional difference between the two phases, with only slight mixing or mingling of the two magmas, that would indicate relatively high crystallinity in the felsic phase (Fernandez and Barbarin 1991). The dioritic phase between the felsic parts of Karvalevä is fine-grained and has a cumulus texture at times. The grains size indicates a rapid cooling after the intrusion, probably

aided by the cooling quartz-monzonite on both sides. The quartz-monzonite and monzonite samples (PIM$-2018-67.1 and PIM$-2018-54.1, respectively) taken close to the contact with the diorite show similar textures to the diorite phase; fine-grained and with a slight cumulus texture. Whereas the quartz-monzonite sample (PIM$-2018-59.1) farther away from the contact shows clear, medium-grained, porphyritic texture. This would indicate that the dioritic magma in the middle mixed slightly with the surrounding quartz-monzonite during its emplacement, and thus has a gradual composition from the marginal quartz-monzonite composition to the diorite in the middle. The intrusion also contains a diabase dyke in the southern area. The diabase is fine-grained and has a slight orientation and similar composition to the diorite, which suggests it is a dyke variation of the diorite.

The mafic phases of the Karvalevä intrusion are magnesian in nature and metaluminous (Fig. 35.a and c), which clearly sets them apart geochemically from the felsic phases. Also, they plot as their own group in the SiO_2 vs. major and trace element diagrams (Fig. 33. and 34.), with a roughly clear continuum, but a gap between the two groups. Thich could indicate two magmatic sources and mixing of these in variable proportions to produce the more felsic intrusions and the dioritic parts of the Karvalevä intrusion. In conclusion, the felsic and mafic phases are cogenetic but not comagmatic. The intrusion of the mostly dioritic phase happened when the felsic phase was cooling, possibly through an early fracture in the host rock. The diorite sample from Sorsakoski and the quartz-monzodiorite from Löytölamminvuori along with the Karvalevä diorite suggest that the input of mafic magma occurred throughout all three intrusions and slightly after the intrusion of the granitic and quartz-monzonitic phases.

9.3. Similarities to the Saarijärvi and Rautalampi suite intrusions

As has been established, the post-kinematic granitoids of CFGC have been studied in detail before (Elliot et al. 1998, Nironen et al. 2000, Rämö et al. 2001). In a report by Mikkola et al. (2016) Löytölamminvuori, Sorsakoski and Karvalevä intrusions have been grouped together with the Saarijärvi suite intrusions, but there remained a question if they should be classified in the same group as the pyroxene-bearing Rautalampi suite

intrusions. Both Saarijärvi and Rautalampi suites have been studied and categorized by Elliot (2001) and Saarijärvi suite further by Mikkola et al. (2018) and Virtanen and Heilimo (2018). The Saarijärvi suite consists of Type 2 to Type 3a post-kinematic plutons, and are coarse grained, alkali-felspar porphyritic granitoids. The Rautalampi suite has been categorized as a Type 3b. It has the lowest SiO_2 contents out of all the post-kinematic plutons and shows different trend in Harker diagrams compared to the rest of the plutons. Even though the Rautalampi pluton has been grouped with the post-kinematic series based on its petrography and non-deformed state, geochemically it falls closer to the syn-kinematic series (Elliott 2001). Based on this, the grouping of Löytölamminvuori, Sorsakoski and Karvalevä together with Saarijärvi suite is more appropriate, because it clearly has a similar geochemical composition as the post-kinematic group, and not calc-alkalic, volcanic arc -type geochemistry like the syn-kinematic group (Elliott 2001).

There are some minor differences between these intrusions and the Saarijärvi suite, as Karvalevä intrusion plots closest to the Type 3b post-kinematic plutons, but in general there are more similarities than deviations. The Saarijärvi suite intrusions are A-type, ferroan, metaluminous to slightly peraluminous, and alkali to alkali-calcic in composition (Virtanen and Heilimo 2018), being slightly more alkalic than Sorsakoski, Löytölamminvuori and Karvalevä. They are enriched in K_2O, Ba and FeO/MgO and depleted in MgO, CaO and Sr, features which are similar in the intrusions studied in this thesis. Saarijärvi suite intrusions also show a shift from Type 3a to Type 2 with increasing SiO_2 content, a similar transition which can be seen in Sorsakoski and Löytölamminvuori intrusions. The dioritic phases associated with Saarijärvi garnitoids form a bimodal magmatic system (Virtanen and Heilimo 2018), also similar to the Sorsakoski, Löytölamminvuori and Karvalevä intrusions. The suites also exhibit a same trend in tectonic discrimination diagrams, plotting on the border of WPG and VAG fields, which would also indicate similar magmatic sources.

9.4. Sources and magmatic evolution

The post-kinematic granitoids of the CFGC and their petrogenesis has been studied previously by Rämö et al. (2001) and Elliott (2003), using geochemical modeling and

isotopes. Based on the findings of these studies it has been suggested that the parental magma for the post-kinematic intrusions was formed by partial melting of mantle derived mafic rocks which mixed with varying proportions of anatectic melts of mafic granulite (Elliott 2003). The differences between the different types are likely a consequence of a varying thickness of the crust and intra-crustal differentiation processes: eastern magmas formed at deeper levels in the lower crust with a lower-degree of partial melting, and in the west the thinner crust resulted in more abundant partial melting and more mixing between different melt proportions. As the studied intrusions conform spatially, mineralogically and geochemically to the Type 2 and Type 3 plutons of the CFGC, can this previously proposed petrogenetic model be also used in explaining their petrogenesis.

9.4.1 Sources of the intrusions

The Löytölamminvuori and Sorsakoski intrusion, and the felsic phases of Karvalevä intrusion, plot geochemically in the A-type group of granitoids, as they are ferroan, alkali-calcic to calc-alkalic and peraluminous. The A-type granitoids with these features are thought to have formed by either partial melting of tonalitic to granodioritic crust (forming peraluminous granitoids at higher pressures and metaluminous granitoids at lower pressures) or by extreme differentiation of basaltic melts (with alkalinity increasing with the growing pressure of differentiation) (Frost and Frost 2011). The presence of pyroxenes in the intrusions points to high temperatures during partial melting and relatively low water activity in the source (Clemens and Vielzeuf 1987). Using the tectonic discrimination diagrams by Pearce et al. (1984), the Löytölamminvuori and Sorsakoski intrusions plot in the border of WPG, VAG, and VAG + syn-COLG fields (Fig. 41). As they have formed in a WPG setting (within plate), the affinity to VAG and VAG + syn-COLG needs to be explained. Crustal contamination of partial melts of mantle-derived basalts could accord to the shift from WPG to VAG field (Pearce et al. 1984). Also, the high aluminum contents of the studied intrusions point to crustal assimilation of moderate degrees. This would be a combination of the two end-member formation models for A-type granitoids by Frost and Frost (2011). The other explanation here could be the mixing with the syn-kinematic magmas, a mode which was suggested by Virtanen and Heilimo (2018). The syn-kinematic magmas had VAG affinities (Heilimo et al. 2018), and the intrusion age (1876$\pm$6 Ma) of Sorsakoski,

Löytölamminvuori and Karvalevä means they formed during the late synorogenic stage of the Svecofennian orogeny, and their age overlaps with the late syn-kinematic magmatism. Based on these observations, the syn-kinematic magmas are a possible contaminant.

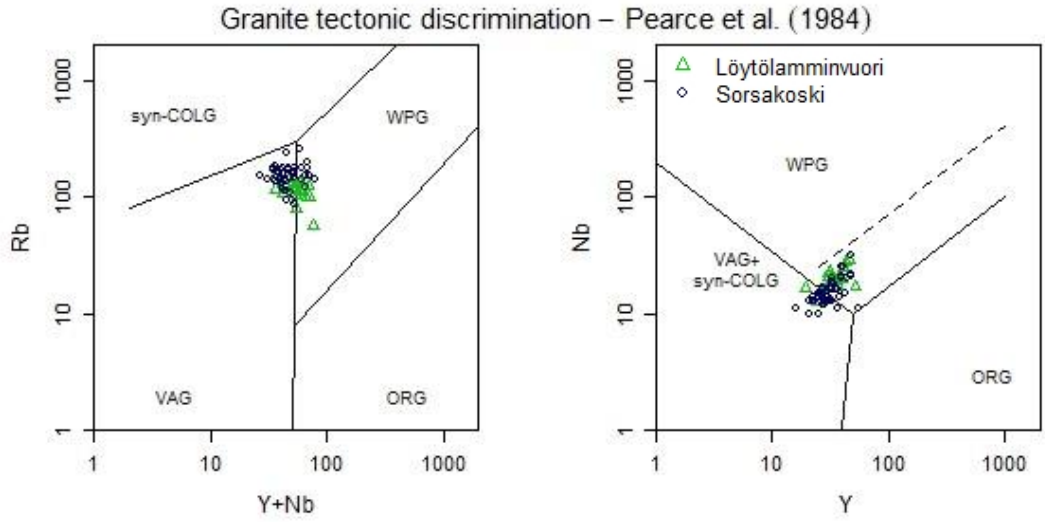

Figure 41. Tectonic discrimination diagrams by Pearce et al. (1984), with Löytölamminvuori and Sorsakoski intrusion samples. The samples plot on the border of WPG, VAG, VAG + syn-COLG fields, with no particular differences between Sorsakoski and Löytölamminvuori intrusions.

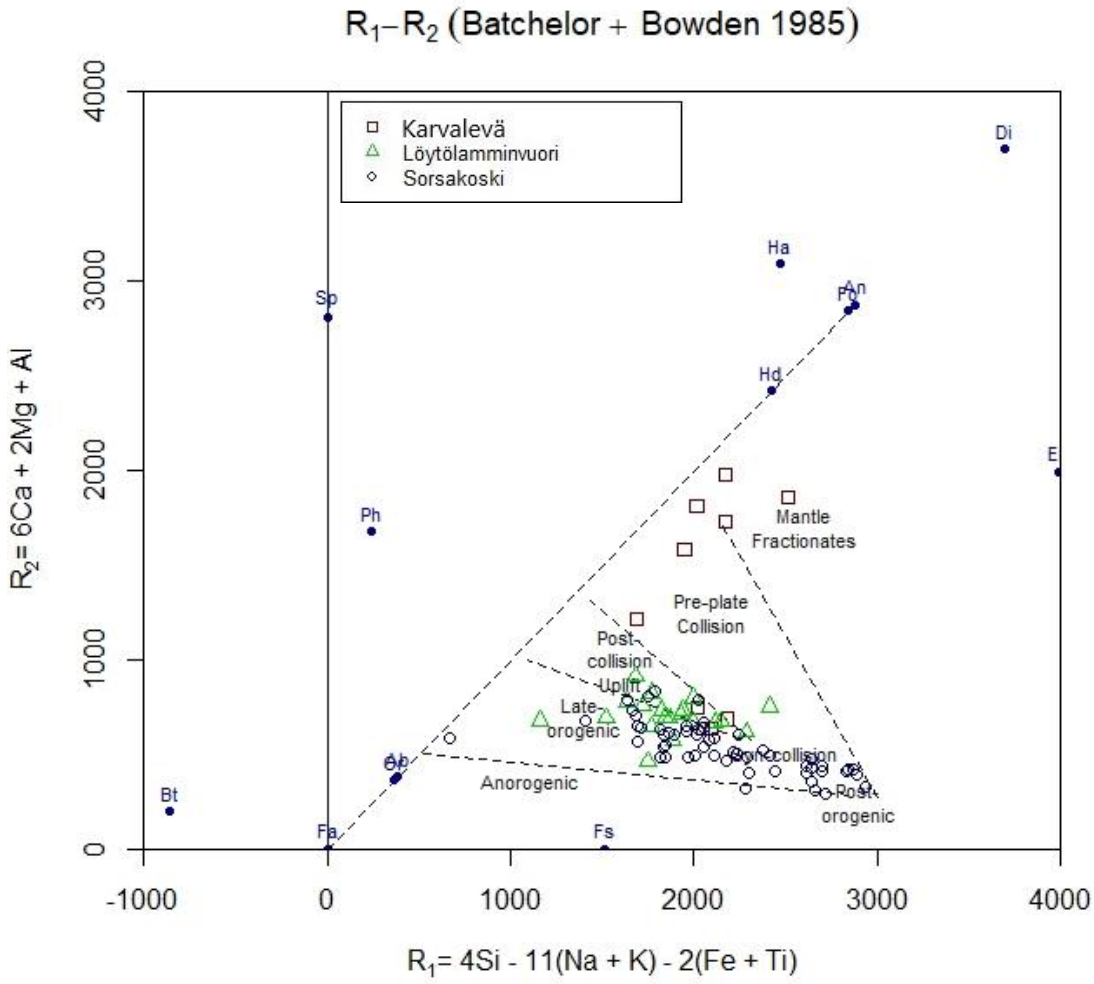

Figure 42. Samples from all three intrusions, plotted using the R1-R2 tectonic discrimination diagram from Batchelor and Bowden (1985). Samples from Löytölamminvuori and felsic samples from Karvalevä plot in the Late-orogenic and Post-collision Uplift fields. Sorsakoski samples plot in the same fields, in addition to some samples reaching Syn-collision field. The mafic samples from the Karvalevä intrusion plot in the Pre-plate Collision and Mantle Fractionates fields.

The R_1-R_2 discrimination diagram by Batchelor and Bowden (1985) places the felsic samples in syn-collisional, post-collisional uplift, and late-orogenic fields (Fig. 42.). These results correlate with the already proposed timing and types of magmatism proposed for other post-kinematic intrusions of the CFGC (Elliott 2003). The mafic samples from Karvalevä intrusion deviate here from the felsic ones, and plot in the pre-plate collision and mantle fractionate fields. As has earlier been established, the mafic magmas differ from the felsic by their geochemistry. The more juvenile compositions would point to a different, mantle derived source with less crustal assimilation. As so, the mafic phases of the Karvalevä intrusion would present the mantle-derived, basaltic

source-component of these intrusions. The formation of A-type magmas in the region has been related to local transtensional and temporary extensional tectonic settings (Heilimo et al. 2018). The shear-zones formed pathways for the magmas to ascend. As the magma which formed the intrusions of Sorsakoski, Löytölamminvuori and Karvalevä originated from deep, lower crustal levels, it needed a conduit to rise. A possible explanation for this is the Raahe-Ladoga Shear-zone, as the intrusions are located in the middle of it.

9.4.2. Magmatic evolution of the intrusions

The REE patterns of the Löytölamminvuori and Sorsakoski samples, and the felsic sample from Karvalevä, are very uniform, showing also similar concentrations of the different elements (Fig. 37.) This indicates that the magmatic evolution of the intrusions has been similar and the magma source same. The felsic samples show moderate negative Eu anomalies, and similar Eu concentrations. This would indicate the incorporation of Eu into earlier crystallizing phases, for example plagioclase in a bimodal, cogenetic magma series (Rollinson 1993). The REE patterns of the two mafic samples from Karvalevä intrusion show flat REE patterns compared to the felsic samples, and all in all lower concentrations of the elements and no visible Eu anomalies. The patterns resemble a MORB (mid-ocean ridge basalt) composition that is slightly enriched in light REE elements, which could be due to the presence of pyroxenes in the dioritic phases (Rollinson 1993). Elliott (2001) studied two mafic intrusions associated with Type 2 post-kinematic intrusions, Perämaa and Kälä gabbros. Compared to these, Karvalevä samples show lower concentrations and lesser enrichment of light REEs. That together with the magnesian affinity of Karvalevä mafic magmas, would indicate a more primitive source or, as is probably the case here, lesser crustal assimilation than in the case of Perämaa and Kälä. In contrast, the REE patterns of the felsic samples from Löytölamminvuori, Sorsakoski and Kiviniemi intrusions are very similar to the other post-kinematic plutons of the CFGC (Elliott 2001), which indicates same sources and similar magmatic evolution.

10. CONCLUSIONS

1) Two larger and one smaller, non-foliated intrusions were studied. The Löytölamminvuori, Sorsakoski and Karvalevä intrusions are located in the schist-zone between the eastern margin of the CFGC and the Archean craton. The intrusions are mineralogically and texturally more similar to the post-kinematic plutons than the syn-kinematic intrusions of the CFGC.

2) Lithology of the studied intrusions ranges from the felsic granite and quartz-monzonite, to the mafic diorite phases. The granites and quartz-monzonites are non-foliated alkali feldspar porphyritic rocks which at times show rapakivi-like ovoid-texture. The main mafic silicates are biotite, hornblende, with additional pyroxenes in the quartz-monzonite phases. The mafic phases are generally fine-grained plagioclase, biotite, and pyroxene rocks, with minor quartz and alkali feldspar.

3) One U-Pb age determination has been performed on the Löytölamminvuori quartz-monzonite phase. The age of 1876$\pm$6 Ma was measured, which places it in the same age group as the other post-kinematic plutons in the eastern parts of the CFGC.

4) Geochemically the studied intrusions show A-type affinity and similarities to the post-kinematic plutons of CFGC. The silica rich granitic parts show similarities to the Type 2 intrusions and the quartz-monzonitic phases, which contain pyroxenes, to the Type 3a. On average the intrusions fit best to the Type 3a plutons with transitional characteristics from Type 2 to Type 3. An earlier comparison with the Saarijärvi suite intrusions has been made, and the studied intrusions show many similarities to Saarijärvi plutons, especially the granitic phases of Löytölamminvuori and Sorsakoski.

5) The intrusions show signs of bimodal mafic-felsic magmatism, the dioritic phases in the Karvalevä intrusion representing the mafic phase, together with one syn-plutonic diorite dyke found in the Sorsakoski intrusion. The dioritic phases were intruded slightly

after the felsic ones, probably during the early cooling period of the felsic magma. The mafic magmatism was coeval, but not comagmatic with the felsic phases, the diorites showing a slight compositional gap to the felsic phases.

6) Based on the petrographic and geochemical features the magmas for Löytölamminvuori, Sorsakoski and Karvalevä intrusions were derived from partial melts from mantle derived basalts, which underwent crustal contamination by partial melts from the lower crust or, possibly, mixed with the magma which formed the syn-kinematic plutons of the CFGC. This fits with the suggested petrogenetic model for the other post-kinematic plutons of CFGC. The mafic phases are geochemically more juvenile and would represent the mantle-derived source component, with less crustal assimilation.

11. ACKNOWLEDGEMENTS

I want to thank my supervisors Perttu Mikkola and Tapani Rämö, whose expertise and knowledge were a great help and improved the contents of this study. I also want to thank the Geological Survey of Finland for providing the field observation data, thin sections, the older whole-rock geochemical data and the U-Pb analysis data, and Labtium Ltd for the whole-rock geochemical data on the new samples. I would also like to thank my friends for keeping me motivated, especially Seppo Karvinen, whose help with the maps and the geochemical data were much appreciated.

12. REFERENCES

Batchelor, R.A. and Bowden, P. 1985. Petrogenetic interpretation of granitoid rock series using multicationic parameters. Chemical Geology, Elsevier, Volume 48, Issues 1-4, pp. 43-55.

Belousova, E.A., Griffin, W.L. and O'Reilly, S.Y. 2006. Zircon crystal morphology, trace element signatures and Hf isotope composition as a tool for petrogenetic modeling: examples from Eastern Australian granitoids. J Petrol 47:329-353

Boynton, W.V. 1984. Geochemistry of the rare earth elements: meteorite studies. In: Henderson, P. (Ed.), Rare Element Geochemistry. Elsevier, Amsterdam, 63–114.

Chappell, B.W. and White, A.J.R. 1974. Two contrasting granite types. Pacific Geology 8, 173–174.

Clemens, J.D. and Vielzeuf, D. 1987. Constraints on melting and magma production in the crust. Earth and Planetary Science Letters. Elsevier, Volume 86, Issues 2-4, pp. 287-306.

De la Roche, H., Leterrier, J., Grandclaude, P. and Marchal, M. (1980) A Classification of Volcanic and Plutonic Rocks Using R1-R2 Diagrams and Major Element Analyses—Its Relationships with Current Nomenclature. Chemical Geology, 29, 183-210.

Elliott, B.A., Rämö, O.T. and Nironen, M. 1998. Mineral chemistry constraints on the evolution of the 1.88–1.87 Ga post-kinematic granite plutons in the Central Finland Granitoid Complex. Lithos 45, 109–129.

Elliott, B.A. 2001. The Petrogenesis of the 1.88-1.87 Ga post-kinematic granitoids of the Central Finland Granitoid Complex. Academic Dissertation, University of Helsinki, department of geology, division of geology and mineralogy, 36 pp.

Elliott, B.A. 2003. Petrogenesis of the Post-kinematic Magmatism of the Central Finland Granitoid Complex II; Sources and Magmatic Evolution. Journal of Petrology 44, 1681–1701.

Fernandez, A.N. and Barbarin, B. 1991. Relative rheology of coeval mafic and felsic magmas: Nature of resulting interaction processes. Shape and mineral fabrics of mafic microgranular encalves. In: Didier, J. and Barbarin, B. (Eds.), Enclaves and Granite Petrology. Elsevier, Amsterdam, 263–275.

Front, K. and Nurmi, P.A. 1987. Characteristics and geological setting of synkinematic Svecokarelian granitoids in southern Finland. Precambrian Research, 35, 207–224.

Frost, C.D. & Frost, B.R. 1997. Reduced rapakivi-type granites: the tholeiite connection. Geology 25, 647-650.

Frost, B.R., Barnes, C.G., Collins, W.J., Arculus, R.J., Ellis, D.J. and Frost, C.D. 2001. A Geochemical Classification for Granitic Rocks. Journal of Petrology 42, 2033–2048.

Frost., C.D. and Frost. B.R. 2011. On Ferroan (A-type) Granitoids: their Compositional Variability and Modes of Origin. Journal of Petrology, volume 52, 1, pp. 39-52

Heilimo, E., Ahven, M. & Mikkola, P. 2018. Geochemical characteristics of the plutonic rock units present at the southeastern boundary of the Central Finland Granitoid Complex. Geological Survey of Finland, Bulletin 407, YY–ZZ, 10 figures and 1 table.

Huhma, H., Mänttäri, I., Peltonen, P., Kontinen, A., Halkoaho, T., Hanski, E., Hokkanen, T., Hölttä, P., Juopperi, H., Konnunaho, J., Layahe, Y., Luukkonen, E., Pietikäinen, K., Pulkkinen, A., Sorjonen-Ward, P., Vaasjoki, M. and Whitehouse, M. 2012. The age of the Archean greenstone belts in Finland. Geological Survey of Finland, Special Paper 54, 74–175.

Lahtinen, R., Korja, A., Nironen, M. and Heikkinen P. 2009. Palaeoproterozoic accretionary processes in Fennoscandia. Geological Society of London, Special Publications, 318, pp. 237-256.

Lahtinen, R, Huhma, H, Lahaye, Y., Lode, S., Heinonen, S., Sayab, M. and Whitehouse, J. 2016. Paleoproterozoic magmatism across the Archean-Proterozoic boundary in central Fennoscadia: Geochronoly, geochemistry and isotopic data (Sm-Nd, Lu-Hf, O). Lithos. Elsevier, Volume 262, pp. 507-525.

Loiselle, M.C. and Wones, D.R. 1979. Characteristics and origin of anorogenic granites. Geological Society of America, Abstracts with Programs 11, 468.

Ludwig, K.R. 2003. User's manual for Isoplot/Ex, Version 3.00. A geochronological toolkit for Microsoft Excel. Berkeley Geochronology Center Special Publication 4, 74 p.

Mikkola, P., Lukkarinen, H. and Luukas, J. 2016. Suonenjoen kartta-alueen 3241 kallioperä ja kivillajiyksiköt. Geological Survey of Finland, Archive Report 227, 29 p.

Mikkola, P., Heilimo, E., Luukas, J., Kousa, J., Aatos, S., Makkonen, H., Niemi, S., Nousiainen, M., Ahven, M., Romu, I. & Hokka, J. 2018. Geological evolution and structure

along the southeastern border of the Central Finland Granitoid Complex. Geological Survey of Finland, Bulletin 407, YY–ZZ, 6 figures and 1 table.

Miyashiro, A. 1970. Volcanic rock series in island arcs and active continental margins. American Journal of Science 274, pp. 321-355.

Müller, W., Shelley, M., Miller, P. and Broude, S. 2009. Initial performance metrics of a new custom-designed ArF excimer LA-ICPMS system coupled to a two-volume laser-ablation cell. Journal of Analytical Atomic Spectrometry 24, 209–214.

Nironen, M. 1997. The Svecofennian Orogen: a tectonic model. Precambrian Research 86, 21–44.

Nironen, M., Elliott, B.A. and Rämö, O.T. 2000. 1.88–1.87 Ga post-kinematic intrusions of the Central Finland Granitoid Complex: a shift from C-type to A-type magmatism during lithospheric convergence. Lithos 53, 37–58.

Nironen, M. 2005. Proterozoic orogenic granitoid rocks. In: Lehtinen, M., Nurmi, P. A. and Rämö, O.T. (Eds.), Precambrian Geology of Finland – Key to the Evolution of the Fennoscandian Shield. Elsevier B. V., Amsterdam, 443–480.

Peacock, M.A. 1931. Classification of Igneous Rock Series. The Journal of Geology, Volume 39, Number 1.

Pearce, J.A., Harris, N.B.W. and Tindle, A.G. 1984. Trace Element Discrimination Diagrams for the Tectonic Interpretation of Granitic Rocks. Journal of Petrology 25, 956–983.

Peccerillo, R. &Taylor, S.R. 1976.Geochemistry of Eocene calc-alkaline volcanic rocks from the Kastamonu area, northern Turkey. Contributions to Mineralogy and Petrology58, 63–81.

Rasilainen, K., Lahtinen, R. and Bornhorst, T. J. 2007. The Rock Geochemical Database of Finland Manual. Geological Survey of Finland, Report of Investigation 164, 38 p

Rollinson, H.R. 1993. Using Geochemical Data: Evaluation, Presentation, Interpretation. Longman, Singapore, 352 p.

Rämö, O.T., Vaasjoki, M., Mänttäri, I., Elliott, B.A. and Nironen, M. 2001. Petrogenesis of the Post-kinematic Magmatism of the Central Finland Granitoid Complex I; Radiogenic Isotope Constraints and Implication for Crustal Evolution. Journal of Petrology 42, 1971–1993.

Shand, S.J. (1943) Eruptive rocks, their genesis, composition, classification, with a chapter on meteorites. Thomas Murby and Co, London

Streckeisen, A.L. 1976. To each plutonic rock its proper name. Earth Science Reviews 12, 1–33.

Van Achterbergh, E., Ryan, C., Jackson, S. and Griffin, W. 2001. Data reduction software for LA-ICP-MS. In: Sylvester, P.J. (Ed.), Laser-Ablation ICPMS in the Earth Sciences: Principals and Applications. St John, Newfoundland, 239–243.

Virtanen, V. J. & Heilimo, E. 2018. Petrology of the geochemically A-type Saarijärvi suite: evidence for bimodal magmatism. Geological Survey of Finland, Bulletin 407, YY–ZZ, 10 figures and 2 tables.

Whalen, J.B., Currie, K.L. and Chappell, B.W. 1987. A-type granites: geochemical characteristics, discrimination and petrogenesis. Contributions to Mineralogy and Petrology 95, 407–419.

Winter, J.D. 2001. An Introduction to Igneous and Metamorphic Petrology, 2nd Edition. Prentice-Hall Inc.

APPENDICES

Appendix 1. Whole-rock geochemical compositions and coordinates of the samples. If concentration is below detection limit, it has been marked with < and detection limit. If element is not analyzed, it has been marked as n.a.

Intrusion	Löytölamminvuori					
Rock type	granite	granite	granite	granite	granite	granite
Sample	91010923	107.1-JHV-97	254.1-ARP-1	421.2-JHV-97	461.1-JHV-97	49.1 -JHV-97
Longitude	523539	524759	522300	526538	522620	524119
Latitude	6941160	6937352	6938681	6934953	6930275	6938411
SiO_2	69,2	64,3	63,3	67,5	65,5	65
TiO_2	0,46	0,81	0,89	0,73	0,74	0,82
Al_2O_3	15,3	15,9	15,8	15	16	15,3
Fe_2O_3t	3,39	6,25	6,75	5,04	5,4	6,52
MnO	0,04	0,07	0,08	0,05	0,07	0,08
MgO	0,66	1,45	1,35	1,3	1,34	1,15
CaO	1,97	3,05	3,31	2,44	2,7	2,95
Na_2O	3,04	3,43	3,34	2,86	2,9	3,18
K2O	5,09	4,1	4,35	4,49	4,55	4,35
P2O5	0,17	0,27	0,29	0,26	0,36	0,29
Total	99,31	99,63	99,46	99,67	99,56	99,63
S	332	1000	762	<100	840	320
Cl	115	190	175	210	90	140
Sc	6,82	<30	<30	<30	<30	<30
V	28,6	87	90	75	79	92
Cr	36,7	55	33	44	48	32
Ni	<20	23	<20	<20	<20	<20
Cu	19,6	28	29	21	24	<20
Zn	70,8	109	114	87	78	106
Ga	24,2	25	26	32	27	31
Rb	142	130	118	146	124	138
Sr	204	265	276	269	301	244
Y	18,1	31	37	32	52	37
Zr	223	318	477	321	388	482
Nb	10,7	19	17	20	17	21
Ba	992	1058	1401	1177	1604	1160
Hf	6,36	n.a.	n.a.	n.a.	n.a.	n.a.
Ta	0,60	n.a.	n.a.	n.a.	n.a.	n.a.
Co	5,55	n.d.	n.d.	n.d.	n.d.	n.d.
Pb	39,3	36	36	37	36	38
Th	12,1	12	14	16	12	26
U	1,6	<10	<10	<10	<10	<10
La	48,1	60	82	73	70	96
Ce	96,8	138	156	171	155	227
Pr	11,5	n.d.	n.d.	n.d.	n.d.	n.d.
Nd	42,1	n.d.	n.d.	n.d.	n.d.	n.d.
Sm	6,91	n.d.	n.d.	n.d.	n.d.	n.d.
Eu	1,08	n.d.	n.d.	n.d.	n.d.	n.d.
Gd	6,52	n.d.	n.d.	n.d.	n.d.	n.d.
Tb	0,77	n.d.	n.d.	n.d.	n.d.	n.d.
Dy	3,26	n.d.	n.d.	n.d.	n.d.	n.d.
Ho	0,66	n.d.	n.d.	n.d.	n.d.	n.d.
Er	1,87	n.d.	n.d.	n.d.	n.d.	n.d.
Tm	0,29	n.d.	n.d.	n.d.	n.d.	n.d.
Yb	1,79	n.d.	n.d.	n.d.	n.d.	n.d.
Lu	0,29	n.d.	n.d.	n.d.	n.d.	n.d.

Appendix 1. Continues.

Intrusion	Löytölamminvuori					
Rock type	granite	granite	granite	granidiorite	granite	granite
Sample	67.1 -JHV-97	79.2 -JHV-97	PIM$-2018-62.1	91010931	113.1-ARP-1	146.1-ARP-1
Longitude	524459	525499	523999	523640	521300	525609
Latitude	6939121	6939631	6932291	6918749	6922378	6919539
SiO_2	64,2	66,8	62,46	64,4	62,9	63,8
TiO_2	0,81	0,67	0,9	0,934	1,06	0,92
Al_2O_3	16,2	15,4	15,37	15,1	15,6	15,3
Fe_2O_3t	6,01	5,04	6,59	6,79	7,51	6,94
MnO	0,07	0,06	0,07	0,1	0,09	0,09
MgO	1,1	0,93	2,05	1,8	1,92	1,6
CaO	3,01	3,01	3,69	2,77	3,08	2,93
Na_2O	3,36	3,38	3,24	3,17	3,45	3,18
K_2O	4,57	4,08	3,52	3,95	3,47	4,51
P_2O_5	0,28	0,22	0,35	0,27	0,27	0,26
Total	99,61	99,59	98,30	99,28	99,36	99,53
S	<100	440	900	1030	567	824
Cl	110	130	300	158	142	117
Sc	<30	<30	17,1	19,7	<30	<30
V	75	66	91,7	77,5	111	95
Cr	47	38	60	58,8	51	49
Ni	<20	<20	40	29,1	<20	23
Cu	22	<20	<20	<20	25	24
Zn	102		100	133	125	110
Ga	28	24	<30	27,4	25	26
Rb	110	105	130	124	111	119
Sr	280	261	310	274	278	284
Y	26	36	27,1	38,4	39	30
Zr	414	375	352	434	562	446
Nb	16	19	16,1	18,7	20	21
Ba	1436	1204	1160	1120	974	1279
Hf	n.a.	n.a.	9,32	12	n.a.	n.a.
Ta	n.a.	n.a.	<1	1,13	n.a.	n.a.
Co	n.d.	n.d.	14,1	11,4	n.d.	n.d.
Pb	38	39	<30	39,6	34	33
Th	<10	10	15,9	13,5	14	<10
U	<10	<10	1,61	2,59	<10	<10
La	49	55	66,5	62,8	78	65
Ce	122	132	132	125	155	107
Pr	n.d.	n.d.	15,1	14,1	n.d.	n.d.
Nd	n.d.	n.d.	58,7	53,8	n.d.	n.d.
Sm	n.d.	n.d.	10,1	9,72	n.d.	n.d.
Eu	n.d.	n.d.	1,82	1,38	n.d.	n.d.
Gd	n.d.	n.d.	8,7	9,07	n.d.	n.d.
Tb	n.d.	n.d.	1,12	1,31	n.d.	n.d.
Dy	n.d.	n.d.	5,91	6,35	n.d.	n.d.
Ho	n.d.	n.d.	1,11	1,23	n.d.	n.d.
Er	n.d.	n.d.	3,1	3,67	n.d.	n.d.
Tm	n.d.	n.d.	0,4	0,531	n.d.	n.d.
Yb	n.d.	n.d.	2,32	3,54	n.d.	n.d.
Lu	n.d.	n.d.	0,35	0,49	n.d.	n.d.

Appendix 1. Continues.

Intrusion	Löytölamminvuori					
Rock type	granite	qtz-monzonite	qtz-monzonite	qtz-monzonite	qtz-syenite	qtz-monzonite
Sample	387.1-PIM-97	91010925	106.1-JHV-97	109.1-JHV-97	408.1-JHV-97	430.1-JHV-97
Longitude	521430	524469	524729	525089	524639	525299
Latitude	6926396	6932644	6937212	6937752	6935303	6936592
SiO_2	67,9	59,7	56,5	59,5	60,5	60,1
TiO_2	0,47	1,12	1,56	1,35	0,82	1,23
Al_2O_3	16,1	16,4	16,3	15,8	17,2	15,8
Fe_2O_3t	3,56	9,32	12,2	9,85	7,05	9,66
MnO	0,038	0,113	0,145	0,117	0,08	0,11
MgO	1,09	1,83	2,47	2,11	0,9	2,13
CaO	0,873	3,53	4,4	3,81	2,77	3,16
Na_2O	3,74	3,3	3,61	3,24	3,19	3,13
K_2O	5,74	3,49	1,94	3,25	6,57	3,84
P_2O_5	0,17	0,386	0,467	0,463	0,317	0,375
Total	99,68	99,19	99,59	99,49	99,40	99,53
S	170	1510	1770	1280	530	1410
Cl	<60	106	90	110	90	130
Sc	<30	28	<30	<30	<30	<30
V	44	95,4	181	154	74	153
Cr	31	63,4	87	68	33	77
Ni	<20	39,7	42	29	<20	36
Cu	<20	28,4	44	39	26	44
Zn	49	154	180	151	126	154
Ga	23	26,9	29	23	30	30
Rb	158	93,2	58	81	136	100
Sr	253	310	310	298	312	313
Y	24	44,2	46	31	38	43
Zr	186	545	733	549	618	546
Nb	13	21,7	29	23	21	28
Ba	1114	1290	757	1227	2774	1551
Hf	n.a.	14,7	n.a.	n.a.	n.a.	n.a.
Ta	n.a.	1,18	n.a.	n.a.	n.a.	n.a.
Co	n.d.	15,9	n.d.	n.d.	n.d.	n.d.
Pb	47	37,1	27	28	44	39
Th	12	19,4	17	<10	<10	15
U	<10	1,64	<10	<10	<10	<10
La	40	82,4	89	41	58	64
Ce	96	166	201	109	140	166
Pr	n.d.	19,4	n.d.	n.d.	n.d.	n.d.
Nd	n.d.	75,5	n.d.	n.d.	n.d.	n.d.
Sm	n.d.	13,5	n.d.	n.d.	n.d.	n.d.
Eu	n.d.	2,13	n.d.	n.d.	n.d.	n.d.
Gd	n.d.	12	n.d.	n.d.	n.d.	n.d.
Tb	n.d.	1,55	n.d.	n.d.	n.d.	n.d.
Dy	n.d.	7,64	n.d.	n.d.	n.d.	n.d.
Ho	n.d.	1,51	n.d.	n.d.	n.d.	n.d.
Er	n.d.	4	n.d.	n.d.	n.d.	n.d.
Tm	n.d.	0,57	n.d.	n.d.	n.d.	n.d.
Yb	n.d.	3,56	n.d.	n.d.	n.d.	n.d.
Lu	n.d.	0,52	n.d.	n.d.	n.d.	n.d.

Appendix 1. Continues.

Intrusion	Löytölamminvuori				
Rock type	granite	qtz-monzonite	qtz-monzonite	qtz-monzonite	granite
Sample	493.1-JHV-97	56.2 -JHV-97	PIM$-2018-63.1	PIM$-2018-64.1	PIM$-2018-65.1
Longitude	524039	524599	523324	523010	523982
Latitude	6936552	6938152	6934571	6939842	6932287
SiO_2	64,3	60,1	63,14	67,69	66,74
TiO_2	0,77	1,16	0,71	0,34	0,51
Al_2O_3	15,8	16	16,37	14,42	15,02
Fe_2O_3t	6,42	8,9	6,21	4,21	4,49
MnO	0,08	0,12	0,07	0,07	0,05
MgO	0,84	1,86	0,49	1,32	0,34
CaO	2,74	3,48	3,22	3,76	2,41
Na_2O	3,27	3,15	3,55	2,97	3,17
K_2O	5,03	4,26	5,35	3,95	5,59
P_2O_5	0,27	0,37	0,29	0,26	0,20
Total	99,53	99,38	99,40	98,97	98,52
S	320	990	300	<100	100
Cl	120	150	100	200	<100
Sc	<30	<30	<20	<20	13,4
V	72	132	50	70	23,3
Cr	30	54	20	20	<20
Ni	<20	23	<20	30	<20
Cu	21	34	<20	<20	<20
Zn	124	141	130	60	90
Ga	27	29	<30	<30	<30
Rb	119	99	<10	<10	118
Sr	242	315	260	420	210
Y	30	41	30	10	19,2
Zr	610	582	680	80	463
Nb	22	25	<20	<20	16,8
Ba	1858	1711	2380	960	2090
Hf	n.a.	n.a.	n.d.	n.d.	11,9
Ta	n.a.	n.a.	n.d.	n.d.	<1
Co	n.d.	n.d.	n.d.	n.d.	3,77
Pb	38	40	<30	<30	<30
Th	<10	16	<30	<30	6,73
U	<10	<10	<10	<10	1,05
La	38	80	<30	<30	64,8
Ce	103	175	<30	40	125
Pr	n.d.	n.d.	n.d.	n.d.	14,1
Nd	n.d.	n.d.	n.d.	n.d.	53,9
Sm	n.d.	n.d.	n.d.	n.d.	8,57
Eu	n.d.	n.d.	n.d.	n.d.	2,16
Gd	n.d.	n.d.	n.d.	n.d.	7,12
Tb	n.d.	n.d.	n.d.	n.d.	0,86
Dy	n.d.	n.d.	n.d.	n.d.	4,24
Ho	n.d.	n.d.	n.d.	n.d.	0,81
Er	n.d.	n.d.	n.d.	n.d.	2,26
Tm	n.d.	n.d.	n.d.	n.d.	0,3
Yb	n.d.	n.d.	n.d.	n.d.	1,91
Lu	n.d.	n.d.	n.d.	n.d.	0,32

Appendix 1. Continues.

Intrusion	Sorsakoski					
Rock type	granite	granite	granite	granite	granite	granite
Sample	91010928	1.1-MMK-98	106.1-MMK-98	106.2-MMK-98	11.1-MMK-98	128.1-MMK-98
Longitude	533086	533046	530217	530217	532266	532426
Latitude	6920349	6920199	6926236	6926236	6921508	6924617
SiO_2	68,1	74,4	72,7	71,8	67,5	70,7
TiO_2	0,52	0,08	0,22	0,60	0,666	0,40
Al_2O_3	15,2	13,5	14	13	14,5	14,3
Fe_2O_3t	4,17	1,1	2,18	4,73	5,55	2,9
MnO	0,06	0,02	0,03	0,05	0,08	0,04
MgO	0,85	0,17	0,2	0,54	1,28	0,55
CaO	1,81	0,41	1,12	1,79	1,37	1,47
Na_2O	3,44	2,99	2,87	2,98	3,8	2,78
K_2O	4,96	6,77	6,25	4,05	4,2	6,27
P_2O_5	0,16	0,06	0,07	0,17	0,21	0,14
Total	99,26	99,50	99,63	99,70	99,15	99,55
S	133	<100	<100	<100	<100	110
Cl	76,9	<60	90	130	<60	140
Sc	10,4	<30	<30	<30	<30	<30
V	32,8	<30	<30	52	69	41
Cr	35,8	124	<30	33	43	<30
Ni	<20	62	<20	<20	<20	<20
Cu	<20	<20	<20	<20	<20	<20
Zn	77,7	<20	34	81	108	46
Ga	24	<20	25	30	22	27
Rb	149	166	216	198	95	174
Sr	210	132	106	93	207	189
Y	34,7	17	35	47	33	28
Zr	276	68	155	349	392	273
Nb	14,5	<10	<10	21	18	12
Ba	1060	269	732	148	1290	1395
Hf	7,76	n.a.	n.a.	n.a.	n.a.	n.a.
Ta	0,944	n.a.	n.a.	n.a.	n.a.	n.a.
Co	4,98	n.d.	n.d.	n.d.	n.d.	n.d.
Pb	42	38	44	41	25	44
Th	15,9	<10	17	28	<10	17
U	2,4	<10	<10	<10	<10	<10
La	55,3	<30	61	68	64	59
Ce	110	43	151	166	141	143
Pr	12,7	n.d.	n.d.	n.d.	n.d.	n.d.
Nd	47,3	n.d.	n.d.	n.d.	n.d.	n.d.
Sm	8,47	n.d.	n.d.	n.d.	n.d.	n.d.
Eu	1,23	n.d.	n.d.	n.d.	n.d.	n.d.
Gd	8,07	n.d.	n.d.	n.d.	n.d.	n.d.
Tb	1,09	n.d.	n.d.	n.d.	n.d.	n.d.
Dy	5,72	n.d.	n.d.	n.d.	n.d.	n.d.
Ho	1,2	n.d.	n.d.	n.d.	n.d.	n.d.
Er	3,47	n.d.	n.d.	n.d.	n.d.	n.d.
Tm	0,52	n.d.	n.d.	n.d.	n.d.	n.d.
Yb	2,96	n.d.	n.d.	n.d.	n.d.	n.d.
Lu	0,47	n.d.	n.d.	n.d.	n.d.	n.d.

Appendix 1. Continues.

Intrusion	Sorsakoski					
Rock type	granite	granite	granite	granite	granite	granite
Sample	13.1-MMK-98	130.1-ARP-2	131.1-ARP-2	131.1-MMK-98	14.1-MMK-98	14.2-MMK-98
Longitude	532306	528897	529307	532306	532376	532376
Latitude	6922338	6930595	6929945	6924647	6922338	6922338
SiO_2	75,2	66,2	70,5	67,9	66,3	66,5
TiO_2	0,34	0,74	0,46	0,66	0,55	0,57
Al_2O_3	12,6	15,1	14,5	14,8	15,7	15,7
Fe_2O_3t	2,26	5,5	3,73	4,91	4,33	4,44
MnO	0,03	0,07	0,05	0,06	0,06	0,07
MgO	0,47	1,16	0,65	1,3	0,86	0,87
CaO	1,38	2,68	1,86	2,35	1,97	2,31
Na_2O	3	3,03	3,22	3,77	3,01	3,37
K_2O	4,33	4,8	4,57	3,44	6,55	5,45
P_2O_5	0,06	0,23	0,18	0,18	0,18	0,19
Total	99,67	99,50	99,72	99,38	99,50	99,46
S	<100	526	149	490	200	300
Cl	80	139	135	110	110	120
Sc	<30	<30	<30	<30	<30	<30
V	35	85	42	75	61	62
Cr	<30	<30	<30	48	44	36
Ni	<20	<20	<20	<20	<20	<20
Cu	<20	<20	21	<20	<20	<20
Zn	42	97	73	77	77	74
Ga	22	30	25	27	27	26
Rb	122	115	175	148	168	167
Sr	110	254	153	215	274	278
Y	23	32	56	36	38	35
Zr	258	357	243	378	326	317
Nb	<10	13	11	16	14	16
Ba	428	1496	683	614	2064	1701
Hf	n.a.	n.a.	n.a.	n.a.	n.a.	n.a.
Ta	n.a.	n.a.	n.a.	n.a.	n.a.	n.a.
Co	n.d.	n.d.	n.d.	n.d.	n.d.	n.d.
Pb	37	36	38	32	50	41
Th	29	13	12	17	12	<10
U	<10	<10	<10	<10	<10	<10
La	78	73	52	72	50	31
Ce	195	127	103	158	131	118
Pr	n.d.	n.d.	n.d.	n.d.	n.d.	n.d.
Nd	n.d.	n.d.	n.d.	n.d.	n.d.	n.d.
Sm	n.d.	n.d.	n.d.	n.d.	n.d.	n.d.
Eu	n.d.	n.d.	n.d.	n.d.	n.d.	n.d.
Gd	n.d.	n.d.	n.d.	n.d.	n.d.	n.d.
Tb	n.d.	n.d.	n.d.	n.d.	n.d.	n.d.
Dy	n.d.	n.d.	n.d.	n.d.	n.d.	n.d.
Ho	n.d.	n.d.	n.d.	n.d.	n.d.	n.d.
Er	n.d.	n.d.	n.d.	n.d.	n.d.	n.d.
Tm	n.d.	n.d.	n.d.	n.d.	n.d.	n.d.
Yb	n.d.	n.d.	n.d.	n.d.	n.d.	n.d.
Lu	n.d.	n.d.	n.d.	n.d.	n.d.	n.d.

Appendix 1. Continues.

Intrusion	Sorsakoski					
Rock type	granite	granite	granite	granite	granite	granite
Sample	14.3-MMK-98	141.1-MMK-98	147.1-MMK-98	148.1-MMK-98	151.1-MMK-98	160.1-MMK-98
Longitude	532376	532246	532256	532416	532536	532856
Latitude	6922338	6924147	6924077	6924197	6924037	6923937
SiO_2	75,4	68,5	75,9	71	70,7	77,5
TiO_2	0,28	0,51	0,04	0,39	0,40	0,11
Al_2O_3	12,6	15	12,6	14,3	14,5	12,1
Fe_2O_3t	1,85	3,81	1,4	2,94	2,94	1,11
MnO	0,03	0,05	0,04	0,04	0,04	0,02
MgO	0,37	0,86	0,02	0,65	0,51	0,19
CaO	1,39	1,84	0,55	1,56	1,75	0,74
Na_2O	2,73	3,02	3,38	3,01	3,13	2,73
K_2O	4,94	5,7	4,94	5,5	5,49	5,24
P_2O_5	0,09	0,15	0,02	0,14	0,12	0,01
Total	99,68	99,43	98,89	99,53	99,58	99,76
S	<100	<100	<100	230	<100	<100
Cl	90	140	<60	150	130	<60
Sc	<30	<30	<30	<30	<30	<30
V	31	65	<30	46	44	<30
Cr	<30	41	<30	33	<30	<30
Ni	<20	<20	<20	<20	<20	<20
Cu	<20	<20	<20	<20	<20	<20
Zn	30	65	36	50	54	<20
Ga	21	24	27	23	26	<20
Rb	127	162	311	172	177	161
Sr	196	226	15	185	183	98
Y	24	25	75	21	22	17
Zr	215	281	101	258	248	127
Nb	<10	14	<10	13	13	<10
Ba	916	1398	44	1031	949	201
Hf	n.a.	n.a.	n.a.	n.a.	n.a.	n.a.
Ta	n.a.	n.a.	n.a.	n.a.	n.a.	n.a.
Co	n.d.	n.d.	n.d.	n.d.	n.d.	n.d.
Pb	39	43	54	41	40	43
Th	13	16	17	17	16	11
U	<10	<10	<10	<10	<10	<10
La	46	46	<30	54	60	<30
Ce	106	129	65	120	123	55
Pr	n.d.	n.d.	n.d.	n.d.	n.d.	n.d.
Nd	n.d.	n.d.	n.d.	n.d.	n.d.	n.d.
Sm	n.d.	n.d.	n.d.	n.d.	n.d.	n.d.
Eu	n.d.	n.d.	n.d.	n.d.	n.d.	n.d.
Gd	n.d.	n.d.	n.d.	n.d.	n.d.	n.d.
Tb	n.d.	n.d.	n.d.	n.d.	n.d.	n.d.
Dy	n.d.	n.d.	n.d.	n.d.	n.d.	n.d.
Ho	n.d.	n.d.	n.d.	n.d.	n.d.	n.d.
Er	n.d.	n.d.	n.d.	n.d.	n.d.	n.d.
Tm	n.d.	n.d.	n.d.	n.d.	n.d.	n.d.
Yb	n.d.	n.d.	n.d.	n.d.	n.d.	n.d.
Lu	n.d.	n.d.	n.d.	n.d.	n.d.	n.d.

Appendix 1. Continues.

Intrusion	Sorsakoski					
Rock type	granite	granite	granite	granite	granite	granite
Sample	17.1-MMK-98	177.1-MMK-98	178.1-MMK-98	2.1-MMK-98	212.1-MMK-98	221.1-MMK-98
Longitude	532436	533995	532426	533056	533296	532996
Latitude	6922278	6923318	6923518	6920269	6922658	6922098
SiO_2	62,4	75,2	67,7	68,2	77,1	65,6
TiO_2	0,29	0,20	0,48	0,68	0,03	0,83
Al_2O_3	20	12,9	15,5	14,1	12,6	14,4
Fe_2O_3t	2,27	2,12	3,5	5,25	1,32	6,99
MnO	0,03	0,03	0,05	0,08	0,05	0,10
MgO	0,33	0,19	0,81	1,18	0,01	1,35
CaO	1,64	0,82	1,79	1,67	0,37	2,62
Na_2O	4,57	3,31	2,98	3,07	3,67	3,37
K_2O	7,7	4,84	6,5	4,64	4,62	4,08
P_2O_5	0,10	0,07	0,14	0,20	0,04	0,24
Total	99,32	99,68	99,45	99,07	99,80	99,58
S	<100	<100	460	<100	<100	320
Cl	<60	<60	120	80	<60	130
Sc	<30	<30	<30	<30	<30	<30
V	34	<30	59	76	<30	101
Cr	<30	<30	41	57	<30	50
Ni	<20	<20	<20	24	<20	<20
Cu	<20	<20	<20	<20	<20	23
Zn	50	60	63	95	31	129
Ga	26	27	24	28	22	26
Rb	236	257	168	155	269	153
Sr	252	61	250	201	12	229
Y	31	43	27	44	55	39
Zr	183	159	302	415	59	458
Nb	13	15	12	20	<10	25
Ba	1372	199	1796	935	25	904
Hf	n.a.	n.a.	n.a.	n.a.	n.a.	n.a.
Ta	n.a.	n.a.	n.a.	n.a.	n.a.	n.a.
Co	n.d.	n.d.	n.d.	n.d.	n.d.	n.d.
Pb	60	50	46	36	40	36
Th	17	24	16	16	<10	16
U	<10	<10	<10	<10	<10	<10
La	79	<30	60	91	<30	65
Ce	173	47	150	205	44	184
Pr	n.d.	n.d.	n.d.	n.d.	n.d.	n.d.
Nd	n.d.	n.d.	n.d.	n.d.	n.d.	n.d.
Sm	n.d.	n.d.	n.d.	n.d.	n.d.	n.d.
Eu	n.d.	n.d.	n.d.	n.d.	n.d.	n.d.
Gd	n.d.	n.d.	n.d.	n.d.	n.d.	n.d.
Tb	n.d.	n.d.	n.d.	n.d.	n.d.	n.d.
Dy	n.d.	n.d.	n.d.	n.d.	n.d.	n.d.
Ho	n.d.	n.d.	n.d.	n.d.	n.d.	n.d.
Er	n.d.	n.d.	n.d.	n.d.	n.d.	n.d.
Tm	n.d.	n.d.	n.d.	n.d.	n.d.	n.d.
Yb	n.d.	n.d.	n.d.	n.d.	n.d.	n.d.
Lu	n.d.	n.d.	n.d.	n.d.	n.d.	n.d.

Appendix 1. Continues.

Intrusion	Sorsakoski					
Rock type	granite	granite	granite	granite	qtz-monzonite	qtz-monzonite
Sample	24.1-MMK-98	248.1-MMK-98	25.2-MMK-98	27.1-MMK-98	27.2-MMK-98	276.1-MMK-98
Longitude	531916	535175	531906	531636	531636	533835
Latitude	6922448	6922148	6922428	6923547	6923547	6919909
SiO_2	74,9	68	74,4	66,4	64,1	73,6
TiO_2	0,40	0,47	0,29	0,63	0,97	0,33
Al_2O_3	12,4	15	13,4	15,6	14,4	13,2
Fe_2O_3t	2,57	3,66	1,66	4,55	7,58	2,74
MnO	0,04	0,04	0,02	0,06	0,09	0,03
MgO	0,42	0,75	0,37	1,09	1,74	0,45
CaO	1,38	1,38	1,4	2,36	2,75	1,49
Na_2O	2,83	2,73	3,03	3,41	3,26	3,11
K_2O	4,6	7,03	5,1	5,2	3,63	4,39
P_2O_5	0,09	0,15	0,06	0,16	0,26	0,11
Total	99,63	99,20	99,73	99,46	98,78	99,45
S	<100	<100	<100	670	<100	<100
Cl	90	150	80	130	160	70
Sc	<30	<30	<30	<30	<30	<30
V	32	50	<30	82	119	<30
Cr	<30	37	<30	48	68	<30
Ni	<20	<20	<20	<20	22	<20
Cu	<20	<20	<20	<20	23	<20
Zn	45	70	24	73	115	55
Ga	22	26	24	25	30	25
Rb	135	183	114	130	123	178
Sr	113	209	179	267	230	131
Y	23	22	22	25	41	36
Zr	266	208	224	354	567	234
Nb	13	14	<10	15	25	11
Ba	405	1830	741	1359	836	553
Hf	n.a.	n.a.	n.a.	n.a.	n.a.	n.a.
Ta	n.a.	n.a.	n.a.	n.a.	n.a.	n.a.
Co	n.d.	n.d.	n.d.	n.d.	n.d.	n.d.
Pb	42	47	40	42	34	41
Th	26	<10	21	18	21	16
U	<10	<10	<10	<10	<10	<10
La	67	38	77	71	64	49
Ce	158	124	142	174	131	141
Pr	n.d.	n.d.	n.d.	n.d.	n.d.	n.d.
Nd	n.d.	n.d.	n.d.	n.d.	n.d.	n.d.
Sm	n.d.	n.d.	n.d.	n.d.	n.d.	n.d.
Eu	n.d.	n.d.	n.d.	n.d.	n.d.	n.d.
Gd	n.d.	n.d.	n.d.	n.d.	n.d.	n.d.
Tb	n.d.	n.d.	n.d.	n.d.	n.d.	n.d.
Dy	n.d.	n.d.	n.d.	n.d.	n.d.	n.d.
Ho	n.d.	n.d.	n.d.	n.d.	n.d.	n.d.
Er	n.d.	n.d.	n.d.	n.d.	n.d.	n.d.
Tm	n.d.	n.d.	n.d.	n.d.	n.d.	n.d.
Yb	n.d.	n.d.	n.d.	n.d.	n.d.	n.d.
Lu	n.d.	n.d.	n.d.	n.d.	n.d.	n.d.

Appendix 1. Continues.

Intrusion	Sorsakoski					
Rock type	granite	granite	granite	granite	granite	granodiorite
Sample	286.1-MMK-98	286.2-MMK-98	287.1-MMK-98	287.2-MMK-98	300.1-MMK-98	303.1-MMK-98
Longitude	531226	531226	531166	531166	531116	530877
Latitude	6920299	6920299	6920569	6920569	6920879	6921059
SiO_2	65,5	73,7	66,7	74,1	61,6	72,9
TiO_2	0,75	0,40	0,71	0,35	1,4	0,35
Al_2O_3	14,9	13,1	14,5	12,7	14,3	13,8
Fe_2O_3t	5,57	2,29	5,75	2,81	9,06	2,07
MnO	0,07	0,03	0,07	0,03	0,12	0,03
MgO	1,34	0,48	1,44	0,53	2,25	0,43
CaO	2,42	1,43	2,02	1,22	3,65	1,11
Na_2O	3,13	2,69	2,96	2,75	3,28	2,72
K_2O	4,85	5,44	4,89	5,07	2,77	5,94
P_2O_5	0,21	0,09	0,19	0,10	0,43	0,07
Total	98,73	99,64	99,23	99,66	98,86	99,43
S	<100	<100	360	<100	<100	<100
Cl	130	110	170	90	190	70
Sc	<30	<30	<30	<30	<30	<30
V	97	35	73	32	165	30
Cr	58	32	55	<30	82	<30
Ni	23	<20	<20	<20	22	<20
Cu	20	<20	30	<20	<20	<20
Zn	88	37	87	46	148	39
Ga	27	24	31	21	29	24
Rb	131	139	169	142	144	156
Sr	265	210	213	129	232	120
Y	26	21	31	21	47	16
Zr	408	220	383	206	441	192
Nb	15	<10	16	10	32	11
Ba	1456	978	1225	596	398	689
Hf	n.a.	n.a.	n.a.	n.a.	n.a.	n.a.
Ta	n.a.	n.a.	n.a.	n.a.	n.a.	n.a.
Co	n.d.	n.d.	n.d.	n.d.	n.d.	n.d.
Pb	42	42	39	40	31	43
Th	16	19	16	17	16	18
U	<10	<10	<10	<10	<10	<10
La	54	63	74	47	41	<30
Ce	158	146	169	118	147	63
Pr	n.d.	n.d.	n.d.	n.d.	n.d.	n.d.
Nd	n.d.	n.d.	n.d.	n.d.	n.d.	n.d.
Sm	n.d.	n.d.	n.d.	n.d.	n.d.	n.d.
Eu	n.d.	n.d.	n.d.	n.d.	n.d.	n.d.
Gd	n.d.	n.d.	n.d.	n.d.	n.d.	n.d.
Tb	n.d.	n.d.	n.d.	n.d.	n.d.	n.d.
Dy	n.d.	n.d.	n.d.	n.d.	n.d.	n.d.
Ho	n.d.	n.d.	n.d.	n.d.	n.d.	n.d.
Er	n.d.	n.d.	n.d.	n.d.	n.d.	n.d.
Tm	n.d.	n.d.	n.d.	n.d.	n.d.	n.d.
Yb	n.d.	n.d.	n.d.	n.d.	n.d.	n.d.
Lu	n.d.	n.d.	n.d.	n.d.	n.d.	n.d.

Appendix 1. Continues.

Intrusion	Sorsakoski					
Rock type	granite	granite	granite	granite	granite	granite
Sample	307.1-MMK-98	310.1-MMK-98	318.1-MMK-98	368.1-MMK-98	368.2-MMK-98	37.1-MMK-98
Longitude	533336	533336	532356	530637	530637	530857
Latitude	6917540	6917120	6926316	6917840	6917840	6923508
SiO_2	69	71,3	67,4	66,8	67	66,8
TiO_2	0,47	0,46	0,69	0,61	0,59	0,59
Al_2O_3	14,8	13,8	14,7	15,2	15,4	15,7
Fe_2O_3t	3,57	3,47	5,22	4,77	4,41	4,31
MnO	0,05	0,05	0,07	0,06	0,06	0,06
MgO	0,77	0,69	1,03	1,09	0,84	1,09
CaO	1,43	1,79	2,28	1,19	1,93	2,21
Na_2O	2,91	3,02	3,12	3,6	2,98	3,4
K_2O	6,37	4,96	4,79	5,1	6,13	5,26
P_2O_5	0,14	0,14	0,22	0,22	0,25	0,16
Total	99,50	99,68	99,52	98,64	99,58	99,57
S	130	110	<100	<100	<100	150
Cl	90	160	140	<60	100	130
Sc	<30	<30	<30	<30	<30	<30
V	41	54	71	63	60	79
Cr	37	<30	39	44	37	50
Ni	<20	<20	<20	<20	<20	<20
Cu	<20	<20	<20	<20	<20	<20
Zn	81	59	90	73	68	72
Ga	26	27	23	24	25	28
Rb	177	159	181	135	176	148
Sr	201	187	217	262	225	264
Y	27	28	39	30	34	33
Zr	274	280	427	380	326	347
Nb	15	13	21	14	18	16
Ba	1377	894	953	1351	1508	1433
Hf	n.a.	n.a.	n.a.	n.a.	n.a.	n.a.
Ta	n.a.	n.a.	n.a.	n.a.	n.a.	n.a.
Co	n.d.	n.d.	n.d.	n.d.	n.d.	n.d.
Pb	48	36	37	31	43	42
Th	13	14	20	16	10	15
U	<10	<10	<10	<10	<10	<10
La	62	47	63	74	38	80
Ce	148	121	173	186	120	170
Pr	n.d.	n.d.	n.d.	n.d.	n.d.	n.d.
Nd	n.d.	n.d.	n.d.	n.d.	n.d.	n.d.
Sm	n.d.	n.d.	n.d.	n.d.	n.d.	n.d.
Eu	n.d.	n.d.	n.d.	n.d.	n.d.	n.d.
Gd	n.d.	n.d.	n.d.	n.d.	n.d.	n.d.
Tb	n.d.	n.d.	n.d.	n.d.	n.d.	n.d.
Dy	n.d.	n.d.	n.d.	n.d.	n.d.	n.d.
Ho	n.d.	n.d.	n.d.	n.d.	n.d.	n.d.
Er	n.d.	n.d.	n.d.	n.d.	n.d.	n.d.
Tm	n.d.	n.d.	n.d.	n.d.	n.d.	n.d.
Yb	n.d.	n.d.	n.d.	n.d.	n.d.	n.d.
Lu	n.d.	n.d.	n.d.	n.d.	n.d.	n.d.

Appendix 1. Continues.

Intrusion	Sorsakoski					
Rock type	granite	granite	granite	granite	granite	granite
Sample	37.2-MMK-98	49.1-MMK-98	5.1-MMK-98	59.1-MMK-98	59.2-MMK-98	60.1-MMK-98
Longitude	530857	530197	532876	530197	530197	530557
Latitude	6923508	6924457	6920819	6924357	6924357	6925417
SiO_2	71,2	75,5	68,8	64,9	74,4	65,1
TiO_2	0,42	0,29	0,57	0,65	0,27	0,63
Al_2O_3	14,2	12,4	14,1	15,8	13,1	16,2
Fe_2O_3t	2,77	2,56	4,45	5,61	1,98	4,83
MnO	0,04	0,03	0,07	0,07	0,02	0,06
MgO	0,66	0,37	1,07	0,9	0,29	0,81
CaO	1,6	1,22	1,52	2,63	1,22	2,73
Na_2O	2,97	2,96	2,74	3,52	2,81	3,41
K_2O	5,62	4,34	5,89	5,14	5,52	5,56
P_2O5	0,10	0,09	0,16	0,28	0,09	0,21
Total	99,57	99,75	99,37	99,50	99,67	99,55
S	<100	<100	<100	140	<100	<100
Cl	120	80	<60	120	80	120
Sc	<30	<30	<30	<30	<30	<30
V	46	<30	59	73	<30	69
Cr	32	<30	47	39	<30	35
Ni	<20	<20	<20	<20	<20	<20
Cu	<20	<20	<20	<20	<20	<20
Zn	45	41	81	97	39	80
Ga	22	26	<20	30	23	26
Rb	142	184	159	151	161	118
Sr	220	98	147	198	137	291
Y	25	66	33	47	27	27
Zr	248	198	345	418	169	406
Nb	10	<10	19	22	<10	15
Ba	1355	298	1184	1246	598	1782
Hf	n.a.	n.a.	n.a.	n.a.	n.a.	n.a.
Ta	n.a.	n.a.	n.a.	n.a.	n.a.	n.a.
Co	n.d.	n.d.	n.d.	n.d.	n.d.	n.d.
Pb	44	36	30	44	46	42
Th	19	21	16	<10	21	<10
U	<10	<10	<10	<10	<10	<10
La	71	55	62	47	80	42
Ce	160	129	138	124	179	117
Pr	n.d.	n.d.	n.d.	n.d.	n.d.	n.d.
Nd	n.d.	n.d.	n.d.	n.d.	n.d.	n.d.
Sm	n.d.	n.d.	n.d.	n.d.	n.d.	n.d.
Eu	n.d.	n.d.	n.d.	n.d.	n.d.	n.d.
Gd	n.d.	n.d.	n.d.	n.d.	n.d.	n.d.
Tb	n.d.	n.d.	n.d.	n.d.	n.d.	n.d.
Dy	n.d.	n.d.	n.d.	n.d.	n.d.	n.d.
Ho	n.d.	n.d.	n.d.	n.d.	n.d.	n.d.
Er	n.d.	n.d.	n.d.	n.d.	n.d.	n.d.
Tm	n.d.	n.d.	n.d.	n.d.	n.d.	n.d.
Yb	n.d.	n.d.	n.d.	n.d.	n.d.	n.d.
Lu	n.d.	n.d.	n.d.	n.d.	n.d.	n.d.

Appendix 1. Continues.

Intrusion	Sorsakoski				
Rock type	granite	granite	granite	granite	granite
Sample	65.1 -KKK-96	69.1-MMK-98	90.1 -KKK-96	PIM$-2018-51.1	PIM$-2018-52.1
Longitude	532986	530647	532676	530591	530908
Latitude	6922118	6925697	6922828	6929206	6930463
SiO_2	65	65,9	68	63,05	61,17
TiO_2	0,82	0,61	0,47	0,81	0,99
Al_2O_3	15	15,7	15,8	15,96	15,7
Fe_2O_3t	6,8	4,91	3,51	6,29	7,67
MnO	0,09	0,07	0,04	0,07	0,08
MgO	1,38	0,87	0,76	1,22	1,65
CaO	2,64	2,59	2,37	3,37	4,11
Na_2O	3,26	3,35	3,56	3,56	3,76
K_2O	4,39	5,32	4,9	4,66	3,15
P_2O_5	0,25	0,20	0,13	0,34	0,39
Total	99,63	99,51	99,55	99,32	98,68
S	770	130	430	500	700
Cl	140	110	160	100	200
Sc	<30	<30	<30	15,3	<20
V	95	70	55	62,7	100
Cr	51	36	33	40	50
Ni	<20	<20	<20	20	40
Cu	22	<20	23	<20	30
Zn	119	78	55	100	120
Ga	25	28	25	<30	<30
Rb	143	114	143	111	<10
Sr	241	308	247	300	300
Y	40	30	27	31,1	40
Zr	463	378	266	374	500
Nb	20	13	16	16,9	<20
Ba	1058	1830	1051	1910	1110
Hf	n.a.	n.a.	n.a.	9,83	n.d.
Ta	n.a.	n.a.	n.a.	<1	n.d.
Co	n.d.	n.d.	n.d.	10,9	n.d.
Pb	34	39	41	<30	<30
Th	14	<10	14	9,34	<30
U	<10	<10	<10	2,07	<10
La	63	41	50	52,9	60
Ce	151	159	122	102	120
Pr	n.d.	n.d.	n.d.	11,8	n.d.
Nd	n.d.	n.d.	n.d.	46,9	n.d.
Sm	n.d.	n.d.	n.d.	8,79	n.d.
Eu	n.d.	n.d.	n.d.	2,29	n.d.
Gd	n.d.	n.d.	n.d.	7,94	n.d.
Tb	n.d.	n.d.	n.d.	1,09	n.d.
Dy	n.d.	n.d.	n.d.	6,19	n.d.
Ho	n.d.	n.d.	n.d.	1,22	n.d.
Er	n.d.	n.d.	n.d.	3,56	n.d.
Tm	n.d.	n.d.	n.d.	0,5	n.d.
Yb	n.d.	n.d.	n.d.	3,16	n.d.
Lu	n.d.	n.d.	n.d.	0,51	n.d.

Appendix 1. Continues.

Intrusion	Sorsakoski			
Rock type	qtz-monzonite	qtz-monzonite	qtz-monzonite	qtz-monzonite
Sample	1.1-MTL-1	129.1-ARP-2	PIM$-2018-49.1	PIM$-2018-49.2
Longitude	528947	528777	529090	529090
Latitude	6932334	6927846	6932010	6932010
SiO_2	61,1	61,8	61,07	62,66
TiO_2	1	0,84	0,71	0,73
Al_2O_3	16,8	17	16,51	16,41
Fe_2O_3t	7,72	6,63	5,53	5,69
MnO	0,09	0,08	0,06	0,06
MgO	1,49	1,1	1,16	1,18
CaO	3,71	3,74	2,77	2,98
Na_2O	3,46	3,51	3,38	3,65
K_2O	3,73	4,47	5,59	4,43
P_2O_5	0,33	0,30	0,23	0,23
Total	99,43	99,47	97,08	98,09
S	995	304	500	500
Cl	100	104	100	100
Sc	<30	<30	13,5	<20
V	107	78	58,1	70
Cr	42	<30	30	40
Ni	23	<20	40	30
Cu	<20	<20	<20	20
Zn	129	118	80	80
Ga	29	27	<30	<30
Rb	88	96	142	<10
Sr	317	318	330	310
Y	33	27	26,6	30
Zr	533	502	338	360
Nb	20	17	14	<20
Ba	1571	1779	2880	2180
Hf	n.a.	n.a.	9,11	n.d.
Ta	n.a.	n.a.	<1	n.d.
Co	n.d.	n.d.	9,85	n.d.
Pb	36	34	<30	40
Th	18	<10	16,2	<30
U	<10	<10	2,38	<10
La	64	47	69,6	60
Ce	135	81	134	90
Pr	n.d.	n.d.	15,2	n.d.
Nd	n.d.	n.d.	59,3	n.d.
Sm	n.d.	n.d.	10	n.d.
Eu	n.d.	n.d.	2,9	n.d.
Gd	n.d.	n.d.	8,52	n.d.
Tb	n.d.	n.d.	1,08	n.d.
Dy	n.d.	n.d.	5,61	n.d.
Ho	n.d.	n.d.	1,07	n.d.
Er	n.d.	n.d.	3,08	n.d.
Tm	n.d.	n.d.	0,42	n.d.
Yb	n.d.	n.d.	2,73	n.d.
Lu	n.d.	n.d.	0,42	n.d.

Appendix 1. Continues.

Intrusion	Karvalevä				
Rock type	monzodiorite	diabase	diabase	diorite	diorite
Sample	PIM$-2018-54.1	PIM$-2018-55.1	PIM$-2018-55.2	PIM$-2018-58.1	PIM$-2018-60.1
Longitude	526179	526233	526242	525971	525913
Latitude	6926975	6926934	6926933	6928495	6928048
SiO_2	59,98	50,81	49,76	51,85	50,4
TiO_2	0,86	0,78	0,77	0,76	0,81
Al_2O_3	17,19	16,86	17,33	16,28	15,99
Fe_2O_3t	8,43	9,35	9,2	9,41	9,96
MnO	0,07	0,14	0,14	0,14	0,15
MgO	3,43	7,35	6,59	6,25	7,59
CaO	1,67	10,86	10,72	8,87	9,72
Na_2O	2,35	1,46	2,48	2,76	2,23
K_2O	3,19	0,40	0,72	1,15	0,52
P_2O_5	0,08	0,14	0,15	0,15	0,12
Total	97,26	98,15	97,85	97,61	97,49
S	1900	700	700	800	600
Cl	100	100	100	100	100
Sc	<20	30	30	30	37,9
V	150	220	220	190	229
Cr	160	440	410	220	270
Ni	90	70	50	40	50
Cu	50	30	20	20	20
Zn	140	70	80	100	90
Ga	<30	<30	<30	<30	<30
Rb	<10	<10	<10	<10	18,7
Sr	220	170	170	190	170
Y	20	20	20	30	24,2
Zr	180	70	70	100	101
Nb	<20	<20	<20	<20	4,15
Ba	1090	210	220	320	180
Hf	n.d.	n.d.	n.d.	n.d.	2,95
Ta	n.d.	n.d.	n.d.	n.d.	<1
Co	n.d.	n.d.	n.d.	n.d.	40,1
Pb	<30	<30	<30	<30	<30
Th	<30	<30	<30	<30	2,76
U	<10	<10	<10	<10	0,66
La	<30	<30	<30	<30	10,9
Ce	50	<30	50	50	24,1
Pr	n.d.	n.d.	n.d.	n.d.	3,05
Nd	n.d.	n.d.	n.d.	n.d.	13,5
Sm	n.d.	n.d.	n.d.	n.d.	3,39
Eu	n.d.	n.d.	n.d.	n.d.	1,02
Gd	n.d.	n.d.	n.d.	n.d.	4,03
Tb	n.d.	n.d.	n.d.	n.d.	0,68
Dy	n.d.	n.d.	n.d.	n.d.	4,51
Ho	n.d.	n.d.	n.d.	n.d.	0,96
Er	n.d.	n.d.	n.d.	n.d.	2,92
Tm	n.d.	n.d.	n.d.	n.d.	0,42
Yb	n.d.	n.d.	n.d.	n.d.	2,71
Lu	n.d.	n.d.	n.d.	n.d.	0,41

Appendix 1. Continues.

Intrusion	Karvalevä				
Rock type	qtz-monzonite	diorite	granite	granite	qtz-monzonite
Sample	PIM$-2018-67.1	PIM$-2018-61.1	PIM$-2018-57.1	PIM$-2018-66.1	PIM$-2018-59.1
Longitude	526168	523899	526748	526131	526265
Latitude	6927246	6929061	6927628	6934386	6928815
SiO_2	48,3	52,32	64,22	66,16	64,01
TiO_2	0,36	1,50	0,91	0,62	0,93
Al_2O_3	18,54	15,58	14,89	15,11	15,53
Fe_2O_3t	8,42	11,07	6,55	4,21	6,15
MnO	0,13	0,15	0,07	0,043	0,07
MgO	8,05	4,26	1,6	1,09	1,52
CaO	11,37	6,54	2,46	2,65	3,38
Na_2O	2,1	3,35	3,18	3,18	3,77
K_2O	0,34	1,26	3,92	4,53	3,11
P_2O_5	0,05	0,36	0,34	0,28	0,36
Total	97,66	96,38	98,14	97,87	98,83
S	800	500	400	100	600
Cl	<100	100	100	300	200
Sc	33,9	<20	<20	<20	19,5
V	201	180	90	60	67,9
Cr	550	60	50	30	50
Ni	70	40	40	30	30
Cu	20	30	<20	<20	30
Zn	60	130	70	70	90
Ga	<30	<30	<30	<30	<30
Rb	9,72	<10	<10	<10	104
Sr	140	300	250	280	280
Y	11,3	30	30	40	35,7
Zr	30	170	430	270	411
Nb	<3	<20	<20	<20	20,6
Ba	80	460	1310	1180	1140
Hf	0,98	n.d.	n.d.	n.d.	10,6
Ta	<1	n.d.	n.d.	n.d.	1,01
Co	46,5	n.d.	n.d.	n.d.	12,1
Pb	<30	<30	<30	<30	<30
Th	<2	<30	<30	<30	20,4
U	0,17	<10	<10	<10	3,81
La	3,65	<30	80	60	77,5
Ce	7,38	40	150	120	154
Pr	0,93	n.d.	n.d.	n.d.	17,5
Nd	4,16	n.d.	n.d.	n.d.	67,6
Sm	1,15	n.d.	n.d.	n.d.	11,5
Eu	0,53	n.d.	n.d.	n.d.	1,99
Gd	1,53	n.d.	n.d.	n.d.	9,79
Tb	0,28	n.d.	n.d.	n.d.	1,3
Dy	1,93	n.d.	n.d.	n.d.	7,12
Ho	0,42	n.d.	n.d.	n.d.	1,44
Er	1,33	n.d.	n.d.	n.d.	4,35
Tm	0,2	n.d.	n.d.	n.d.	0,63
Yb	1,23	n.d.	n.d.	n.d.	3,92
Lu	0,2	n.d.	n.d.	n.d.	0,62

Appendix 2. In-situ U-Pb measurements of zircon grains of Löytölamminvuori sample A2434.

Spot no.	Ages & 1 σ errors (Ma)						Ratios			Rho	Concordance (%)	Pb	Th	U
	$^{207}Pb/^{2006}Pb$		$^{207}Pb/^{235}U$		$^{206}Pb/^{238}U$		$^{207}Pb/^{206}Pb$*	$^{207}Pb/235U$*	$^{206}Pb/^{238}U$*					
Löytölamminvuori intrusion (sample A2434)														
151006 1a	1885	20	1943	16	1998	30	0,1154	5,7804	0,3634	0,81	106	181	499	445
151006 1b	1896	20	1969	16	2039	30	0,1160	5,9505	0,3720	0,81	108	183	479	441
151006 2	1884	21	1913	17	1941	29	0,1153	5,5822	0,3513	0,79	103	64	36	163
151006 3	1945	19	1939	16	1934	29	0,1192	5,7522	0,3499	0,82	99	469	34	1204
151006 3b	1883	21	1893	17	1902	29	0,1152	5,4517	0,3431	0,81	101	101	45	274
151006 4	1871	22	1914	17	1954	29	0,1144	5,5850	0,3541	0,79	104	62	15	157
151006 5	1862	20	1886	16	1908	29	0,1139	5,4102	0,3445	0,82	102	448	62	1170
151006 6	1877	21	1916	16	1954	29	0,1148	5,6023	0,3540	0,80	104	85	42	217
151006 7	1880	20	1889	16	1897	29	0,1150	5,4257	0,3422	0,81	101	170	79	450
151006 8	1858	21	1909	17	1956	29	0,1136	5,5520	0,3544	0,80	105	72	53	185
151006 10a	1872	23	1876	17	1879	29	0,1145	5,3421	0,3383	0,77	100	37	26	100
151006 10b	1897	21	1856	16	1819	28	0,1161	5,2196	0,3261	0,80	96	73	42	205
151006 11	1890	20	1892	16	1894	29	0,1156	5,4462	0,3416	0,81	100	189	190	510
151006 12	1878	20	1909	16	1937	29	0,1149	5,5532	0,3506	0,81	103	144	110	379
151006 13	1889	21	1900	16	1910	29	0,1156	5,4962	0,3449	0,81	101	106	44	284
151006 14	1861	21	1871	17	1881	29	0,1138	5,3163	0,3389	0,80	101	85	26	233
151006 14b	1875	21	1871	16	1869	29	0,1147	5,3164	0,3363	0,80	100	99	26	274
151006 15	1864	21	1917	17	1967	30	0,1140	5,6075	0,3568	0,81	106	107	93	278
151006 16	1860	21	1855	16	1850	28	0,1137	5,2127	0,3324	0,81	99	137	38	383
151007 1	1897	21	1862	17	1831	28	0,1161	5,2574	0,3285	0,80	96	94	37	269
151007 1b	1881	21	1856	16	1835	28	0,1151	5,2233	0,3292	0,81	98	130	78	372
151007 2	1876	22	1865	17	1856	29	0,1147	5,2787	0,3337	0,80	99	71	24	201
151007 3	1859	21	1869	17	1878	29	0,1136	5,2984	0,3381	0,80	101	88	41	246
151007 4	1899	20	1932	17	1963	30	0,1162	5,7063	0,3560	0,81	103	199	39	530

151007 4b	1870	21	1899	17	1925	30	0,1144	5,4883	0,3480	0,82	103	254	89	706
151007 5	1887	24	1892	18	1897	29	0,1155	5,4477	0,3422	0,77	100	33	19	91
151007 6	1889	23	1885	17	1882	29	0,1156	5,4036	0,3391	0,78	100	44	33	123
151007 8a	1866	20	1893	17	1918	29	0,1141	5,4544	0,3466	0,82	103	248	139	687
151007 8b	1879	22	1873	17	1868	29	0,1149	5,3268	0,3362	0,80	99	80	31	228
151007 10	1872	21	1865	17	1859	29	0,1145	5,2761	0,3342	0,80	99	98	49	282
151007 11a	1864	22	1891	17	1916	30	0,1140	5,4391	0,3461	0,80	103	87	29	241
151007 11b	1858	22	1885	17	1909	30	0,1136	5,3981	0,3447	0,80	103	83	39	232
151007 12	1870	22	1870	17	1870	29	0,1144	5,3071	0,3365	0,79	100	63	37	182
151008 1	1867	22	1894	17	1920	30	0,1142	5,4599	0,3469	0,79	103	75	20	212
151008 2	1868	22	1910	17	1948	30	0,1142	5,5581	0,3528	0,80	104	85	24	237
151008 3	1860	22	1909	17	1954	30	0,1138	5,5526	0,3540	0,80	105	87	27	242
151008 4	1892	21	1925	17	1957	30	0,1157	5,6604	0,3547	0,81	103	147	73	410
151008 5	1890	22	1890	17	1889	30	0,1157	5,4297	0,3405	0,80	100	83	44	240
151008 5b	1881	22	1883	17	1886	30	0,1151	5,3914	0,3398	0,79	100	70	43	204
151008 5c	1876	22	1894	17	1910	30	0,1147	5,4566	0,3449	0,80	102	122	75	354
151008 6	1856	21	1895	17	1931	30	0,1135	5,4643	0,3493	0,82	104	330	215	939
151008 7a	1898	23	1914	18	1930	31	0,1161	5,5881	0,3489	0,79	102	282	364	821
151008 7b	1883	22	1942	17	1999	31	0,1152	5,7732	0,3635	0,80	106	82	24	227
151008 8	1899	22	1924	17	1947	31	0,1162	5,6508	0,3526	0,80	102	86	31	243
151008 8b	1848	21	1954	17	2056	32	0,1130	5,8525	0,3756	0,82	111	1080	284	2884
151008 9	1877	22	1939	17	1997	31	0,1148	5,7484	0,3631	0,81	106	124	21	343
151008 10	1865	22	1937	17	2005	31	0,1141	5,7388	0,3648	0,81	107	190	158	523
151008 10b	1888	21	1946	17	2000	31	0,1155	5,7948	0,3637	0,81	106	220	47	610
151008 11	1875	22	1906	18	1935	30	0,1147	5,5367	0,3501	0,80	103	81	41	235
151008 12	1866	23	1927	18	1984	31	0,1141	5,6704	0,3604	0,79	106	72	47	201
151008 13	1876	23	1905	18	1933	31	0,1147	5,5314	0,3497	0,79	103	66	22	192